# Decision Support Algorithms for Power System and Power Electronic Design

by
Maziar Heidari

A thesis submitted to the Faculty of Graduate Studies of
the University of Manitoba
in partial fulfillment of the requirements of the degree of

## Doctor of Philosophy

Department of Electrical and Computer Engineering
University of Manitoba
Winnipeg, MB

# Acknowledgement

Joining the doctoral program at the University of Manitoba was not only a great academic practice, but also a valuable life experience for me. It gave me the opportunity to meet many people from all over the world, which taught me a lot about different cultures and life styles.

I would like to express my deepest thankfulness to my parents, who lovingly supported me during my whole life in a way that cannot be expressed by words. Without their help and support it was not possible for me to come to Canada.

I would also like to thank my thesis advisor Prof. Ani Gole and my thesis co-advisor Prof. Shaahin Filizadeh who helped me during the course of this program. In the past few years Shaahin was not only my advisor but also a good friend who helped me to go through the difficulties and the problems I had either in the research or in my personal life. Working with Dr. Gole was also a great pleasure as his knowledge and experience was a great guide during the course of my research.

Finally, I would also like to thank all my friends and colleagues who helped me during the course of this program.

# To my loving parents

who made my life meaningful by their love
and enjoyable by their wisdom, patience and hard work

# Abstract

The thesis introduces an approach for obtaining higher level decision support information using electromagnetic transient (EMT) simulation programs. In this approach, a suite of higher level driver programs (decision support tools) control the simulator to gain important information about the system being simulated. These tools conduct a sequence of simulation runs, in each of which the study parameters are carefully selected based on the observations of the earlier runs in the sequence. In this research two such tools have been developed in conjunction with the PSCAD/EMTDC electromagnetic transient simulation program. The first tool is an improved optimization algorithm, which is used for automatic optimization of the system parameters to achieve a desired performance. This algorithm improves the capabilities of the previously reported method of optimization-enabled electromagnetic transient simulation by using an enhanced gradient-based optimization algorithm with constraint handling techniques. In addition to allow handling of design problems with more than one objective the thesis proposes to augment the optimization tool with the technique of Pareto optimality. A sequence of optimization runs are conducted to obtain the Pareto frontier, which quantifies the tradeoffs between the design objectives. The frontier can be used by the designer for decision making process.

The second tool developed in this research helps the designer to study the effects of uncertainties in a design. By using a similar multiple-run approach this sensitivity analysis tool provides surrogate models of the system, which are simple mathematical functions that represent different aspects of the system performance. These models allow the designer to analyze the effects of uncertainties on system performance without having

to conduct any further time-consuming EMT simulations. In this research it has been also proposed to add probabilistic analysis capabilities to the developed sensitivity analysis tool. Since probabilistic analysis of a system using conventional techniques (e.g. Monte-Carlo simulations) normally requires a large number of EMT simulation runs, using surrogate models instead of the actual simulation runs yields significant savings in terms of shortened simulation time. A number of examples have been used throughout the thesis to demonstrate the application and usefulness of the proposed tools.

# Table of Contents

# List of Figures

# List of Tables

# Chapter 1  Introduction

Methodologies for design of power systems have evolved from simplified analytical methods to sophisticated computer-aided ones over the course of several decades. As complexity of systems escalated over time design of power systems using conventional techniques, which rely on analytical studies, became increasingly difficult. Modern large interconnected networks, which include power electronic devices, are perhaps among the most challenging systems for analysis and design. As the cost of conducting field tests is extremely high, use of digital simulation is often the only feasible solution for power system design problems.

Nowadays, there are several methods available for computer simulation of power systems. Examples include power flow simulation [1], transient stability simulation [2], small signal stability simulation [3], and electromagnetic transient (EMT) simulation [4]. Power flow simulation is useful for determining whether consumer power demand can be delivered without violating transmission system limits. Although this type of simulation is carried out for the steady state condition and it is not capable of dealing with transient behaviour or stability of power systems, it is still a fundamental tool for any power system design problem. Small signal stability simulation, on the other hand, is capable of analyzing the transient behaviour and stability of the system. In this type of simulation a linearized model of power system is used for finding its eigen-values. This is especially important for design of control systems in power networks. In order to increase accuracy of simulation, transient stability and electromagnetic transient simulation programs model

power elements with more details, and they also consider nonlinearity of power system elements. Based on the type and duration of the transient phenomenon under study, a designer selects one of these methods. Transient stability simulation is used for studying longer-term transients caused by severe and large disturbances such as faults and switching. The simulation period in this type of study is usually in the range of a few seconds and it is mainly done to make sure the system retains synchronism after a disturbance.

In electromagnetic transient (EMT) simulation, power system elements are modeled in far more detail compared to transient stability and small signal stability studies, so that the models are valid over a large frequency spectrum and they also represent the nonlinearities involved in power system elements. This makes the EMT simulation tools even capable of simulating fast transients of power systems in the range of milliseconds or microseconds. In addition the ability of modeling power electronic switches makes these programs suitable for studying power electronic devices in power networks [5] and [6]. Benefiting from the above factors EMT simulation is a suitable tool for power electronic and power system design problems; however, as this type of simulation is highly detailed, the computation time required for EMT simulation is usually long. Moreover design is inherently a repetitive cycle that usually requires several simulations before obtaining a final solution. Therefore, it is important to minimize the total number of EMT simulations in the design procedure of power systems to shorten the overall design cycle.

Conventionally use of the EMT simulation programs for power system design requires an expert to conduct several simulation runs to study different aspects of the design problem. This process usually takes a long time and it requires the expert to be available during the whole process. In order to facilitate the design procedure, this thesis introduces the concept of decision support tools for power system and power electronic applications. Decision support tools utilize intelligent supervisory algorithms, which are capable of conducting several simulation runs in an adaptive manner to aid in different aspects of the design problem. In this context a mathematical algorithm plays the role of the human expert and analyzes the simulation results after each run and makes decisions about the parameter values for the next run. As a result these tools significantly improve the computer-aided design cycle by automating the process that would otherwise require repetitive human intervention.

## 1.1      Motivation and Background

One of the major steps in a design problem is to select the values of the system parameters (e.g. control system parameters, size of the system elements, etc.) to optimize the system performance under different operating conditions. Although there are several analytical methods available for analyzing and selecting parameters for power systems [103] and [104], it is always necessary to tune the system parameters with a highly detailed simulation program to finalize a design, and to make sure that the design objectives are actually met. This is because analytical methods are often not easily applicable to complex and large systems and simplifications are required before they can

be conveniently applied. As mentioned before in a power system design procedure an expert conducts several simulation runs before the design can be finalized. In this process the expert selects a different set of parameter values for each run. The starting parameter values for this trial and error based approach are typically obtained from simplified analytical methods. At the end of each simulation run, based on the results observed and using his/her experience the expert selects a new set of parameter values, which in his/her opinion are likely to be an improvement for the next run. This procedure continues until a satisfactory system performance is achieved. Although in this process the intelligence and experience of the designer may reduce the number of required EMT simulation runs (by sensibly selecting the parameter values for each run), this procedure does involve significant user intervention, which typically results in extra design cost and length.

In order to reduce human interaction the first approach was to automate the simulation runs by using primitive run-control techniques. The multiple-run simulation feature [9] – [11], which is offered by many of the EMT simulation programs, is an example of such techniques. This feature allows the designer to automatically conduct several simulation runs with sequentially or randomly selected parameter values. The user therefore does not need to manually change the parameter values following each simulation run, and he/she can analyze the results once all the simulation runs are done. Additionally in order to facilitate the selection of the final parameter set among the typically large number of simulation cases, an objective function (or an error function) is used in the multiple-run simulation process. This is a user-defined mathematical function that quantifies the simulated performance of the system by penalizing any undesirable

behaviour of the system. Having the objective function makes the parameter selection straightforward, as the parameter set that produces the lowest objective function is selected. This feature does reduce the human interaction to a large extent, but since in this procedure the human supervision is eliminated, using multiple-run simulations in practice significantly increases the number of required simulation runs. This is because in a multiple-run approach the parameter values for each run are selected regardless of the results obtained in the previous runs; as opposed to a supervised approach in which the expert uses the results obtained in the previous runs to avoid conducting simulation runs that are less likely to cause an improvement.

Recently the concept of optimization-enabled EMT simulation has been proposed [13], in which an optimization algorithm replaces the primitive brutal-force multiple-run approach for conducting the EMT simulation runs. This was an attempt to give the simulation program the ability to make wise choices based on the previous experience accumulated during past simulations. In this method an optimization algorithm plays the role of the human expert in the sense that it uses the previous experience (in terms of the previously obtained values of the objective function) to select a new parameter set that is likely to be an improvement in the system performance (i.e. results in a lower objective function value).

The idea of using such supervisory algorithms for conducting multiple-run simulations was the main motivation of this research. This thesis is aimed to enhance the capabilities of the optimization enable EMT simulation and to find other opportunities for automating the design procedure as described in the following section.

## 1.2      Problem Definition and Research Objectives

In order to enhance existing methodologies for computer-aided design this thesis introduces the concept of decision support tools. A decision support tool is a supervisory algorithm that takes control of the multiple-run simulations and judiciously selects parameter values for each run. By analyzing the EMT simulation results following each run, a decision support tool is capable of selecting the new set of parameter values in a wise manner to use the time consuming simulation runs efficiently. Depending on the application these tools can also be used for post-processing of the simulation results after all the simulation runs are done. The post-processing stage could be simply an algorithm for sorting the results or it may involve advanced statistical and mathematical manipulation of the data. This makes the simulation results more usable for the designers, which in turn expedites the design procedure. With the above view the existing optimization-enabled EMT simulation is indeed a decision support tool, which uses a nonlinear optimization algorithm for supervising the multiple-run simulation process. The concept of decision support tools is however not limited to an optimization algorithm and encompasses other algorithms as briefly stated in the following sub sections.

### 1.2.1      Uncertainty Analysis

This research proposes to employ the decision support tools for uncertainty analysis of power systems. It is well-known that power system elements are manufactured with tolerances, which means their actual characteristics are expected to vary within certain tolerance bands around their nominal values. In addition to

manufacturing tolerances, there are other factors such as aging and operating conditions that may cause deviations from nominal design values and hence introduce a level of uncertainty in a design process. Such uncertainties may cause degradation in the performance of a system after implementation. Therefore it is imperative that their impact be studied to ensure that the actual performance remains within acceptable limits even in the presence of perceived uncertainties. One approach to handle this problem at the design level is to use multiple-run EMT simulations. In this approach several simulation runs are conducted with parameter values varying in their permissible ranges around the nominal design values. The performance of the system is then studied using the simulation results. Lightning studies is perhaps one the most widely investigated applications of the multiple-run EMT simulations for uncertainty analysis [45] – [47]. In these studies the transmission line over-voltages caused by lighting strikes are simulated by an EMT simulation program to estimate the chance of occurrence of a flashover. As the lightening strokes have a random nature, the flashover rate of the transmission lines cannot be determined just by simulating a single lightening strike and it is determined by Monte-Carlo simulation of many lightening strikes (a multiple-run approach with randomly selected values for the strike parameters). Although this method is an effective method for uncertainty studies, it is not efficient in terms of the number of simulation runs. As mentioned before multiple-run approach requires a large number of EMT simulation runs, completion of which takes a long time.

Another approach for handling uncertainties is to adopt a sensitivity analysis method [12]. In these methods a number of performance indices (or performance

measures) are defined to quantify different aspects of the design performance. These functions are then approximated around the operating point, and the designer uses the changes in the values of these functions to assess the impact of uncertainties on the system performance. If uncertainty levels are small one common method is to use linear approximation of the performance indices around the operating point and use simulation-based methods to find parameters of the linear functions [27] – [31]. Note that once these linear functions are developed using a relatively small number of EMT simulations, they replace the actual simulation for rapid evaluations of the respective performance indices.

Although using linear approximation of the performance indices lowers the simulation burden of uncertainty analysis, linear approximations have two main drawbacks. Firstly, linear approximations are not valid when the parameter variations are large. Secondly in case of systems operating at optimal points, these approximations fail to adequately represent the system performance. Therefore, recently the concept of surrogate models has been introduced [48], [49]. A surrogate model is a mathematical function that approximates a performance index (response variable) over a range of system parameters. With this definition the conventional linear functions, discussed above can also be considered as surrogate models. However, to add more detail to the models, this thesis proposes to use second-order polynomial surrogate models for uncertainty analysis of optimal systems. Second-order functions are capable of representing optimal operating points (which often manifest quadratic-like behaviour) while still retaining a simple form. Simplicity of the model makes it possible to find the parameters of the surrogate model with minimum number of EMT simulation runs, and

the thesis introduces a decision support tool for finding those parameters. As uncertainty studies are usually carried out in two forms of worst-case analysis [40] – [43] (in which the goal is to find the worst-case scenario of the system performance) and statistical analysis [44] – [49] (in which the probability of different performance levels is estimated) the tool was enhanced so it becomes capable of providing probabilistic as well as deterministic information.

## 1.2.2     Extensions on Simulation-Based Optimization

Another aspect of the research in this thesis is to improve and expand the concept of simulation-based optimization. As mentioned earlier simulation-based optimization is considered as one of the decision support tools, which uses a nonlinear optimization algorithm as the supervisor for conducting multiple-run simulations. This thesis expands the previous work on the optimization-enabled transient simulation [13] by adding the capability of handling multi-objective optimization problems. Normally a design problem consists of several objectives, which have to be satisfied simultaneously. A good example of such a problem is cost-performance optimization, which is an important aspect in many engineering designs [25], [26]. This is normally done by defining sub-objective functions for different aspects of the design and combining them into one aggregate objective function using a linear weighted combination. Although it might be possible to satisfy these sub-objectives at the same time for some special cases, such luxury is often unavailable in practical cases, which implies improvement in one of the sub-objectives results in deterioration of at least one of the other ones. Therefore, it is important to find a

compromised solution for such optimization problems. This thesis aims to address the multi-objective optimization problem by using the concept of Pareto optimality [24]. The goal of the Pareto optimization is to obtain the Pareto frontier of all the sub-objectives, a curve or a surface that shows the tradeoffs between the sub-objectives. This curve plays an important role in the design procedure as it helps the designer to decide about the relative significance of each sub-objective to achieve a compromised design. Therefore, in this thesis the technique of Pareto optimization is implemented in the optimization tool to enable it to deal with multi-objective problems. Similar to the previous work, in this research the PSCAD/EMTDC electromagnetic transient simulation program [7], [8] has been selected as the simulation core. The reason for selecting PSCAD/EMTDC is that this program is an established commercial program, developed by the Manitoba HVDC Research Center, which has made technical support accessible during the course of this research.

Another important step for the optimization tool is to implement a gradient-based optimization algorithm in the tool. There are many instances of using gradient-based optimization algorithms for the design purposes in the electrical engineering area [14] − [19]. This is mainly because of two reasons. Firstly these methods are simple and effective and secondly they can be expedited by using fast gradient calculation methods [18] − [23], or by parallelizing the process of their calculation [17]. As a result implementing a gradient-based optimization algorithm provides the opportunity for future improvement of the optimization tool by using the above techniques.

As a last step for the optimization tool, the tool was modified by implementing constraint handling techniques. In most engineering problems the system parameters cannot assume arbitrary values, and are usually limited within certain ranges; therefore, it is necessary to devise methods to impose constraints during the optimization process.

## 1.3      Organization of the Thesis

This thesis starts with a description of the first decision support algorithm, i.e. the optimization. Chapter 2 provides background review of the simulation-based optimization techniques. A simple illustrative example of an optimization problem is presented to demonstrate the role of the optimization in the design procedure. Chapter 3 starts with a brief explanation of the Fletcher-Reeves optimization algorithm, which has been utilized in the developed optimization tool. The chapter also discusses the multi-objective optimization problems, and the concept of Pareto optimality. Implementation stages of the optimization tool in the PSCAD/EMTDC transient simulation program are also explained in this chapter.

Chapter 4 contains a number of application examples to demonstrate the usefulness of the developed optimization techniques. The first case study considers the application of the developed tools for designing a three-level static compensator (STATCOM). In this example, the control system of the STATCOM is tuned using simulation-based developed optimization. An important issue in the STATCOM design is selecting the size of its dc capacitor. In general, the larger the dc capacitor the better is the performance of the STATCOM; however, a large dc-side capacitor means higher

capital cost. The example deals with the problem of selecting a suitable capacitor size as a multiple objective problem, which involves the tradeoffs between the capacitor size and the system performance. In the second example an induction motor drive system is optimized, where the tradeoffs are between high quality steady state response and fast transient response.

In Chapter 5 the other decision support algorithm, the uncertainty analysis tool is introduced. This chapter starts by defining terminology in the context of uncertainty analysis. The chapter discusses two major uncertainty analysis problems namely, sensitivity analysis and tolerance analysis. Under each topic the chapter presents a brief review of literature. The techniques used in development of the uncertainty analysis tool in PSCAD/EMTDC are also explained in this chapter.

The thesis continues in Chapter 6 with a number of case studies that demonstrate the application of the developed uncertainty analysis tool. Selective harmonic elimination technique is the first case study considered in this chapter. This example shows how the optimization, sensitivity analysis, and statistical analysis are useful in studying the harmonic performance of a selective harmonic elimination switching scheme. In the second example uncertainty analysis is used to study the effect of system parameter variations on the transient response of a three-level STATCOM following a load interruption. The sensitivity analysis is conducted to relate the duration of transient phenomena to the values of the system parameters, and then statistical analysis is performed to estimate an expected duration for the transient phenomena when the parameters vary within their permitted ranges.

The thesis ends with the conclusions and recommendations for the future work. In addition at the end of the thesis a number of gradient-based optimization methods are briefly explained in an appendix.

# Chapter 2  Simulation-Based Optimization Background

The complexity of modern power systems, which results from nonlinearity and complexity of individual system elements and their intricate interactions, makes selection of the optimal parameters for a power system a time-consuming and difficult process. As mentioned in the previous chapter, the traditional method for tuning the system parameters using an electromagnetic transient simulation program requires an expert to conduct several simulations and follow a trial and error approach to find an optimal set of system parameters. The multiple-run feature, which is offered in many of the EMT simulation programs [9], [10] reduces the human interaction to some extent. This feature allows the user to automatically conduct several simulation runs with randomly or sequentially selected parameter values. After the multiple run procedure is completed, the designer can scrutinize the results and select the best performing set of system parameters among the ones simulated. The advantage of this method is that it significantly reduces the human interaction, as the designer does not need to run the simulation cases manually. However, since this process entirely eliminates the role of human supervision, a typically large number of simulation runs are often conducted, which normally includes parameter combinations that could have been eliminated by minimal inspections. In practice, this makes the multiple-run simulation process an unaffordably long process.

One way to reduce the number of required simulation runs without involving repetitive human interactions is to implement supervisory methods that conduct the

multiple-run process in an intelligent way. The technique of optimization-enabled electromagnetic transient simulation (OE-EMTS) [13] is one such method, which uses a supervisory nonlinear optimization algorithm to conduct a sequence of runs on an electromagnetic transients simulator. The closeness of the simulation results with the desired performance is quantified by a suitable metric known as the objective function (OF). In this thesis the selected metrics are such that the closer the results to the desired, the smaller is the value of the objective function. Observing the behaviour of the OF from earlier runs can yield information on how to adjust parameters for further improvement in the design. This is achieved by utilizing a nonlinear optimization algorithm as will be discussed later in this chapter.

There are several reports on application of computer-aided optimization in different areas of electrical engineering [13] − [16] and [63] − [73]. Perhaps one of the first attempts in this field was the matching of given frequency response curves to realizable filter transfer functions [63]. Subsequently powerful tools were created by coupling nonlinear optimization programs to electronic circuit simulators for the design of microelectronic circuits [14], [15], [65], [66]. Utilization of computer-aided optimization techniques for high-power applications originated in the power electronics area, where electronic-circuit simulators such as SABER and PSpice were used [16] , [64]. Recent developments extended simulation-based optimization to modern power system transient simulators [13]. Implementation of these tools in EMT simulation programs makes the simulator especially suitable for power electronics and power system

applications as EMT simulation programs are able to accurately model a wide range of power system and power electronic equipment [4].

## 2.1 Optimal Design Example: Minimum Cost Filter

In order to illustrate the concept of optimal design, in this section an example of a minimum cost filter design is presented. Filters are used to reduce the effects of harmonics (produced by nonlinear components) in power systems. There are several filter topologies available for power systems that vary in complexity and performance; however, since this section is only meant to show the essential aspects of the optimization approach, it uses a simplified scheme. The design objective in this section is to find a set of values for the filter elements that result in the lowest cost. Practical power system design examples are presented in Chapter 4 of this thesis.

A commonly used filter topology is the doubly-tuned scheme shown in Figure 2.1. This type of filter is capable of eliminating two harmonic components simultaneously, which makes the design more economical and more compact [101], as in many cases nonlinear loads introduce more than one harmonic current that needs to be eliminated.

The frequency response of a doubly-tuned filter, tuned to eliminate $5^{th}$ (300Hz) and $7^{th}$ (420Hz) harmonics, is shown in Figure 2.2. As shown in the figure, the impedance of the filter tends to zero at two different resonance frequencies (in this case the filter is designed for eliminating the $5^{th}$ and $7^{th}$ order harmonics). The resonance frequencies can be calculated using equation (2.1).
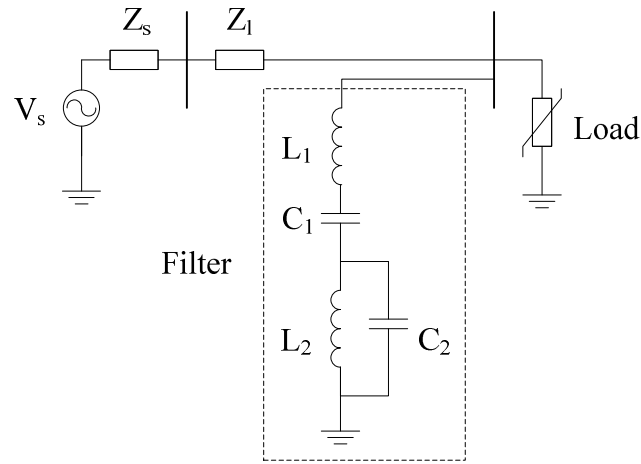
**Figure 2.1  Doubly-Tuned Filter**
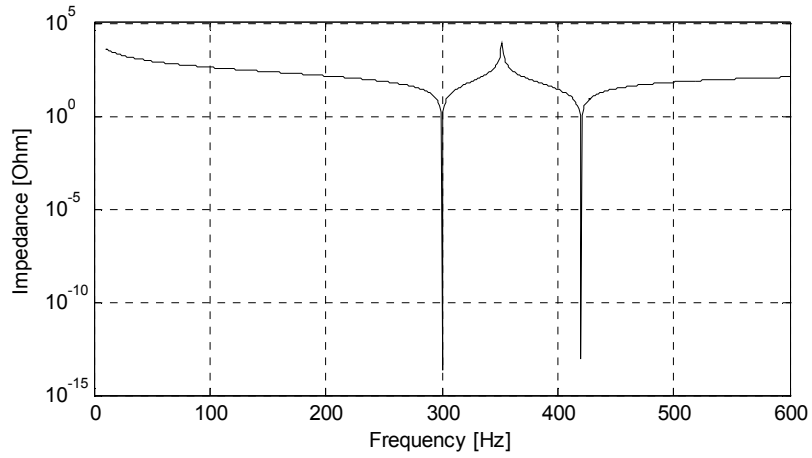


**Figure 2.2  Frequency response of a doubly-tuned filter**

$$\omega_1^2 = \frac{(L_1C_1 + L_2C_2 + L_2C_1) + \sqrt{(L_1C_1 + L_2C_2 + L_2C_1)^2 - 4L_1L_2C_1C_2}}{2L_1L_2C_1C_2}$$

$$\omega_2^2 = \frac{(L_1C_1 + L_2C_2 + L_2C_1) - \sqrt{(L_1C_1 + L_2C_2 + L_2C_1)^2 - 4L_1L_2C_1C_2}}{2L_1L_2C_1C_2}$$

(2.1)

where $f_1 = \omega_1/2\pi$ and $f_2 = \omega_2/2\pi$ are the resonance frequencies of choice. As it can be seen in (2.1) the number of parameters ($L_1$, $L_2$, $C_1$, and $C_2$) is more than the number of equations to be satisfied, which provides flexibility in the design. For a given set of resonance frequencies, two of the variables can be arbitrary selected and the other two can be expressed as functions of those two, e.g., $L_1$ and $C_1$ can be expressed as functions of $L_2$ and $C_2$ as shown in (2.2) and (2.3). However in this case $L_2$ and $C_2$ are constrained through the condition that $L_1$ and $C_1$ have to be positive.

$$L_1 = \frac{-L_2}{\left(1 - \omega_1^2 L_2 C_2\right)\left(1 - \omega_2^2 L_2 C_2\right)} \tag{2.2}$$

$$C_1 = -\frac{\left(1 - \omega_1^2 L_2 C_2\right)\left(1 - \omega_2^2 L_2 C_2\right)}{\omega_1^2 \omega_2^2 L_2 C_2} \cdot \frac{1}{L_2} \tag{2.3}$$

A similar approach to the one presented in [101] can be used for finding the element values that yield the minimum cost design. This involves finding the cost of the filter in terms of the filter parameters and minimizing the cost function. The filter consists of four reactive elements and the cost of each element depends on its power rating, which is determined by both the fundamental frequency and the harmonic currents in the element. As in this case the filter is designed to eliminate $5^{th}$ and $7^{th}$ order harmonics, those harmonics are the ones included in calculation of power rating of each element (assuming that the effect of other harmonic currents is negligible). For example the power rating of $C_1$ is:

$$P_{rC1} = \frac{V_1^2}{|Z_s|^2 \omega_s C_1} + \frac{I_{h5}^2}{5\omega_s C_1} + \frac{I_{h7}^2}{7\omega_s C_1} \tag{2.4}$$

where $V_1$ is the rms value of the fundamental phase-voltage, $I_{h5}$ is the 5th order harmonic current, $I_{h7}$ is the 7th order harmonic current, and $Z_s$ is the impedance of the filter at the fundamental frequency calculated as shown in equation (2.5):

$$Z_s = j\left( \omega_s L_1 - \frac{1}{\omega_s C_1} + \frac{\omega_s L_2}{1 - \omega_s^2 L_2 C_2} \right) \tag{2.5}$$

Similarly, the power ratings of the other elements ($L_1$, $C_2$, and $L_2$) are:

$$P_{rL1} = \frac{V_1^2}{|Z_s|^2} \omega_s L_1 + I_{h1}^2 h_1 \omega_s L_1 + I_{h2}^2 h_2 \omega_s L_1 \tag{2.6}$$

$$P_{rC2} = \left| \frac{V_1}{Z_s} \cdot \frac{\omega_s L_2}{\omega_s L_2 - \frac{1}{\omega_s C_2}} \right|^2 \frac{1}{\omega_s C_2} + \left| I_{h1} \cdot \frac{h_1 \omega_s L_2}{h_1 \omega_s L_2 - \frac{1}{h_1 \omega_s C_2}} \right|^2 \frac{1}{h_1 \omega_s C_2} + \left| I_{h2} \cdot \frac{h_2 \omega_s L_2}{h_2 \omega_s L_2 - \frac{1}{h_2 \omega_s C_2}} \right|^2 \frac{1}{h_2 \omega_s C_2} \tag{2.7}$$

$$P_{rL2} = \left| \frac{V_1}{Z_s} \cdot \frac{-\frac{1}{\omega_s C_2}}{\omega_s L_2 - \frac{1}{\omega_s C_2}} \right|^2 \omega_s L_2 + \left| I_{h1} \cdot \frac{-\frac{1}{h_1 \omega_s C_2}}{h_1 \omega_s L_2 - \frac{1}{h_1 \omega_s C_2}} \right|^2 h_1 \omega_s L_2 + \left| I_{h2} \cdot \frac{-\frac{1}{h_2 \omega_s C_2}}{h_2 \omega_s L_2 - \frac{1}{h_2 \omega_s C_2}} \right|^2 h_2 \omega_s L_2 \tag{2.8}$$

Having expressed the power ratings, the cost of the filter can be obtained using the per kVAR cost of inductor ($U_L$) and capacitor ($U_C$) as shown by equation (2.9):

$$K_d = U_L (P_{rL1} + P_{rL2}) + U_C (P_{rC1} + P_{rC2}) \tag{2.9}$$

Note that $K_d$ is eventually a function of the $L_1$, $C_1$, $L_2$, and $C_2$ values. In this example it is assumed that $I_{h5}$ = 70A and $I_{h7}$ = 50A, $V_1$ = 235kV, $U_C$ = 3.5\$/kVAR, and $U_L$ = 8.0\$/kVAR. A contour map of filter cost as a function of $L_2$ and $C_2$ is shown in Figure 2.3. The minimum cost point (indicated by "☆") is approximately at $C_2$ = 14.3µF and $L_2$ = 13.8mH. Using (2.2) and (2.3) $C_1$ and $L_1$ are calculated to be $C_1$ = 1.66µF and $L_1$ = 124mH, which results in the minimum cost of \$92,200 per phase.
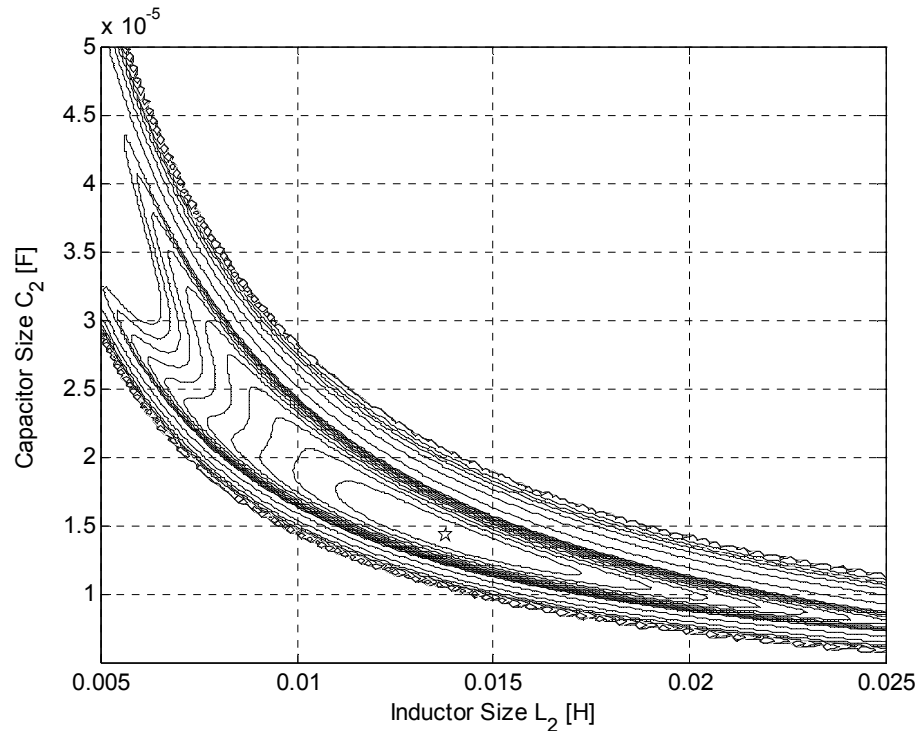


**Figure 2.3  Contour map of the doubly-tuned filter cost**

Note that generation of a contour such as the one shown in Figure 2.3 requires numerous function evaluations over the entire search space of $C_2$ and $L_2$. Alternatively use of an optimization algorithm significantly reduces the amount of calculations required for

finding the minimum cost (for example using an initial guess of $L_2$ = 10mH and $C_2$ = 20μF the optimization steps of a steepest descent optimization algorithm are shown in Figure 2.4).
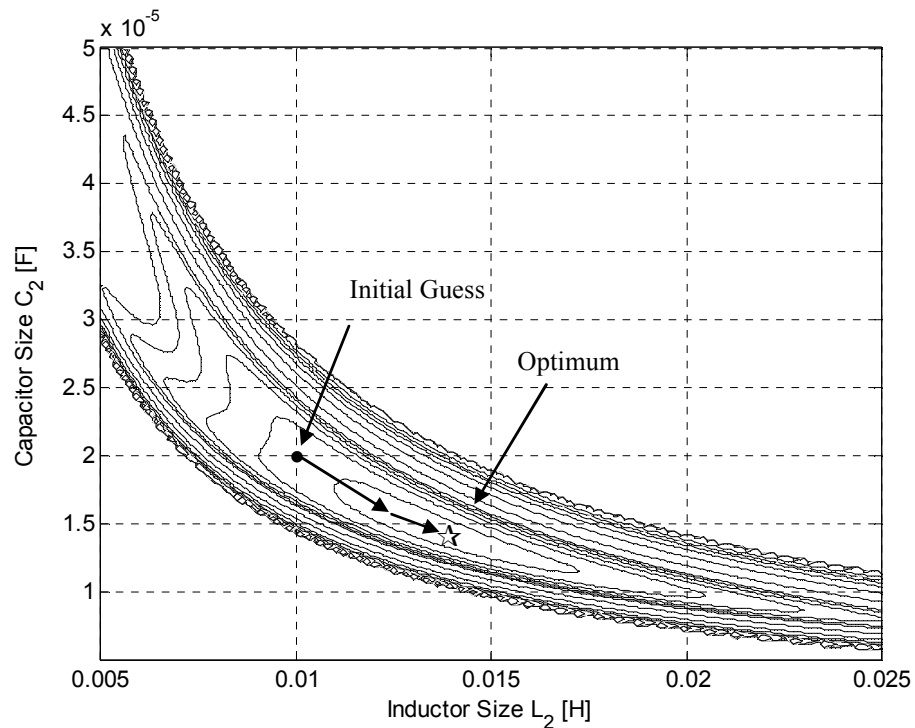


**Figure 2.4  Steepest descent method for finding the minimum cost filter**

In addition, for complex systems, derivation of a closed-form representation for the objective function (e.g. the one shown in Eq. 2.9) in terms of optimization parameters may be practically impossible. As described in the next section, a simulation method can be used in lieu of an analytical objective function, thus facilitating the use of an optimization algorithm for optimal design.

## 2.2      Simulation and Optimization

As mentioned in the previous section, it is difficult or impossible to express the objective function in terms of the optimization parameters for large and complex systems. This is the main motivation behind the development of simulation-based optimization methods [13]. In these methods instead of developing an analytical form for the objective function (as in 2.9), the objective function is calculated based on the simulation results obtained for each set of parameter values. The concept of simulation-based optimization is illustrated in Figure 2.5.
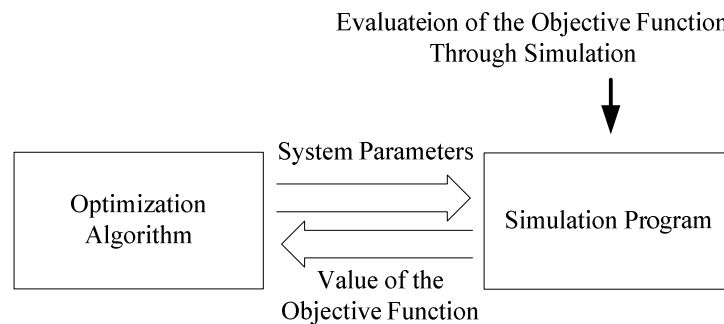


**Figure 2.5  Simulation-Based Optimization**

In each step the optimization algorithm passes a set of trial values for system parameters to the simulation program (in case of the filter design problem these are the inductor and capacitor sizes); the program simulates the circuit for the given set of system parameters and returns the corresponding value of the objective function. Since simulation programs are capable of handling large and complex systems, optimization of such systems becomes possible through this synergetic combination.

As an application example of simulation-based optimization, the filter design problem presented earlier is solved using the method described above. The

PSCAD/EMTDC simulation program has been used for representing the circuit and calculation of the objective function with the Nelder-Mead nonlinear optimization algorithm [13] as the optimization routine. The progress of the optimization procedure is shown in Figure 2.6 with the '☆'s denoting the generated trial points. For this simple case the contour plot of the objective function, obtained earlier, is superposed on the sequence of the trial points to demonstrate the quality of the convergence.
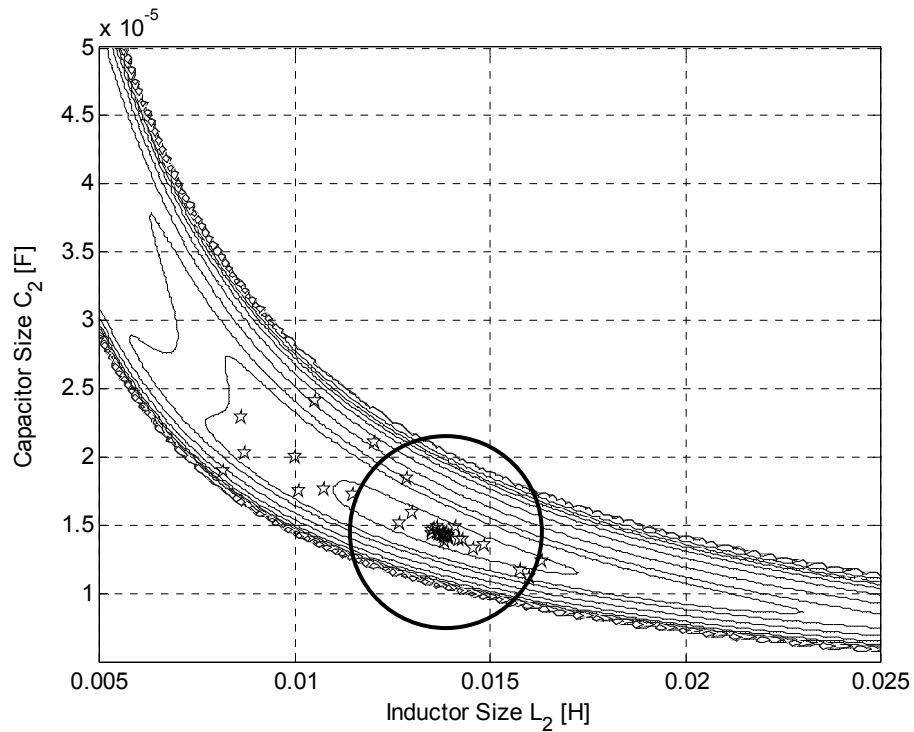


**Figure 2.6  Simulation-based optimization of the minimum cost filter**

In the figure, the minimum cost to which the algorithm converges is located in the area where the density of the trial points is highest (implying convergence). In this example the optimization process started with the initial values of $L_2 = 10$mH and $C_2 = 20\mu$F, at which the cost of the filter is around \$97,100. During each run of the trial

sequence the Nelder-Mead algorithm generates a new set of trial values for $L_2$ and $C_2$ based on the objective function values (filter costs) obtained from the previous runs, which eventually leads to an optimum cost of \$92,200 after about 30 simulation runs.

## 2.3      Nonlinear Optimization Methods

Selection of the optimization algorithm is a key factor in development of the simulation-based design methods. Although a large number of nonlinear optimization algorithms exist, these methods can be classified into three categories of direct search methods, gradient-based methods, and heuristic methods. In this section each of these methods are briefly explained and their main advantages and disadvantages are discussed.

### 2.3.1      Direct Search Methods

The main feature of direct methods is that they only use the values of objective function (obtained at a limited number of sample points) in their search. From these sample evaluations, a candidate direction for moving the search is determined, and additional points are generated. This is done by selecting the new samples in the vicinity of the points with lower objective function values (assuming a minimization problem). Methods of Nelder-Mead, Hooke-Jeeves, and Powell's conjugate directions are typical examples.

The main advantage of direct search methods is their simplicity, in that they do not require explicit calculations of derivatives as would be required in gradient based

method, hence earlier approaches to optimization enabled electromagnetic transients simulation [13] have used such methods.

## 2.3.2     Gradient-Based Optimization Methods

These methods not only use sampled values of objective function, but they also use derivative information of the function at each point. Derivatives of a function indicate the local rate of change of the function with respect to its parameters. Therefore this information can be used for selecting an effective and suitable direction for reducing the objective function. In a simulation-based approach, however, the derivative information is not available and derivatives have to be numerically calculated using samples of the objective function. This reduces the optimization speed to some extent; however as  is shown in the thesis, the overall speed of the optimization still remains satisfactory due to their fast convergence rate. In addition calculation of the derivatives is a highly parallelizable task, which can be accelerated using parallel-processing platforms. Examples of gradient-based methods are Cauchy's method, Newton's method, and Marquardt's method.

## 2.3.3     Heuristic Optimization Methods

Heuristic methods are those methods which are mainly inspired by nature (as opposed to direct and gradient-based methods which have a mathematical foundation). These methods are mainly used for their capability of finding the global optimum of a function. In the past few decades several heuristic methods have been developed and

examples include genetic algorithm (GA), particle swarm optimization (PSO), simulated annealing (SA), and ant colony. The main drawback of these methods is that they require a relatively large number of samples to provide reasonably accurate results. Since EMT simulation of large power systems itself is an extremely lengthy process, use of heuristic methods for these applications is not recommended.

## 2.4      Selection of the Optimization Method

The thesis uses electromagnetic transient simulation for objective function evaluation.  This is the most detailed method for simulating power system transients and can handle the full range of power system phenomena, ranging from high frequency lightning transients, to power electronic switching transients and even to electromechanical machine transients. However, the high level of detail makes these methods computationally very slow, with simulation times for individual runs ranging from several seconds to an hour. Hence, minimizing the number of simulation runs in the optimization process is extremely important. Therefore, utilization of heuristic optimization methods (which normally require a large number of simulation runs) is not recommended for such studies.

The previously reported research on simulation-based optimization used Nelder-Mead method as the nonlinear optimization algorithm. This method is one of the direct search methods, i.e., it does not require the derivative information (gradient) of the objective function. The advantage of not calculating the gradient is that finding the

direction in which the trial point is moved from run to run typically does not require more than one function evaluation.

Gradient-based optimization methods on the other hand require several function evaluations, and at the first glance appear to be computationally expensive; however, as discussed in the next chapter gradient-based methods provide more exact information as to the steepest descent direction of the objective function, and therefore potentially converge in a smaller number of iterations. In addition these methods lend themselves to implementation on parallel computers, resulting in potential speed improvements.

Another advantage of having derivative information of an objective function is that such information can be used for sensitivity analysis of the system under study. In practice the system components cannot be made so that they have the exact values obtained from the optimization process, and such tolerances may cause deterioration in the system performance. As discussed in the next chapters, having the derivative information of the objective function makes it possible to approximate the function around an operating point. This allows the designer to quantify the resulting degradation in the performance when the system parameters have small variations.

Based on above in this research a gradient-based optimization algorithm has been chosen as the main core of the optimization process.

# Chapter 3  Improved Approaches for Simulation-Based Optimization

As indicated in the previous chapter, simulation-based optimization is an effective approach for parameter tuning in design of highly complex power systems. It not only reduces human interactions during the design process but also reduces the required number of simulation runs. This thesis extends the previously developed non-gradient simulation-based optimization approach [13] by adding gradient-based optimization capability. This allows potentially faster convergence, enables proper scaling of variables, and paves the way for assessment of design sensitivity through a gradient-based sensitivity assessment algorithm.

Moreover the concept of Pareto optimality [24] has been used in conjunction with the simulation-based optimization to make it possible to deal with multi-objective design problems. The Pareto frontier is drawn in the space of all the sub-objective functions, and it permits the understanding of tradeoffs between competing sub-objectives. This helps the designer make an informed decision on the weight of each sub-objective in the design.

In the next sections, the gradient-based optimization algorithm, used in this research, is explained. Moreover, other practical issues such as scaling and constraint handling are also discussed.

## 3.1     Gradient-Based Optimization

As mentioned before, in this research a gradient-based optimization algorithm has been used in conjunction with an electromagnetic transient simulation program to construct a gradient-based simulation-based optimization facility. Even though gradient-based algorithms may not always be the fastest methods available, and are not able to handle objective functions with discontinuity, they are popular in the area of electrical engineering due to the following reasons:

1.  Although calculation of the gradient vector is generally a time-consuming process (especially when the number of system parameters is large) there are a number of circuit-based methods available for fast calculation of the gradient vector, which can expedite the process [18] – [23].

2.  Even when the gradient has to be calculated numerically via significant computational effort, the number of steps to convergence, taken by the algorithm, may be less, making the method comparable to direct methods in time penalty. This is shown by an example later in Chapter 4.

3.  Gradient-based methods are highly parallelizable, and can be conveniently implemented on parallel processing platforms, which in turn results in accelerated optimization [17].

4.  There is past evidence of successful use of gradient-based methods for electrical engineering applications [14] – [23].

Gradient-based optimization methods constitute a major category of classical optimization methods. In this section the main characteristics of these methods are explained and their advantages and disadvantages are outlined. Additional details about the gradient-based methods are also presented in Appendix A of this thesis. Without loss of generality, the following describes gradient-based methods for a minimization problem. Any maximization problem can be reformed as a minimization problem for example by negating the objective function.

As mentioned before, an optimization problem is defined as finding the optimum value of an objective function $f(\mathbf{x})$, in which $\mathbf{x} = \{x_1, \ldots, x_n\}$ is a point (decision vector) in the search space. Gradient-based methods use the derivative information of the objective function to find a suitable search direction ($\mathbf{d}$), which results in a decrease in the objective function evaluation. Having found the direction, a step is taken in that direction as shown in equation (3.1):

$$\mathbf{x}^{(k+1)} = \mathbf{x}^{(k)} + s^{(k)}\mathbf{d}^{(k)} \tag{3.1}$$

where $\mathbf{x}^{(k+1)}$ is the new point, $\mathbf{x}^{(k)}$ is the previous point, $s^{(k)}$ is the current step length (determined using a line search method as described later), and $\mathbf{d}^{(k)}$ is the current direction vector. The algorithm proceeds by calculating the direction vector, and by taking an appropriately-sized step in that direction until an optimum is achieved.

Cauchy's method is arguably the simplest gradient-based method. In this method the opposite direction of the objective function gradient ($\nabla f$) is chosen for $\mathbf{d}$. The gradient vector shows the direction of the maximum increase in value of the objective

function; therefore, its opposite direction shows the direction of the steepest descent. The

algorithm is represented mathematically in (3.2), in which $\nabla f$ has replaced $\mathbf{d}$ in (3.1):

$$\mathbf{x}^{(k+1)} = \mathbf{x}^{(k)} - s^{(k)} \nabla f\left(\mathbf{x}^{(k)}\right) \tag{3.2}$$

The step length $s^{(k)}$ is determined by a single variable search, in which the variable

is $s^{(k)}$ and the objective function is evaluated at $f(\mathbf{x}^{(k+1)})$ where $\mathbf{x}^{(k+1)}$ is calculated from

(3.2).

Although Cauchy's method is straightforward and works well for simple objective

functions, it has excessively slow convergence rate when the objective function has a

complex shape. Other methods have therefore been developed to deal with complicated

objective functions, and are available in the literature. In this research the Fletcher-

Reeves optimization algorithm, which is an improved version of the Cauchy's method,

has been selected for the purpose of optimal design. This method is described in the next

section. Appendix A presents more information about these two and other gradient-based

optimization methods.

## 3.1.1     Fletcher-Reeves Method

The Fletcher-Reeves optimization algorithm is one of the most effective gradient-

based optimization methods as it benefits from a fast convergence rate [74] and it only

uses the first order-derivatives of the objective function (which reduces computation time

and numerical error in the optimization process). In this method movement from the

current point $\mathbf{x}^{(k)}$ to the new point $\mathbf{x}^{(k+1)}$ occurs along a direction vector as shown in (3.3):

$$\mathbf{d}^{(k)} = -\nabla f^{(k)} + \frac{\left|\nabla f^{(k)}\right|^2}{\left|\nabla f^{(k-1)}\right|^2}\mathbf{d}^{(k-1)}$$

$$\mathbf{d}^{(0)} = -\nabla f^{(0)}$$

(3.3)

As seen in the first equation in (3.3) the current gradient vector ($\nabla f$), as well as the previous direction vector, are used to generate the new direction vector. The Fletcher-Reeves method belongs to a class of gradient-based optimization algorithms called the conjugate gradient methods. In these methods, instead of looking for a direction in which the objective function decreases the most, the algorithm provides a number of different directions (conjugate directions) that result in the minimum number of line searches in the optimization process. In order to explain the concept of conjugate directions, consider a generic $N$-variable quadratic function as shown in equation (3.4):

$$f(\mathbf{x}) = a + \mathbf{b}^\mathrm{T}\mathbf{x} + \frac{1}{2}\mathbf{x}^\mathrm{T}\mathbf{C}\mathbf{x}$$

(3.4)

where $a$ is a constant, $\mathbf{b}$ is a $N \times 1$ vector, and $\mathbf{C}$ is an $N \times N$ matrix. Directions $\mathbf{d}_1$, ... , $\mathbf{d}_N$ are called $\mathbf{C}$ conjugate if the condition shown in (3.5) is satisfied:

$$\mathbf{d}_i^\mathrm{T}\mathbf{C}\mathbf{d}_j = 0 \qquad \text{for any } i \neq j$$

(3.5)

It can be proved that starting from any point on the surface of the $N$-variable quadratic function, $N$ line searches along the above directions lead to the optimum value of the function [74]. As any well-behaved function can be approximated by a quadratic form in at least a sufficiently small area around its optimum, using conjugate gradient methods

significantly reduces the number of function evaluations in the optimization process. For a quadratic function, it can be proved that the direction vectors produced by Fletcher-Reeves method (3.3) are conjugate to each other [74]. In order to illustrate and compare the performance of the Cauchy and the Fletcher-Reeves methods Figure 3.1and Figure 3.2 show the optimization steps of the objective function shown in (3.6) using each of the two methods.

$$f(x,y) = \left(\frac{x}{3}\right)^2 + y^2 - \frac{xy}{3} \qquad\qquad (3.6)$$
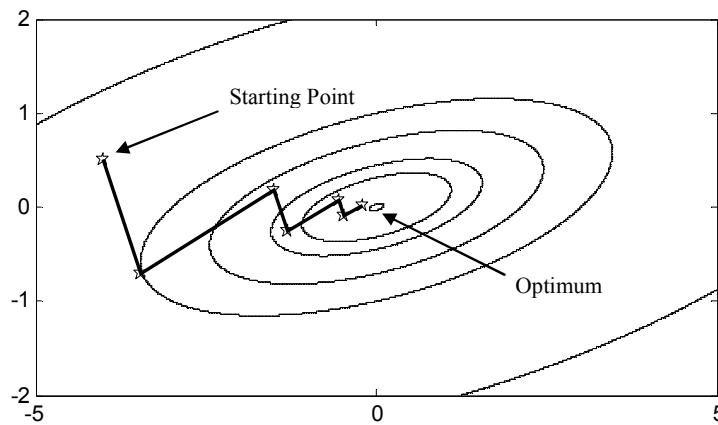


**Figure 3.1  Cauchy's method of optimization**
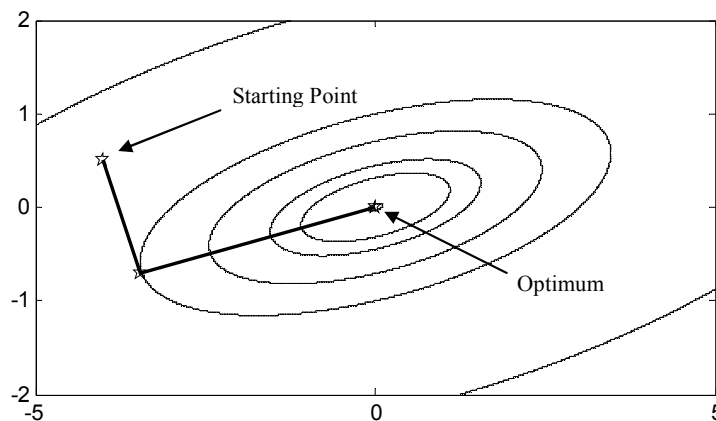


**Figure 3.2  Fletcher-Reeves method of optimization**

As it can be seen in the figures, with the same starting point the Cauchy's method has not reached the optimum even after seven trial points, whereas the Fletcher-Reeves method converges to the optimum only after two iterations, as expected from a conjugate gradient method.

## 3.1.2     Constraint Handling Technique

Most engineering applications have constraints on the optimization parameters imposed either by physical properties (e.g. inductor values should be non-negative) or other engineering limitations. Therefore, there is a need for constraint handling techniques in the simulation-based optimization to ensure that the search is conducted within allowed boundaries. In general in an optimization problem there are two types of constraints, namely equality constraints and inequality constraints. There are several methods available to deal with each of the above types of constraints [74]. These methods, however, can be classified in two major groups. The first group suggest the objective function to be modified, so that a constrained problem is converted to an unconstrained problem (e.g. method of Lagrange multipliers) [74]. The second ones suggest modifying the optimization algorithm itself, so it becomes capable of handling design constraints (e.g. method of feasible directions) [74].

In this research the optimization algorithm has been modified to address inequality constraints that put a limit on the range of the system parameters. Figure 3.3 shows the constraint handling technique that has been incorporated in this research [15]. The figure shows the contour plot of an objective function with two parameters $x_1$ and $x_2$,

and a rectangle (hypercube in higher dimensions) outlining the boundaries of the search

variables.
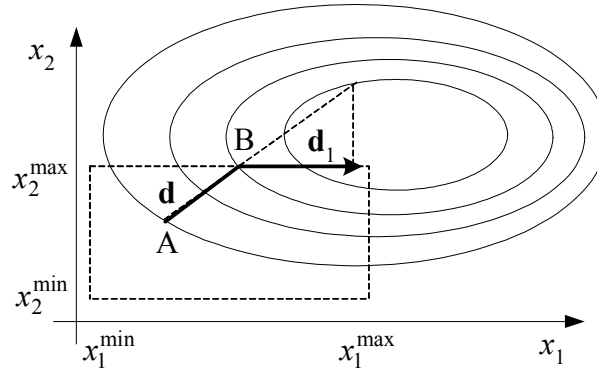


**Figure 3.3  The constraint handling method**

Assume that the search for the optimum is currently at point '**A**', and a move in

direction **d** is recommended by the algorithm. The movement along **d** intersects the

boundary at point '**B**'; at this stage the motion in direction **d** is discontinued in favour of

the motion in direction $\mathbf{d}_1$, where $\mathbf{d}_1 = (\mathbf{d}.\mathbf{i}_1)\mathbf{i}_1$ is the projection of **d** on the constraint

boundary, and $\mathbf{i_1}$ is the unit vector for $x_1$ axis.

## 3.2    Interfacing the Optimization Algorithm with the EMT Simulator

In the previous sections the methods used for gradient-based optimization were

briefly explained; however, during the actual interfacing of these methods with the

simulator, further considerations had to be made to overcome implementation difficulties.

In this section different steps of interfacing the Fletcher-Reeves optimization algorithm

with the simulation program are discussed. Although the discussion is general, in this

thesis the PSCAD/EMTDC electromagnetic transient simulation program has been used as the simulation core, and the optimization algorithm has been implemented in FORTRAN programming language.

## 3.2.1     Structure of the Simulation-Based Optimization Facility

A block diagram of the optimization-simulation interface is shown in Figure 3.4. As shown, the optimization process starts by numerical calculation of the derivatives of the objective function. In this process the simulator is used for evaluation of the objective function at each point. A new direction vector is then constructed based on the above derivatives and the previous direction vectors. This direction is used for a line search, which also involves several simulation runs to find a new point with a lower value of the objective function. The process is repeated until the optimization process converges to an optimum. The convergence condition in the optimization process is satisfied when none of the parameter values change more than a prescribed amount (according to user's choice) in two successive iterations.

## 3.2.2     Scaling of the Variables

Optimization of electrical networks involves dealing with numbers in markedly different orders. For example resistors may assume values in range of kilo-ohms ($10^3\Omega$) and capacitors may assume values in range of micro-Farads ($10^{-6}$F). Such differences in the orders of the numbers can make the problem numerically ill-conditioned.
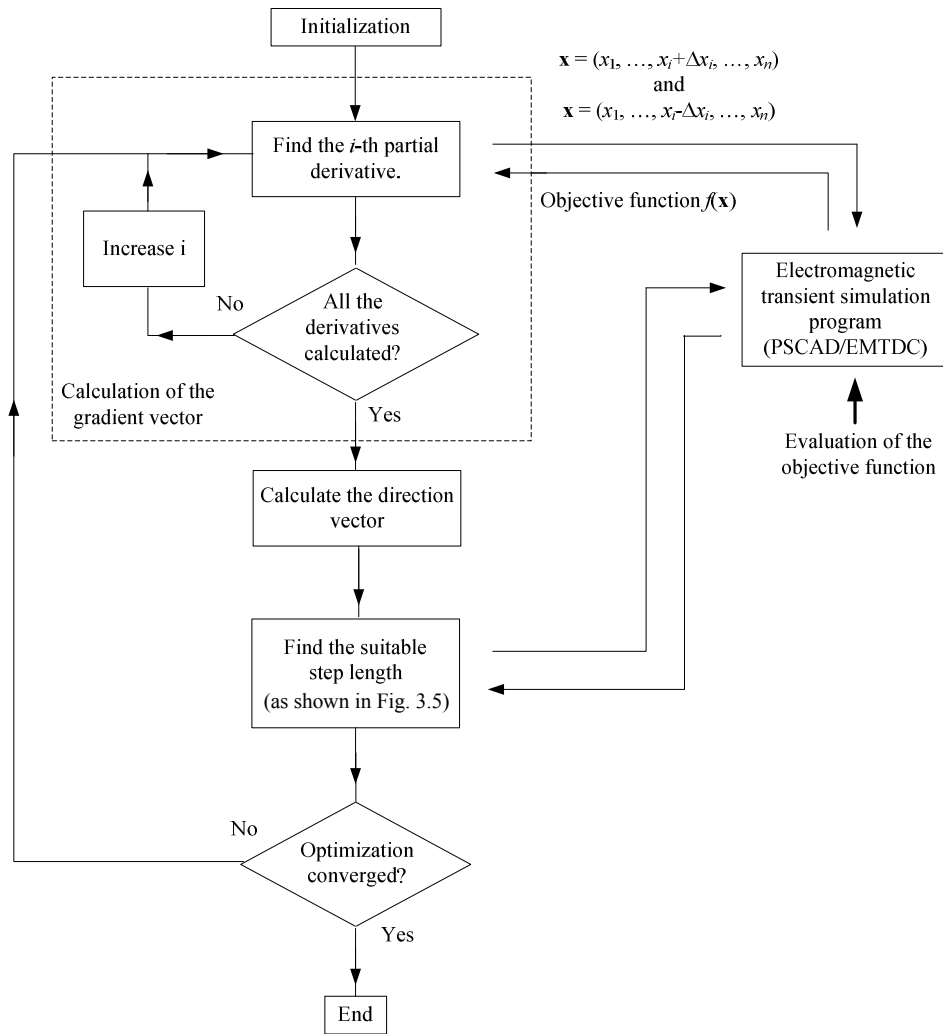
**Figure 3.4  The optimization-simulation interface**

Pre-scaling of the variables to convert the original values to scaled values over a given range ([-10, 10] in this case) is an important step that improves numerical performance of the method. The formula shown in (3.7) has been used for scaling.

$$x_i^* = \frac{10x_i}{\max(|x_i|)} \qquad\qquad (3.7)$$

In the above formula $x_i^*$ is the scaled value of the $i$-th parameter ($x_i$). For example if the search range of a capacitor is [0.1µF, 200µF] and its initial value is 20µF, the above formula yields the scaled value of the initial capacitor as $\dfrac{10 \times 20\,\mu F}{200\,\mu F} = 1$. At the same time if the acceptable range of a resistor is [0.5kΩ, 50 kΩ] and its initial value is 2kΩ, the above formula yields a value of 0.4. It is obvious that although the original values for the capacitor and the resistor are totally different, the scaled values reside in a smaller interval.

## 3.2.3 Numerical Evaluation of the Gradient and Direction Vector

In each iteration of the Fletcher-Reeves optimization method, a direction vector must be calculated using (3.3). However, since a closed-form representation of the objective function is unavailable, the gradient in (3.3) must be calculated numerically. To calculate the partial derivatives ($\partial f / \partial x_i$) used in the gradient vector, the objective function is evaluated at ($x_{10}, \dots, x_{i0} - \Delta x_{i0}, \dots, \Delta x_{n0}$) and ($x_{10}, \dots, x_{i0} + \Delta x_{i0}, \dots, \Delta x_{n0}$) by conducting two separate simulation runs. (3.7) is then used to evaluate the partial derivatives. In PSCAD/EMTDC this is done using the multiple-run feature of the program.

$$\frac{\partial f}{\partial x_i} \approx \frac{f\left(x_{10}, \cdots, x_{i0} + \Delta x, \cdots, x_{n0}\right) - f\left(x_{10}, \cdots, x_{i0} - \Delta x, \cdots, x_{n0}\right)}{2\Delta x} \qquad (3.8)$$

where $\mathbf{x}_0 = (x_{10}, \dots, x_{n0})$ is a vector that indicates the current point, and $f(\mathbf{x})$ is the objective function.

An important observation regarding calculation of the direction vector is resetting certain terms when intersecting a constraint boundary. As discussed in section 3.1.2 when one of the variables reaches a boundary, the value of that specific parameter is kept constant unless a move toward the inner area of the boundary is suggested by the algorithm. In order to improve the performance of the Fletcher-Reeves method, the direction vector for the variables that are located on the boundary is set to zero unless a move toward the inner area of the boundary is suggested by the algorithm. For example if (3.3) suggests $\mathbf{d}^{(k)} = [d_1^{(k)}, \ldots, d_N^{(k)}]$ as the direction vector, and the $m$-th variable is located on the boundary, then $\mathbf{d}^{(k)} = [d_1^{(k)}, \ldots, d_{m-1}^{(k)}, 0, d_{m+1}^{(k)}, \ldots, d_N^{(k)}]$ is used for the direction vector unless a move towards the inner area of the boundary is suggested.

## 3.2.4    Determination of the Optimum Step Length

Once the direction vector is determined, a step with a suitable length in that direction must be taken. The step length $s^{(k)}$ in (3.1) is found by optimizing the objective function as a function of $s^{(k)}$ (referred to as a line search) [74]. However, as the evaluation of the objective function requires time consuming electromagnetic transient simulations, using such a line search method makes the optimization process slow. Therefore, instead of using a classical line search method the algorithm shown in Figure 3.5 has been used. Although this algorithm does not lead to the "optimal" step length, it helps to find a suitable step length in a smaller number of simulation runs.

In the algorithm an initial step length is selected, and the objective function is evaluated by simulation using parameter values of $\mathbf{x}$ as suggested by (3.1). If the objective function is reduced, the search direction is deemed to be a good one, and an

acceleration factor $p$ is applied to the step length to yield a larger step; otherwise the step length is reduced by the factor $p$. If the increase in step length does not result in a decrease in the value of objective function, a smaller acceleration factor $q < p$ is used. A similar approach is used when the initial step length does not result in a reduction (as indicated by Figure 3.5).
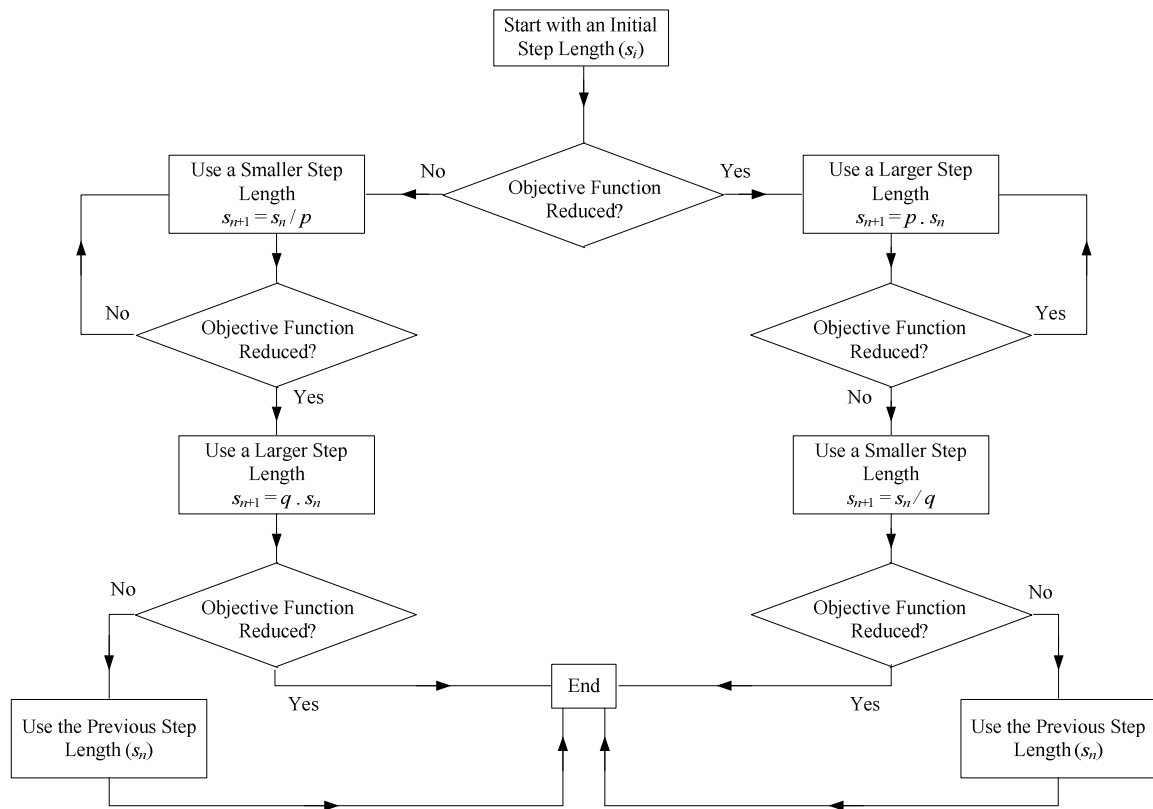


**Figure 3.5  The algorithm used for finding the suitable step length**

In the actual implementation of the algorithm the factors $p$ and $q$, shown in Figure 3.5, have been selected as $p = 2$ and $q = 1.5$. In order to avoid excessively large and small step lengths in this method the step length is limited within a range. In addition, in order to accelerate the procedure after each iteration the step length is adjusted based on the

previous results, i.e. if in the previous iteration the suitable step length was much larger than the initial step length, the starting value of the step length in the following iteration increases.

## 3.3     Multi-Objective Optimization

This section describes a major contribution of the thesis that addresses problems with multiple, often competing, objectives. Engineering optimization problems usually involve multiple objectives that have to be satisfied simultaneously. One way to handle such problems is to construct a composite objective function, which is a weighted sum of the individual sub-objective functions. An ordinary optimization algorithm can then be used for optimizing the system performance. However, in this method selection of a suitable set of weights for sub-objective functions is difficult, as the weight selection requires prior knowledge about the impact of each sub-objective function on the other ones. Another way to handle the multi-objective problems is to use the concept of Pareto optimality [24] and [75] – [79]. The Pareto frontier, which is a set of all the Pareto optimums, clearly shows the tradeoffs between sub-objective functions in a multi-objective problem. In this thesis the Pareto optimization has been used to address design problems with multiple objectives. The method is described in the next sections.

### 3.3.1     Definition of a multi-objective optimization problem

In a multi-objective problem [24], rather than a single scalar objective function a vector of individual objective functions is used. This vector consists of all the single objective functions, as shown in (3.9):

$$\mathbf{f}(\mathbf{x}) = [f_1(\mathbf{x}), \cdots, f_m(\mathbf{x})]^T, \quad \mathbf{x} = [x_1, \cdots, x_n]^T \tag{3.9}$$

where $x_i$ is the $i$-th parameter to be optimized and $f_j$ is the $j$-th objective function. The vectors $\mathbf{f}$ and $\mathbf{x}$ are referred to as the objective vector and the decision vector, respectively.

## 3.3.2    Pareto Optimality

One of the methods for handling multiple objective optimization problems is to use the concept of Pareto optimality [75] – [79]. Without loss of generality the concept is presented for a minimization problem. A Pareto minimum is a decision vector ($\mathbf{x}$) that provides a compromised solution for which none of the corresponding sub-objectives can be further reduced without an increase in at least one of the other ones [24]; in other words $\mathbf{x}^*$ is a Pareto optimum if:

$$\begin{aligned} &\text{For any } \mathbf{x} \neq \mathbf{x}^*, \text{ if } f_i(\mathbf{x}) < f_i(\mathbf{x}^*) \\ &\text{then } f_j(\mathbf{x}) > f_j(\mathbf{x}^*) \text{ for at least one } j \neq i \end{aligned} \tag{3.10}$$

where $f_i(\mathbf{x})$ is an element of the decision vector in (3.9). A Pareto optimal set or a Pareto frontier is the set of all Pareto optima in the entire search space. Consider Figure 3.6, which is drawn for a problem with two sub-objectives $f_1(\mathbf{x})$ and $f_2(\mathbf{x})$. The figure shows different combinations of $f_1(\mathbf{x})$ and $f_2(\mathbf{x})$ resulting from all possible choices of the optimization parameters ($\mathbf{x}$). The space can be divided into two regions; one contains the feasible function pairs and the other where no point exists. The boundary between the two regions is the Pareto frontier. It is evident that any point on the frontier satisfies the

Pareto optimality condition given in (3.10). For example consider point 2, for which any further improvement in $f_1(\mathbf{x})$ results in a degradation in $f_2(\mathbf{x})$ (as the points on the left side of the Pareto frontier are not feasible); however, if one considers any of the interior points (i.e. one of the circles) $f_1(\mathbf{x})$ can be improved (by a horizontal move towards the Pareto frontier) without degrading the other objective function.
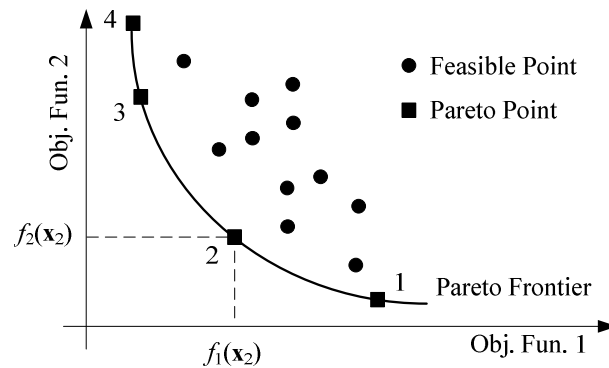


**Figure 3.6  Pareto optimality and Pareto frontier.**

There are several methods for obtaining the Pareto optimal set for a specific design [75] – [80]. A simple method for generating the Pareto frontier is to use the linear weights method. In this method, the multiple objectives are amalgamated into a single scalar objective function as shown in (3.11):

$$f(\mathbf{x}) = \sum_{i=1}^{i=m} w_i \cdot f_i(\mathbf{x}) \qquad \sum_{i=1}^{i=m} w_i = 1 \qquad\qquad (3.11)$$

This single function $f$ (note that $f$ is a scalar function of the decision vector $\mathbf{x}$) is optimized for a particular set of weights $W_n = \{w_{n1}, w_{n2}, \ldots\}$. It can be easily proved that the resulting optimum is also a Pareto optimum in the space of sub-objective functions (if not there should be at least one $f_i$ that can be improved without degrading the other sub-

objective functions, which is in contradiction with the fact that $f$ is at an optimum). Several optimizations are carried out with the weight-set spanning the space of possible weights. The values for the individual functions for each set of weights are plotted as a point in $m$-dimensional space in the form of a parametric plot.

Figure 3.6 show a Pareto frontier for an optimization problem with two sub-objectives. Any point on this frontier is a Pareto optimum. For example the point '2' gives the smallest value of $f_1$ (say $f_1(\mathbf{x}_2)$) that can be achieved when $f_2$ has the value of $f_2(\mathbf{x}_2)$, and vice versa. Therefore the Pareto frontier shows the tradeoffs involved in optimizing both sub-objectives. For example if the operating point is moved from point 1 to point 2 the first objective function can be improved significantly while the second objective function deteriorates to some extent; however if the operating point is at point 3 further improvement in $f_1(\mathbf{x})$ results in significant deterioration of the second objective function. Selecting a compromised set of parameters is an important step in many design studies involving multiple objectives, and the Pareto frontier helps the designer in properly selecting the operating parameters.

### 3.3.3    Generation of Pareto Frontier by Coupling to an EMT Simulator

The Pareto frontier algorithm was interfaced to the PSCAD/EMTDC electromagnetic transient simulation program; however, the approach is general and can be applied to other simulation programs as well. The Pareto frontier algorithm is shown schematically in Figure 3.7. It automatically performs a sequence of optimizations, each requiring several runs of the EMT simulation program.

Similar to the approach used for the single objective optimization, the method described in the previous section was successfully combined with the EMT simulation program. This approach allows the Pareto frontier to be developed for complex power system cases, where an explicit form of the sub-objective functions is not possible and they must be derived by observation of the simulation results.
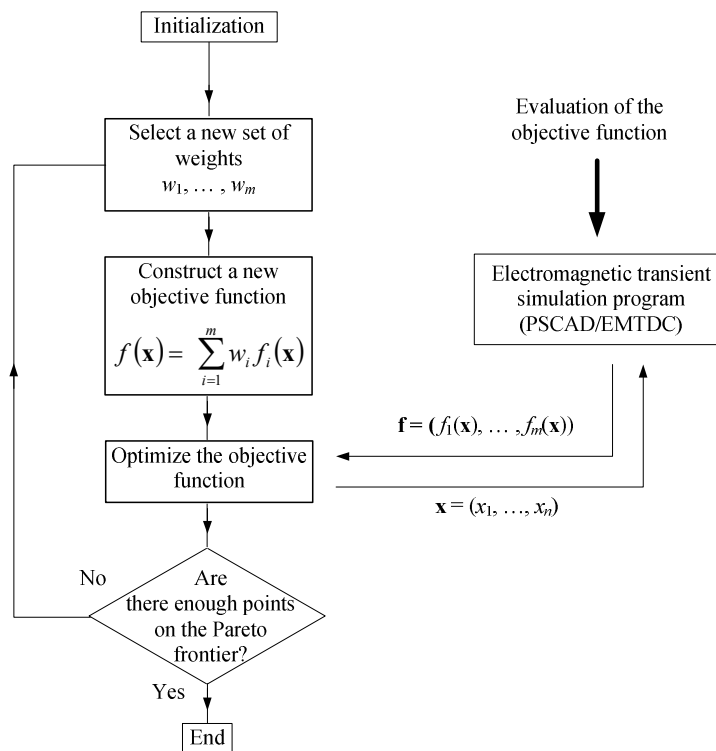


**Figure 3.7  Generation of the Pareto frontier**

In each of the optimizations the weights (gains) of the sub-objective functions are changed, so that a new point on the Pareto frontier is obtained. At the end the results are stored in a file, and they can be plotted as a Pareto frontier in an *m*-dimensional space. This method is able to generate the Pareto frontier with high efficiency because it reduces

the number of simulation runs as much as possible. The key to doing this is to use a sequential variation of the weights for subsequent optimizations that produces relatively continuous points on the Pareto frontier. By doing so, a previously obtained decision vector can be used as a suitable starting point, which usually generates the next point with only a small number of additional simulations.

# Chapter 4  Application Examples of Simulation-Based Optimization

In this chapter a number of power system and power electronic design examples are used to show the effectiveness of the developed simulation-based optimization methods. Development of an analytical objective function for the examples presented is prohibitively difficult; therefore a simulation-based design approach becomes necessary. This closely resembles the situation in the majority of practical design cases as well.

## 4.1     Optimal Design of a Static Compensator

In this example the developed optimization tool is used to improve the response of a three-level Static Compensator (STATCOM) during a power network transient. Parameters of the control system, i.e. its proportional gains and integral time constants, are optimally tuned. This example demonstrates the effectiveness of the developed tools as for this case an analytical formulation of the objective function is practically unattainable. The example also presents an application of the Pareto optimality concept in the analysis of the tradeoffs between cost and performance considering the size of the dc-side capacitor. The concept of Pareto optimality is used for selecting a suitable dc capacitor size to make a reasonable compromise between the cost and performance of the STATCOM.

## 4.1.1    Description of the System Model

A STATCOM is a FACTS (Flexible Alternating Current Transmission System) device, which is mainly used for fast VAR compensation and voltage regulation in power networks [91]. In addition a STATCOM may also be used for other purposes such as voltage balancing [92] and oscillation damping [93]. in power networks. A typical structure of a STATCOM is shown in Figure 4.1. It consists of a voltage sourced converter (VSC) connected to a capacitor on the dc side and to the power network (through a power transformer) on the ac side. By controlling the magnitude and phase of the STATCOM output voltages (the three-phase ac voltages), the STATCOM is able to exchange different amounts of real and reactive power with the ac network. The real and reactive power control is mainly used for voltage regulation of the dc capacitor and the ac network [94] and [95]; however, it can also be used for other purposes such as oscillation damping [93].

Figure 4.1 also shows the schematic diagram of the ac network used in this example. The data pertinent to the network are given in Table 4.1. The STATCOM uses a three-level voltage sourced converter with sinusoidal pulse-width modulation (SPWM) as shown in Figure 4.2. The three-level converter operates on the same concepts as the two-level converter, (a brief explanation of a two-level VSC is presented in section 6.1.3); however, the extra switches used allow a three-level converter to produce an additional voltage level of 0V at the output terminal. This extra voltage level can be leveraged to craft voltage waveforms with improved harmonic spectrum without increasing the switching losses.
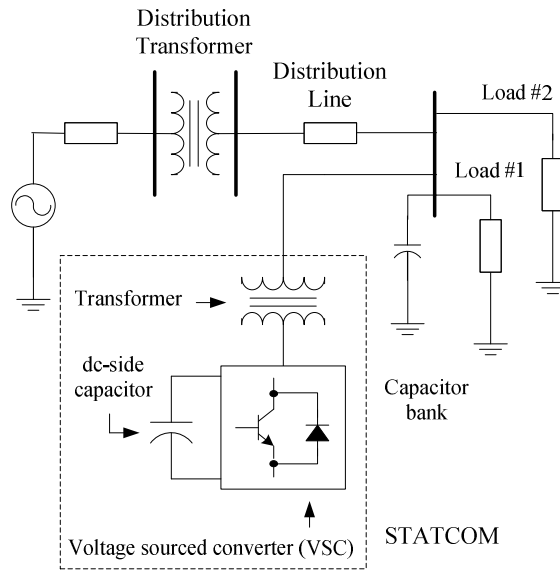
**Figure 4.1 STATCOM system**

**Table 4.1 System parameters**

| AC network | 115 kV, SCMVA = 500 MVA at 80º |
|---|---|
| Distribution transformer | 115 kV / 20 kV, 30 MVA, $X_l$ = 10% |
| Distribution line | Resistance = 0.04 pu, Reactance = 0.10 pu |
| Load #1 | 10.0 MVA, pf = 0.9 lagging |
| Load #2 | 10.0 MVA, pf = 0.85 lagging |
| STATCOM converter | 3.3 kV, 10 MVA, $C$ = 0.5 pu |
| STATCOM transformer | 20 kV/3.3 kV, 10 MVA, $X_l$ = 14% |
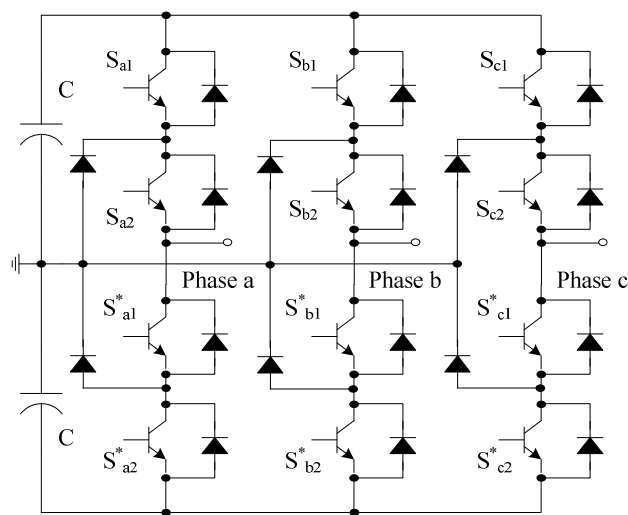


**Figure 4.2 The three-level diode clamped converter used in the STATCOM**

Gate pulses for the upper ($S$) and lower ($S^*$) half-bridges are generated by comparing a sinusoidal reference waveform with two triangular waveforms (carriers) as shown in Figure 4.3 [96]. When the reference waveform (the sinusoid) is higher than both carriers (the triangular waveforms), both $S_{x1}$ and $S_{x2}$ ($x$ is a, b or c depending on the phase) switches are ON, which results in a voltage $+V_{dc}$ at the output. When the reference lies between the two triangular waves, $S_{x1}$ is OFF but $S_{x2}$ is ON, which results in 0V at the output. Finally when the reference wave is lower than both triangular waves, $S_{x1}$ and $S_{x2}$ are both OFF, which results in a voltage level $-V_{dc}$ at the output. Note that $S_{xx}$ ($xx$ is a1, a2, b1, b2, c1, or c2) switches are complementary switches for $S^*_{xx}$ switches, which means if $S_{xx}$ is ON, $S^*_{xx}$ is OFF, and if it is OFF, $S^*_{xx}$ is ON.
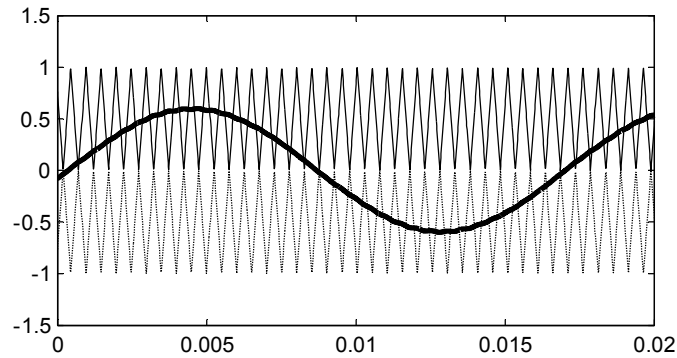


**Figure 4.3 .  Generation of the gate signals.**

Control of the dc-bus voltage and the ac network voltage is conducted through a de-coupled control system [94], [95] as shown by the dotted enclosure in Figure 4.4. This controller regulates the direct (d) and quadrature (q) components of the STATCOM current to their desired reference values $i_d^*$ and $i_q^*$ (indirectly controlling the real and reactive power delivered to the network).
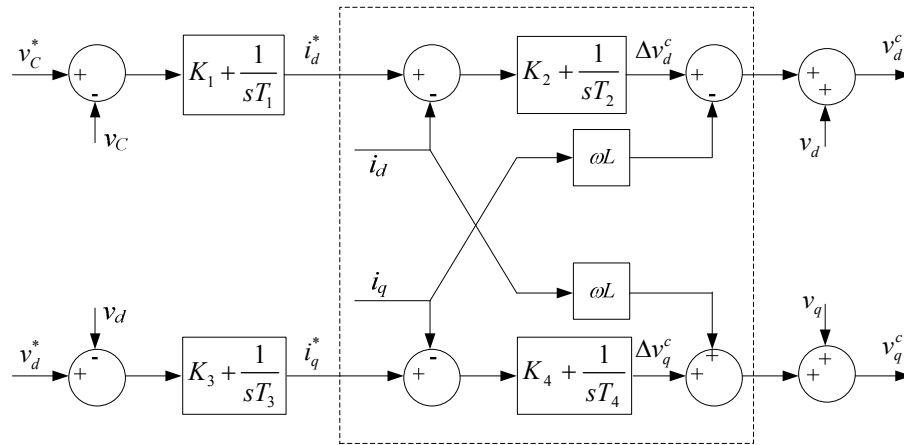
**Figure 4.4  STATCOM de-coupled control scheme**

A synchronously rotating reference frame is locked to the positive sequence of the load bus-bar voltage. Hence in the steady-state $v_d = V_m$ and $v_q = 0$, where $V_m$ is the peak of the phase voltage. The q-axis current order $i_q*$ (indirectly the generated reactive power) for the decoupled controller is generated by an upstream proportional-integral (PI) controller that regulates the terminal voltage $v_d$ to its reference value $v_d*$. Another controller generates the direct axis current order (indirectly the generated real power) to charge or discharge the capacitor so as to regulate its voltage $v_d$ to the desired reference capacitor voltage $v_C*$.

The STATCOM generates harmonic voltages, as is typical for switched power-electronic equipment. In order to reduce harmonic-related contamination of the controller's input signals a set of signal conditioning filters are normally used prior to the controller inputs. In this example first order low-pass filters, as shown in Figure 4.5, are used for this purpose.
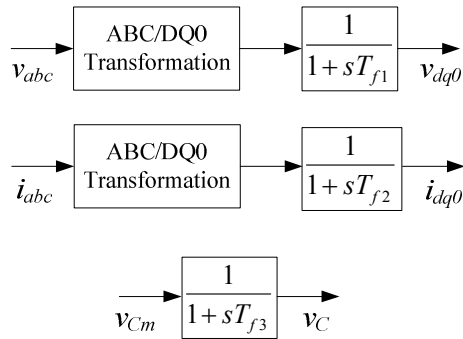
**Figure 4.5  Input filters for the STATCOM**

## 4.1.2     Optimization of the STATCOM Dynamic Response

This section demonstrates the application of the developed optimization methods for designing the STATCOM. At first the transient performance of the STATCOM is optimized by selecting proper control system settings using the optimization method described before. Such optimization is useful if the STATCOM already exists and it is desired to improve its performance.

On the other hand, if the STATCOM has not yet been constructed, further flexibility is possible in the design stage because in addition to the control settings, the selection of the hardware components can also be part of the performance and cost optimization. To demonstrate this aspect, the dc-capacitor size is next included as an optimization variable in the second stage of this example. This added flexibility of an additional optimizable component provides the potential for improving the performance; however, changing the capacitor size also affects the cost of the STATCOM. Therefore having a small capacitor size can be considered as another objective for this problem. The developed Pareto optimality technique is used to study the tradeoffs between the capacitor size and the dynamic performance of the compesator.

## 4.1.2.1 Single Objective Optimization

The developed gradient-based optimization can be used to select parameters (gains and time constants) for the control system of the STATCOM in order to improve its transient performance. This section demonstrates the effectiveness of the proposed simulation-based approach, as in this case an analytical solution is prohibitively difficult to obtain. The objective function (4.1), which is a function of the controller parameters shown in Figure 4.4, is used. It penalizes the deviations in the capacitor voltage $v_C$ and ac network voltage $v_d$ from their respective set-points devoted by $V_C^*$ and $V_d^*$ respectively.

$$f_p(\mathbf{x}) = 1000 \int_{t_s}^{t_e} \frac{\left| v_d - V_d^* \right|}{V_d^*} dt + 200 \int_{t_s}^{t_e} \frac{\left| v_C - V_C^* \right|}{V_C^*} dt$$

$$\mathbf{x} = \left[ K_1, T_1, K_2, T_2, K_3, T_3, K_4, T_4, T_{f1}, T_{f2}, T_{f3} \right]^T$$

(4.1)

Note that this objective function (OF) penalizes both poor transient response as well as steady state ripple due to harmonics; as in either case, there will be non-zero deviations. Also because the control of the ac voltage is the principal purpose of the STATCOM, more weighting is given to the ac network voltage deviation. Although the relative weights were pre-selected here, the procedure of Pareto optimization to follow in the next section could have also been employed in their selection. The objective function (OF) in (4.1) is minimized using the procedure described in Chapter 3 to yield the optimal parameter values.

In this example, the STATCOM in Figure 4.1 is subjected to a load rejection (in this case load #1) at $t = 1.0$ s with a subsequent reconnection of the load at $t = 1.5$ s. The OF is evaluated over the interval $[t_s, t_e] = [0.75s, 1.75s]$. Table 4.2 shows the pre- and

post-optimization values of the control system parameters. Note that the optimization process reduces the OF from a large value of 27.8 to a significantly reduced value of 10.1. The performance improvement is clear from the pre- and post-optimization plots for the capacitor voltage (Figure 4.6) and network voltage (Figure 4.7).

**Table 4.2  Pre- and post-optimization values**

|  |  | Before optimization | After optimization |
|---|---|---|---|
| DC-capacitor voltage controller | $K_1$ | 0.1 | 0.17 |
|  | $T_1$ | 0.15 | 0.13 |
| $i_d$ controller | $K_2$ | 3.0 | 1.8 |
|  | $T_2$ | $0.2\times10^{-2}$ | $0.40\times10^{-2}$ |
| Network voltage controller | $K_3$ | $0.2\times10^{-1}$ | $0.40\times10^{-1}$ |
|  | $T_3$ | $0.2\times10^{-1}$ | $0.32\times10^{-1}$ |
| $i_q$ controller | $K_4$ | 5.0 | 17.3 |
|  | $T_4$ | $0.1\times10^{-2}$ | $0.57\times10^{-3}$ |
| Filter time constants | $T_{f1}$ | $0.1\times10^{-1}$ | $0.47\times10^{-2}$ |
|  | $T_{f2}$ | $0.1\times10^{-2}$ | $0.32\times10^{-3}$ |
|  | $T_{f3}$ | $0.1\times10^{-1}$ | $0.80\times10^{-2}$ |
| Objective function |  | 27.8 | 10.1 |
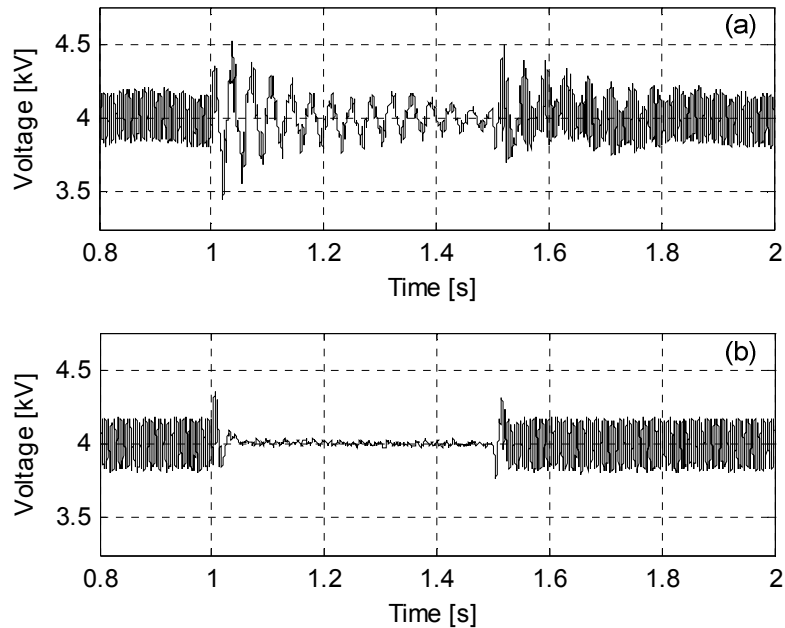


**Figure 4.6  DC capacitor voltage before (a) and after (b) optimization**
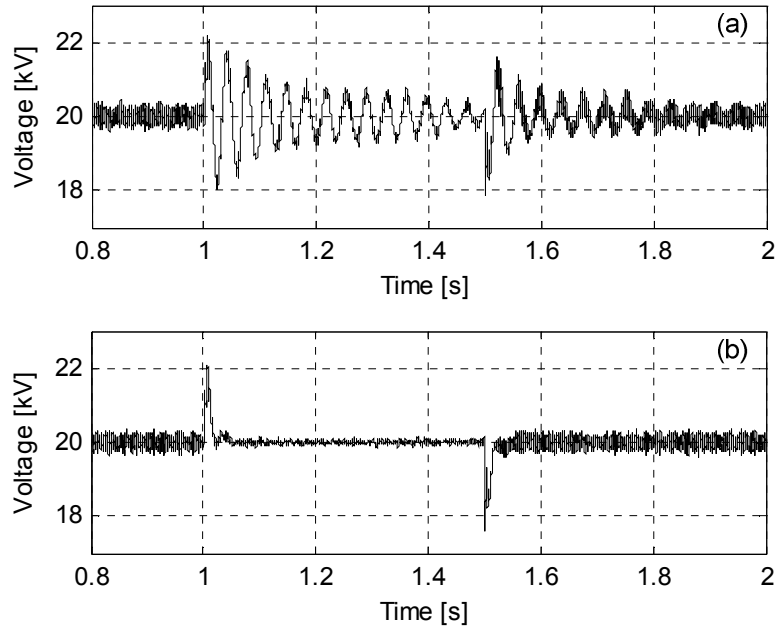
**Figure 4.7  Network voltage before (a) and after (b) optimization**
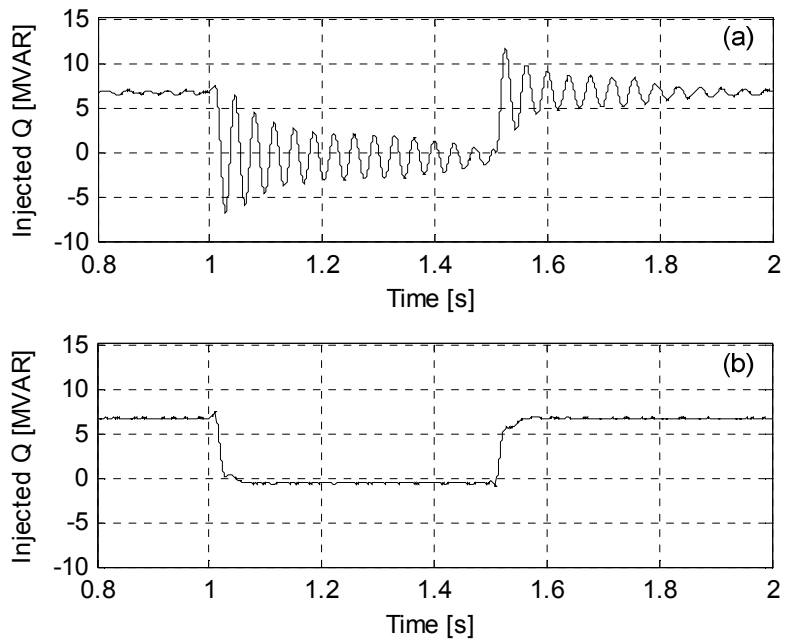


**Figure 4.8  Injected reactive power before (a) and after (b) optimization**

Note that the capacitor voltage transients damp much faster and with less overshoot after optimization. The optimized network voltage ($v_d$) also shows significant improvements both during the disturbance and after it. In addition, the injected reactive power waveform for initial and optimized parameters is shown in Figure 4.8 where the improvement of response is clearly visible.

## 4.1.2.2    Comparison of Non-Linear Simplex (Nelder-Mead) and Gradient Based Optimization

As was mentioned in Chapter 3, earlier wisdom was that gradient-based methods would be too slow when combined with EMT simulation, because of the considerable effort involved in calculating the derivative. However, the total number of steps to convergence may be significantly reduced, resulting in a total simulation time which is not significantly different from that of the direct method.
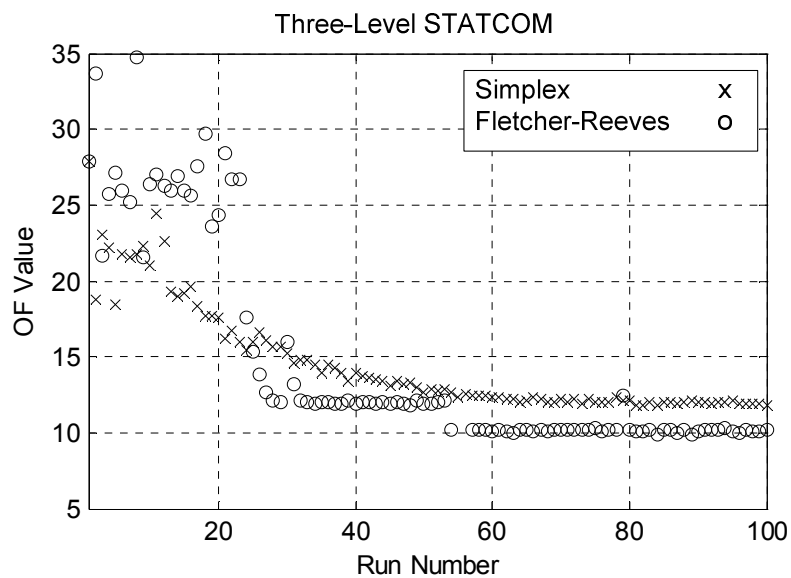


**Figure 4.9  Convergence rate comparison**

**The simplex method of Nelder-Mead vs. the Fletcher-Reeves method**

Figure 4.9 shows the optimization progress (in terms of the OF evaluations vs. run number) of the same case using both the Nelder-Mead and the Fletcher-Reeves methods. Although the gradient-based method requires 22 simulations to calculate the gradient vector, still due its faster convergence rate, both methods converge to the optimum at about the same time. Also it should be noted that with parallel computers, the gradient based approach would have a much better advantage as each partial derivative can be computed using a different processor. The above optimization process takes approximately 33min (Using a computer with 4GB of RAM and a 3GHz AMD Athlon™ 64 X2 Dual Core Processor).

## 4.1.2.3    Multi-Objective Optimization

The optimization case in the previous section considered only the control system parameters, and their tuning for optimal performance. This section includes the additional parameter of the dc-capacitor size in the optimization. Although changes in the control settings are easy and inexpensive to implement, changes in the size of the dc-capacitor have an additional financial implication. It is therefore necessary to evaluate the trade-off between the capacitor size (or cost) and system performance in order to determine the smallest capacitor size that will also yield acceptable performance.

The Pareto frontier discussed in Chapter 3 provides a useful visualization of the tradeoffs involved for multiple objectives. The Pareto optimization tool developed in this thesis automatically generates the Pareto frontier when supplied with a single OF, which

is derived by a weighted sum of the sub-objectives. For the problem at hand, the vector of sub-objectives is expressed in (4.2), where $\mathbf{x}$ and $f_p$ are as defined in (4.3) and $C_{pu}$ is the capacitor size in pu. The Pareto optimization method outputs the frontier shown in Figure 4.10.

$$\mathbf{f}\left(\mathbf{x}, C_{pu}\right) = \left[f_p, C_{pu}\right]^T \tag{4.2}$$

$$f\left(\mathbf{x}, C_{pu}\right) = wf_p + (1-w)C_{pu}; \quad w \in [0,1] \tag{4.3}$$
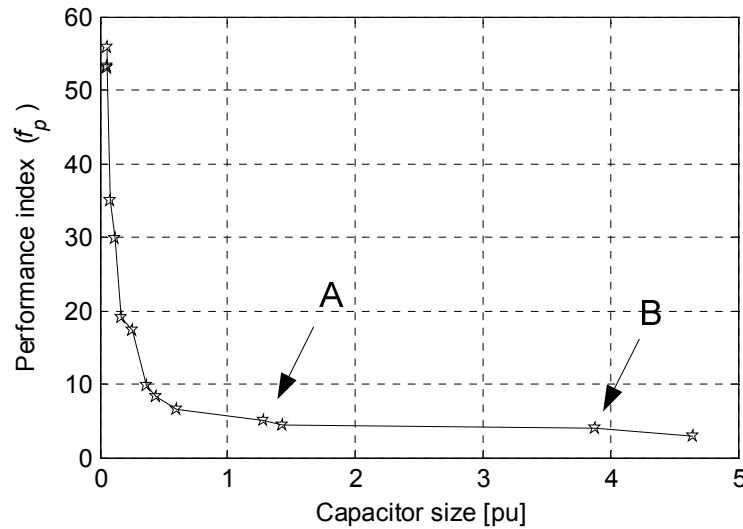


**Figure 4.10  Pareto frontier of the dc capacitor size and the performance**

The Pareto frontier is developed by conducting a sequence of optimizations for several values of the relative weight $w$. For each optimization, the corresponding sub-objective values are plotted against each other. For this example, the two sub-objectives are the performance index $f_p$ and the capacitor size $C_{pu}$. The Pareto frontier in Figure 4.10 indicates that the performance can be optimized by selecting increasing values of $C_{pu}$;

however, once the capacitor size reaches approximately 0.75 pu, performance improvement is marginal. For example, at point 'A' on the diagram the capacitor value is 1.3 pu, with a performance index of $f_p$ = 5.0. To improve the performance by an additional 20% ($f_p$ = 4.0), the capacitor size must be increased by almost 300% corresponding to point 'B' where $C_{pu}$ = 3.9 pu. Rather than try to optimize the performance any further, thereby increasing the size (and hence cost) of the capacitor, the designer may choose to select a capacitor size in the neighbourhood of 0.75 pu.



**(a) $C$ = 0.17pu**



**(b) $C$ = 0.36pu**
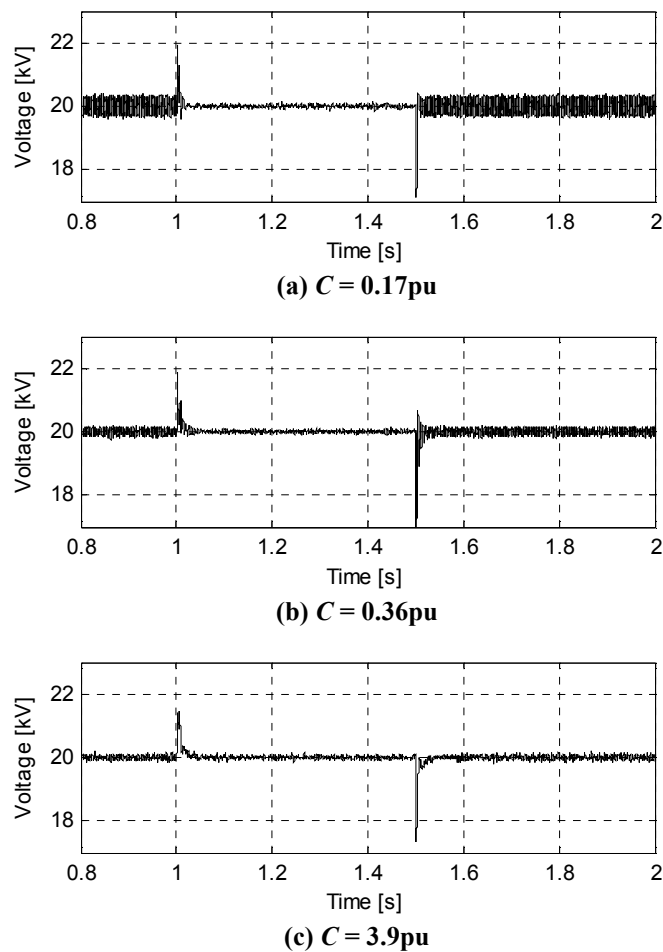


**(c) $C$ = 3.9pu**

**Figure 4.11  STATCOM performance for different values of the dc capacitor**

Figure 4.11 shows the network voltage when the size of the dc capacitor is (a) 0.17 pu (b) 0.36 pu and (c) 3.9 pu. As it can be seen in the results when the capacitor size increases from 0.17 pu to 0.36 pu the steady state ripple on the network voltage considerably reduces by almost 50%. However, further increase in the size of the dc capacitor (from 0.36 pu in Figure 4.11b to 3.9 pu in Figure 4.11c) does not improve the response significantly. The above waveforms confirm the results obtained from the Pareto analysis. Note that as the injected reactive power from $t = 1$s to $t = 1.5$s is almost zero during this period the ripple is very small and the same for all the above cases.

## 4.2    Multi-Objective Optimal Design for an Induction Motor Drive System

In this example the simulation-based Pareto optimization method is used for the multi-objective optimal design of an induction motor drive system. Using this approach, an optimal set of system parameters is selected, which achieves a reasonable trade-off between two competing objectives: (i) a low steady state ripple and (ii) a fast transient response in the developed electrical torque. As opposed to the previously shown STATCOM case, in which the competing objectives were cost versus performance, in this example the competing objectives are two different aspects of the system's dynamic performance.

## 4.2.1        Description of the Drive System

Induction motors are perhaps the most widely used type of electric machinery. In many installations, torque and speed control of these machines is achieved by utilizing a variable frequency drive systems, such as the one shown in Figure 4.12.  The induction motor is driven by a voltage sourced converter (VSC), and by changing the magnitude and frequency of the output voltage of the VSC, the desired speed and torque can be obtained. The DC voltage required by the VSC is produced by a three-phase controlled rectifier.
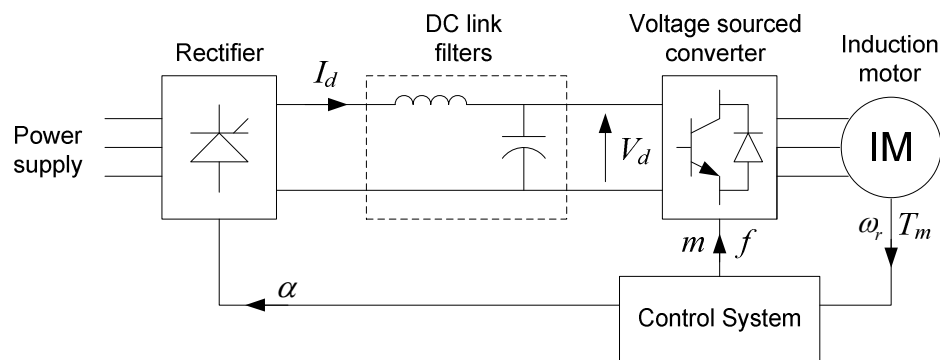


**Figure 4.12  A variable frequency induction motor drive system**

In this example a controlled six-pulse rectifier and a two-level VSC with sinusoidal PWM have been used for the drive system. The control system uses a constant slip-speed control strategy to regulate the output torque of the induction machine. In this strategy, the frequency of the VSC is changed so that the motor always has a constant slip. This way by changing the magnitude of the voltage, the output torque of the motor can be controlled. Figure 4.13 shows the schematic diagram of the control system.
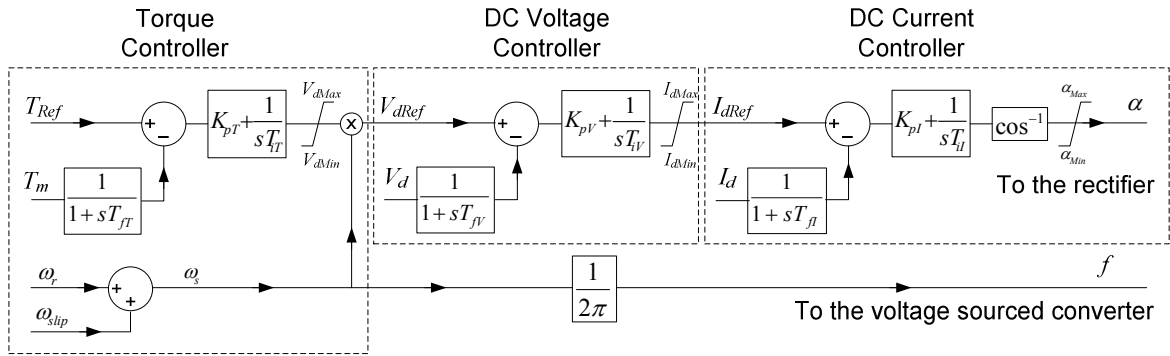
**Figure 4.13  Constant slip speed control strategy**

As in this specific case the magnitude of the output voltage is controlled by changing the dc voltage, a constant modulation index ($m$), adjusted to 1.0, is used for all operating conditions. Controlling the output voltage by changing the dc voltage reduces the switching losses at low speeds, as lower voltage means less switching losses. The parameters of the drive system are given in Table 4.3.

**Table 4.3  Drive system parameters**

|  |  | Rated Values |
|---|---|---|
|  | Voltage | 4160V |
|  | VA | 1.045MVA |
| Induction Motor | Current | 145A |
|  | Frequency | 60Hz |
|  | Speed | 3600rpm |
| Voltage Sourced Converter | Switching Frequency | 10kHz |
| Rectifier | Number of Pulses | 6 |
|  | Voltage | 5.6kV |
| Input AC Network | Frequency | 60Hz |
|  | Impedance | $0.96\Omega\angle78°$ at 60Hz |

## 4.2.2    Optimization of the System Performance Using the Pareto Approach

The drive system should be optimized so that the ripple on the dc voltage and dc current is reduced. Doing so reduces the voltage harmonics at the output of the VSC, the

current harmonics at the input of the rectifier and the ripple current in the dc capacitor. This requires proper selection of the control system parameters as well as the filter elements (smoothing inductor and dc capacitor). However, improving the filtering performance typically requires the use of larger energy storage elements, and consequently degrades transient performance. Therefore it is necessary to find optimal values for the system parameters, which result in an acceptable compromise between the competing objectives of fast transient response and low ripple level.

As the output torque of the induction motor is regulated by the controller, the torque order (the reference torque) is changed at $t = 4.0$s and $t = 6.0$s, so that the transient response of the control system can be measured. In order to quantify both aspects of the system performance, the objective functions shown in (4.4) have been defined to assess transient and steady state performance of the system.

$$
\begin{aligned}
f_{SS} = 10000 \times \Bigg( & \int_{t=3.75}^{t=3.95} \left( \frac{i_d - i_d^*}{0.16} \right)^2 dt + \int_{t=5.75}^{t=5.95} \left( \frac{i_d - i_d^*}{0.16} \right)^2 dt + \int_{t=7.75}^{t=7.95} \left( \frac{i_d - i_d^*}{0.16} \right)^2 dt \\
& + \int_{t=3.75}^{t=3.95} \left( \frac{v_d - v_d^*}{6.785} \right)^2 dt + \int_{t=5.75}^{t=5.95} \left( \frac{v_d - v_d^*}{6.785} \right)^2 dt + \int_{t=7.75}^{t=7.95} \left( \frac{v_d - v_d^*}{6.785} \right)^2 dt \Bigg)
\end{aligned}
$$
(4.4)

$$
f_{Tr} = 100 \times \Bigg( \int_{t=3.8}^{t=4.8} \left( \frac{T_m - T_m^*}{0.9} \right)^2 \cdot w_t(t) \cdot dt + \int_{t=5.8}^{t=6.8} \left( \frac{T_m - T_m^*}{0.9} \right)^2 \cdot w_t(t) \cdot dt \Bigg)
$$
(4.5)

In equations (4.5) and (4.5), variables $i_d$, $v_d$ and $T_m$ are the dc current, dc voltage, and mechanical output torque. The objective function $f_{SS}$ penalizes the ripple in steady state. by measuring the steady state integral of the squared error. The selection of the

integration limits avoids the region where step changes are applied, so that the function only reflects the steady state performance. The objective function $f_{Tr}$ penalizes a slow transient response and penalizes any discrepancy between ordered and measured torque. Weighting function $w_t$ discounts the immediate instants at which the reference changes (i.e. at $t = 4.0$s and $t = 6.0$s). Weighting function $w_t$ is shown in the following figure.
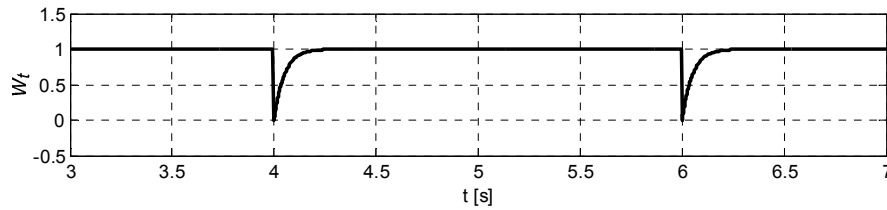


**Figure 4.14** $f_t$ **function which has been used in the objective function**

The parameter space in this problem consists of nine parameters of the control system ($T_{fT_2}$, $K_{pT}$, $T_{iT}$, $T_{fV_2}$, $K_{pV}$, $T_{iV}$, $T_{fI_2}$, $K_{pI}$, $T_{iI}$) and 2 parameters of the power circuit ($L_{dc}$ and $C_{dc}$). The two-objective optimization has been carried out using the developed Pareto optimization method, with the objective functions defined in (4.4) and (4.5). The following figure shows the Pareto frontier of the objective functions.
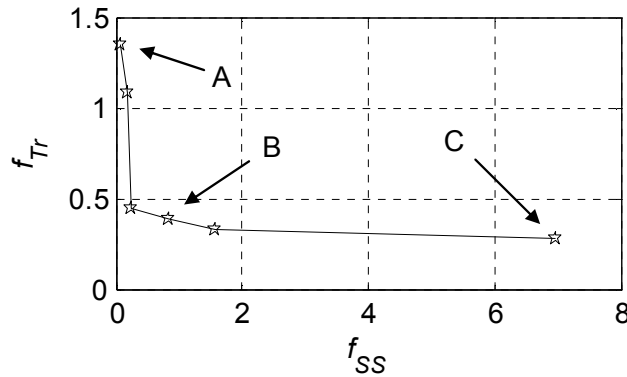


**Figure 4.15  Pareto frontier of the drive system**

Development of this frontier takes about 25 hours (Using a computer with 4GB of RAM and a 3GHz AMD Athlon™ 64 X2 Dual Core Processor). As seen in the figure, improvements in the transient response (lower $f_{Tr}$) results in increased steady state ripple (higher $f_{SS}$). The following figures show the response of the system for two extreme points on the Pareto frontier (i.e. A and C).
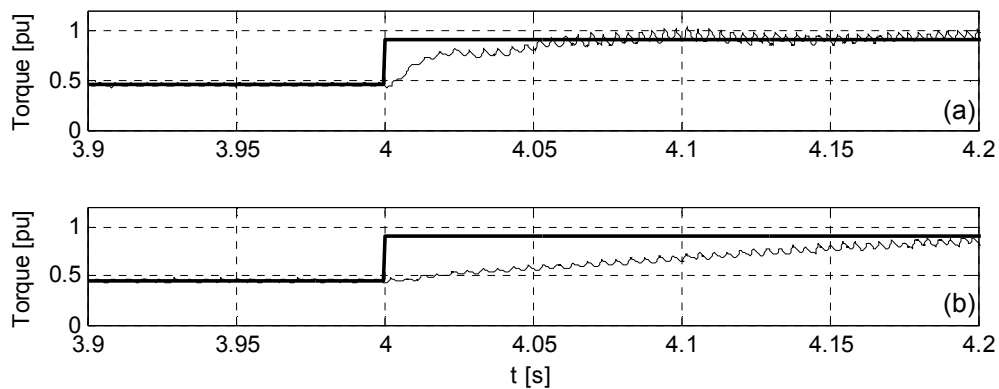


**Figure 4.16  System response to torque order change (a) point A (b) point C**
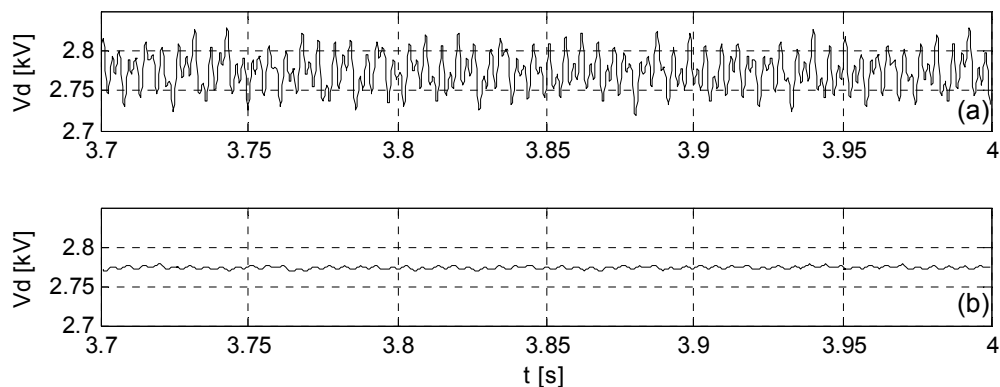


**Figure 4.17  Steady state ripple on the dc voltage (a) point A (b) point C**
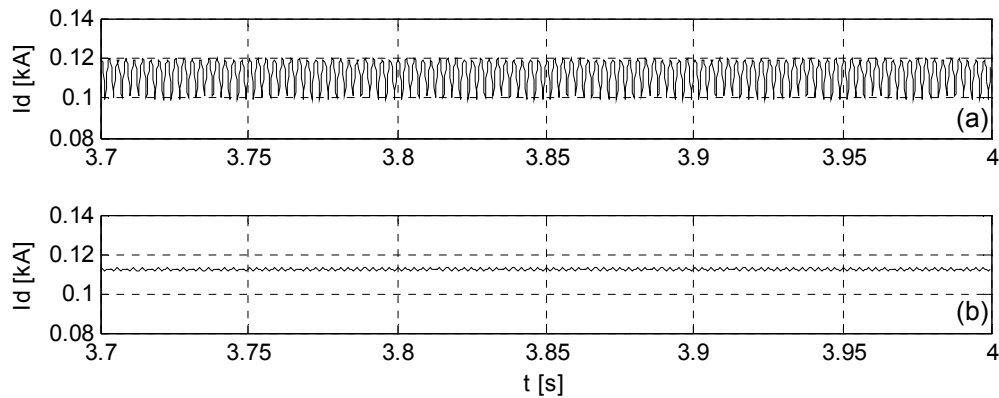
**Figure 4.18  Steady state ripple on the dc current (a) point A (b) point C**

As seen in Figure 4.16 to Figure 4.18, although operating point A results in a much faster

transient response Figure 4.16 (a), the amount of ripple at this point is high. On the other

hand at point C the dc voltage and current are relatively smooth Figure 4.17 (b) and

Figure 4.18 (b). However, this results in a slower transient response Figure 4.16 (b).

Finally point B, which is at the middle of the Pareto frontier, results in a response that is

both fast and smooth. The system response at point B is shown in Figure 4.19 and Figure

4.20.
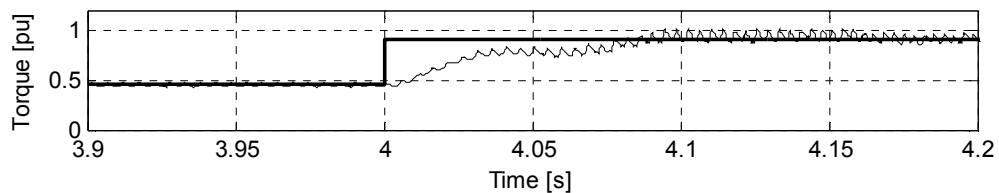


**Figure 4.19  System response to torque order change at the operating point B**
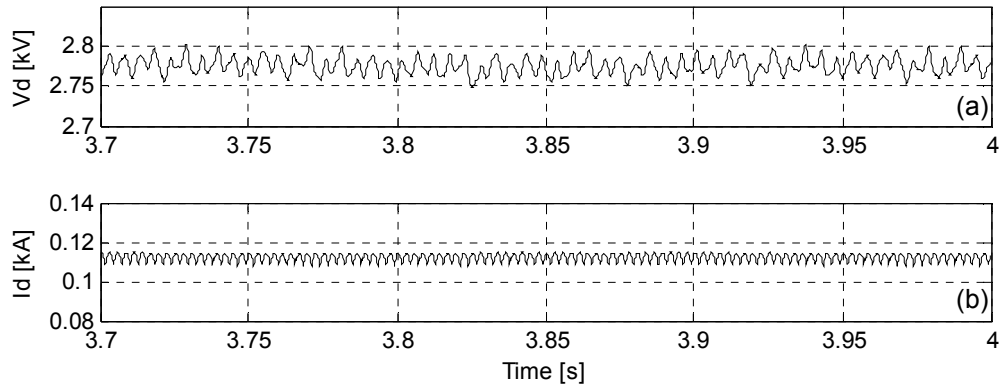
**Figure 4.20  Steady state ripple on the (a) dc voltage and (b) dc current**

Table 4.4 shows the parameter values of the drive system for each of the three operating points. As it can be seen in the table operating point B shows a compromised performance compared to the other points.

**Table 4.4  Parameter values of the drive system for three different Pareto optimums**

|          | A       | B      | C      |
|----------|---------|--------|--------|
| $T_{fT}$ | 0.0285  | 0.0224 | 0.0217 |
| $K_{pT}$ | 1.22    | 0.174  | 0.304  |
| $T_{iT}$ | 0.255   | 0.0493 | 0.0445 |
| $T_{fV}$ | 0.00870 | 0.0341 | 0.0344 |
| $K_{pV}$ | 0.871   | 0.661  | 0.570  |
| $T_{iV}$ | 0.0504  | 0.0270 | 0.0187 |
| $T_{fI}$ | 0.00712 | 0.0304 | 0.0320 |
| $K_{pI}$ | 2.82    | 2.87   | 1.89   |
| $T_{iI}$ | 0.268   | 0.417  | 0.350  |
| $L_{dc}$ [mH] | 1670 | 391    | 120    |
| $C_{dc}$ [µF] | 3510 | 624    | 401    |
| $f_{Tr}$ | 1.34    | 0.386  | 0.274  |
| $f_{SS}$ | 0.0703  | 0.740  | 6.99   |

Note that every point on the Pareto frontier is an optimal solution of the problem for a specific set of relative weights for each of the sub-objective functions. The Pareto frontier shows the tradeoffs between the objectives as the relative weights are varied. It is the

designer's responsibility to select a suitable point on the frontier, which satisfies the multiple objectives to a degree deemed adequate by the designer. Based on this rather subjective choice, point B appears to be a reasonable tradeoff, as midway between two directions of diminishing return. However, if there were a strong requirement for transient performance (for example $f_{Tr} <= 0.3$), point B would be unacceptable, and the most acceptable point would be point C.

# Chapter 5  Simulation-Based Uncertainty Analysis for Design

Due to practical limitations such as manufacturing tolerances and component aging the parameter values in the physical implementation of a system may not be identical to those originally obtained through optimization or otherwise decided by the designer. In addition imprecise knowledge of the system (e.g. measurement errors) increases the level of uncertainty in the design. In order to quantify the potential degradation in performance resulting from such parameter variations and to ensure that the system performance remains satisfactory in the presence of uncertainties, it is essential to perform uncertainty analysis of the design.

This thesis proposes to use a set of simulation-based facilities to automate the uncertainty analysis process and to reduce the human interactions in such studies. Similar to the simulation-based optimization method described in the previous chapters, simulation-based uncertainty analysis also alleviates the need for analytical calculations by using an electromagnetic transient simulation program as an evaluator of system performance under different scenarios.

## 5.1     Definitions

Uncertainty analysis has a long history in engineering applications, and a wide variety of methods exist for such studies. However, existing literature on uncertainty

analysis does not use a common terminology for various concepts. In the following, necessary terms and definitions are outlined as they are used in the context of this thesis.

## 5.1.1       Definition of Performance index

A performance index (also called performance function [39] or response variable [49]) is a mathematical function of the system outputs, which quantifies certain aspects of design performance. For uncertainty analysis of a system a number of different performance indices are usually defined to cover different aspects of the design. A performance index may for example measure the amount of remnant harmonics in a filter subject to component aging, or the changes in the overshoot of a control system step response due to the variations in the system operating conditions.

## 5.1.2       Definition of Sensitivity analysis

Sensitivity analysis is a mapping that relates small changes in the system input parameters to the changes in the performance index. This is equivalent to developing a simplified or "surrogate" model of the system that relates the performance index to its input parameters. Since analytical development of a full model that is accurate in the entire range of system parameters is difficult, several alternative methods are used for such analysis. The most common one of those methods is first-order (linear) approximation of the performance indices around an operating point. Use of more complex methods for sensitivity analysis has also been reported in the literature [39], [48], [49], [51], and [59]. These methods in general enhance the accuracy of the analysis;

however, the added complexity increases the required computation time for such methods.

### 5.1.3      Definition of Tolerance Analysis

In tolerance analysis, the variation of the performance index is estimated from a known spread in the input parameter values of the system. This is done to ensure that the input parameter tolerances will not cause the performance index to lie out of its acceptable range. In many cases, the result of tolerance analysis is the probability distribution of the performance index or even simply its worst-case value. Once sensitivity-based surrogate models are obtained, tolerance analysis can be done using these models [49]. It should be noted that the sensitivity-based approach is not the only solution to the tolerance analysis problem, and other approaches such as direct Monte-Carlo analysis [81] and interval mathematics [55] can also be used to address this problem.

## 5.2      Uncertainty Analysis Background

Uncertainty analysis covers a wide range of studies; however, based on the literature, such studies can be divided into two major categories of (1) sensitivity analysis and (2) tolerance analysis. As mentioned before, sensitivity analysis is performed to develop models (often simple ones) that relate performance indices to the input parameters of a system. These simple models can then be used for optimization and/or

tolerance analysis of the system, when computational power or time constraints do not allow use of full-detailed system models.

Tolerance analysis is also used for estimation of the system performance under uncertainties. However, as opposed to sensitivity analysis, tolerance analysis is not meant to relate each set of input parameters to a specific set of performance indices. It rather aims to solve the problem as a whole, and in this analysis the goal is to find a boundary for the system response when the input parameters vary within their tolerance ranges. There are two major classes of tolerance analysis problems, namely (a) worst-case tolerance analysis and (b) statistical tolerance analysis. In worst-case tolerance analysis an extreme limit is found for each performance index, in such a way that the performance index never passes that limit when the system parameters are within their tolerance ranges. Rather than a single limit, statistical tolerance analysis provides probabilistic information about the performance indices. Using this type of analysis the designer can estimate the probability of having different performance levels.

The thesis introduces a simulation-based sensitivity analysis scheme, which allows modeling of performance indices using a second-order Taylor's series. This not only increases the accuracy of analysis for regular operating points (compared to the conventional first-order sensitivity analysis), but also allows sensitivity analysis of optimal operating points, where the first-order analysis fails to provide useful results, due to vanishing first-order derivatives. In addition, the thesis proposes to use the sensitivity models to perform tolerance analysis (as defined above). As will be discussed later, using

sensitivity models for tolerance analysis significantly reduces the computational burden of the analysis while still providing accurate results.

## 5.3      Simulation-Based Sensitivity Analysis

In this section the sensitivity analysis problem is described and different stages of development of a simulation-based sensitivity analysis facility are discussed. Initially a brief background on sensitivity analysis is presented, and then the concept of simulation-based sensitivity analysis is introduced. The section also discusses different stages of developing the proposed sensitivity analysis facility and explains the implementation details of this method.

### 5.3.1      Background

Sensitivity analysis of linear circuits was perhaps one of the first efforts in the area of sensitivity analysis of electrical systems [12]. In its simplest form, the sensitivity of a performance index (normally a network function) to the variations of the system parameters can be represented as a linear function. The well-known Bode logarithmic sensitivity function (shown in 5.1) is a commonly used form of sensitivity analysis for electrical networks [12].

$$S_x^T = \lim_{\Delta x \to 0} \frac{\Delta T / T}{\Delta x / x} = \frac{x}{T} \frac{\partial T}{\partial x} = \frac{\partial \ln(T)}{\partial \ln(x)} \tag{5.1}$$

In the above expression $T$ is a network function (the performance index) and $x$ is a network parameter. Using such a simple formulation allows the designer to easily

approximate the relative variation in the network function $T$ resulting from small relative

changes in the system parameter $x$, as shown in equation (5.2):

$$\frac{\Delta T}{T} = S_x^T \frac{\Delta x}{x}$$                                                                     (5.2)

Such sensitivity models were originally derived analytically by developing a

closed-form equation relating the output (performance index) to the inputs, and by

analytical calculation of derivatives (5.1). However, for large and complex systems,

which are usually analyzed thorough computer simulation, sensitivity analysis using

closed-form formulation of performance indices becomes impossible as formulation of

the problem is prohibitively difficult. Therefore, computer-aided techniques were

developed for such studies and simulation programs were utilized for the purpose of

sensitivity analysis [28] – [35]. This trend was accelerated by the development automatic

design tools for linear electronic circuits. In these tools gradient-based optimization

techniques were used for parameter tuning of analog electronic circuits. Since gradient-

based optimization methods rely on sensitivity information (gradients) of their objective

function, significant amount of research was dedicated to development of computer-aided

sensitivity analysis methods, which were capable of fast calculation of the required

sensitivity information [29], [33], and [34].

Researchers also found sensitivity information useful in tolerance analysis of

different systems, as using the sensitivity information expedites the tolerance analysis

process (this topic will be discussed in greater detail later on in this chapter). As such

techniques expanded to other areas in electrical engineering, it was found that first-order

sensitivities are not sufficient for tolerance analysis of complex and nonlinear systems; therefore, more accurate and more complex models (such as second-order models) have been developed for sensitivity analysis of complex systems [39], [49], [51], [52], [53], and [59].

An important contribution of this thesis is in the area of sensitivity analysis of optimal systems. At an optimal operating point all first-order derivatives of the objective function with respect to system parameters are zero. As a result, conventional first-order (linear) sensitivity analysis is not capable of providing accurate results on the sensitivity of optimal systems to parameter variations. In this research second-order polynomial models are used to address sensitivity analysis problem for optimal systems.

## 5.3.2     Use of Simulations for Sensitivity Analysis

As mentioned earlier, in modern large power systems it is often difficult to analytically obtain a closed form representation of a performance index in terms of system parameters, and the behaviour of the system is usually determined by simulation. Therefore, computer-aided methods have to be used for sensitivity analysis of such systems. One such method is to conduct several simulation runs with slightly perturbed parameter values around an operating point to numerically determine the variation of the performance with respect to system parameters. The results are then used for creating a closed-form approximation of the performance index around that point [33], [48], [49], [52], and [53].

In this thesis a general-purpose simulation-based sensitivity analysis method is proposed for power system applications. In this method the sensitivity information is obtained automatically using numerical techniques combined with multiple-run simulations. This way the designer becomes capable of conducting sensitivity analysis of a power system conveniently by modeling the system in an electromagnetic transient simulation program.

### 5.3.3    Sensitivity Analysis Using Multiple-Run Simulations

One way to calculate the derivatives of a performance index without recourse to analytical expressions is to use numerical differentiation methods. In this method the simulation program is used to evaluate the performance index at a given operating point. A sensitivity analysis algorithm is then used to change the system parameters using a multiple-run simulations procedure. In each simulation, one (or two in case of mixed-derivatives) of the parameter values is slightly perturbed from its original value, and the performance index is evaluated using the EMT simulation program for this slightly altered set of parameter values. By the end of the multiple-run simulations the sensitivity analysis algorithm calculates the derivatives using the numerical formula (shown in 5.3), based on the performance index values obtained during the multiple-run simulation.

$$\frac{\partial f}{\partial x_i} \approx \frac{f(x_1,\cdots,x_i+\Delta x_i,\cdots,x_n)-f(x_1,\cdots,x_i-\Delta x_i,\cdots,x_n)}{2\Delta x_i} \tag{5.3}$$

In the above formula $f$ is the performance index and $x_1$, …, $x_n$ are the system parameters. In this research the PSCAD/EMTDC electromagnetic transient simulation

program has been used as the main core of the computer-aided sensitivity analysis tool. This makes the tool especially suitable for power systems containing power electronic apparatus.

## 5.3.4      Sensitivity Analysis of Optimized Systems

A first-order approximation of a performance index is often all that is necessary, particularly when the parameter variations are sufficiently small. A first-order approximation is obtained by calculating the first-order derivatives of the performance index at the operating point of interest and using the Taylor's expansion for the approximation. Once all the derivatives are determined (using 5.3), one can assess the effect of single or multiple parameter variations ($\Delta x_i$) on the system performance (represented by $f$) using the expression given in equation (5.4):

$$f\left(x_1 + \Delta x_1, \cdots, x_n + \Delta x_n\right) \approx f\left(x_1, \cdots, x_n\right) + \frac{\partial f}{\partial x_1}\Delta x_1 + \cdots + \frac{\partial f}{\partial x_n}\Delta x_n \tag{5.4}$$

Note that sensitivity analysis assumes that the objective function is continuous and differentiable at the point of interest; if this were not so, derivatives would not exist. Based on (5.4) it can be seen that first-order sensitivity analysis fails to provide any useful insight when the sensitivity around an optimum solution is considered. This is because all first-order derivatives of a function tend to zero around an optimum (unless the optimum lies on the boundary of a constrained optimization). At first glance it does not seem to cause any problem as zero sensitivity implies that the performance index is in a locally flat, i.e. insensitive, area. However, the sensitivity information of an optimum

becomes important (1) when comparing different optimal solutions with each other and (2) when sensitivity-based tolerance analysis of an optimal operating point is necessary (as will be discussed later in this chapter). For example consider Figure 5.1, in which the objective function shown has one optimum at $x = 1$ and another one at $x = 3$. The optimum solution at $x = 1$ is clearly much more sensitive to the parameter variations than the one at $x = 3$, as evidenced by the steep variations of the objective function around this point; however, first-order sensitivity analysis shows zero sensitivity for both optima due to first-order function derivatives approaching zero. Such different optima typically result when the optimization algorithm is started from different starting points.
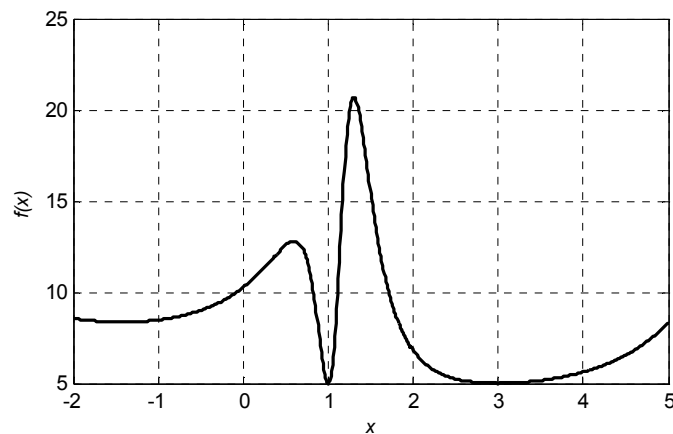


**Figure 5.1  A function with two optima**

To allow assessment of sensitivity around optimal point(s) of a given performance function second-order sensitivity analysis is proposed. In this method second as well as first-order derivatives of the performance function are used to assess the effect of parameter variations on the performance. Unlike first-order derivatives, second-order derivatives of the objective function do not necessarily tend to zero at optimal points. In addition, they increase the accuracy of sensitivity assessment around non-optimal points

by providing a more accurate representation of the performance index. Using a Taylor series expansion, one can obtain an estimation of a given multi-variable function by considering both first and second-order terms as shown in equation (5.5):

$$f(x_1 + \Delta x_1, \cdots, x_n + \Delta x_n) \approx f(x_1, \cdots, x_n) + \frac{\partial f}{\partial x_1} \Delta x_1 + \cdots + \frac{\partial f}{\partial x_n} \Delta x_n + \frac{1}{2} \frac{\partial^2 f}{\partial x_1^2} \Delta x_1^2 + \cdots$$

$$+ \frac{1}{2} \frac{\partial^2 f}{\partial x_n^2} \Delta x_n^2 + \frac{\partial^2 f}{\partial x_1 \partial x_2} \Delta x_1 \Delta x_2 + \cdots + \frac{\partial^2 f}{\partial x_1 \partial x_n} \Delta x_1 \Delta x_n + \frac{\partial^2 f}{\partial x_2 \partial x_3} \Delta x_2 \Delta x_3 + \cdots \qquad (5.5)$$

$$+ \frac{\partial^2 f}{\partial x_{n-1} \partial x_n} \Delta x_{n-1} \Delta x_n$$

The above formula can be written in a matrix form as given in equation (5.6):

$$f(\mathbf{x} + \Delta\mathbf{x}) \approx f(\mathbf{x}) + \mathbf{J}\Delta\mathbf{x} + \frac{1}{2} \Delta\mathbf{x}^T \mathbf{H} \Delta\mathbf{x} \qquad (5.6)$$

Where,

$$\mathbf{J} = \begin{bmatrix} \dfrac{\partial f}{\partial x_1} & \cdots & \dfrac{\partial f}{\partial x_n} \end{bmatrix} \quad and \quad \mathbf{H} = \begin{bmatrix} \dfrac{\partial^2 f}{\partial x_1^2} & \cdots & \dfrac{\partial^2 f}{\partial x_1 \partial x_n} \\ \vdots & \ddots & \vdots \\ \dfrac{\partial^2 f}{\partial x_n \partial x_1} & \cdots & \dfrac{\partial^2 f}{\partial x_n^2} \end{bmatrix} \qquad (5.7)$$

Note that although second-order derivatives provide more accurate results and enhances the sensitivity analysis capabilities, calculation of second order derivatives requires significantly more simulation runs and hence computer time, than calculation of first-order derivatives.

## 5.3.5 High Precision Sensitivity Models

It is possible to increase the accuracy of the sensitivity models by using higher-order derivatives, or by using other forms of approximation (e.g. using Lagrange polynomials [39]). However, obtaining such accuracy increases the required number of simulation runs for finding the parameter values of the models. For example the number of partial derivatives required for an *m*-th order Taylor's approximation of a function can be calculated from equation (5.8):

$$N = \underbrace{\sum_{i_1=0}^{1}\sum_{i_2=i_1}^{1}\cdots\sum_{i_{n-1}=i_{n-2}}^{1}1}_{n-1 \;\; terms} + \underbrace{\sum_{i_1=0}^{2}\sum_{i_2=i_1}^{2}\cdots\sum_{i_{n-1}=i_{n-2}}^{2}1}_{n-1 \;\; terms} + \cdots + \underbrace{\sum_{i_1=0}^{m}\sum_{i_2=i_1}^{m}\cdots\sum_{i_{n-1}=i_{n-2}}^{m}1}_{n-1 \;\; terms} \qquad (5.8)$$

Where *n* is the number of parameters of the function. As can be seen in (5.8) the number of required partial derivative significantly increases as the order of approximation increases. In case of polynomial representation of the performance index improving the polynomial order increases the required number of runs significantly. Therefore in this thesis as a reasonable compromise between high accuracy and amount of computation, derivatives of the performance index up to and including the second-order are considered.

## 5.3.6 Development of a Simulation-Based Sensitivity Analysis Procedure

There are a number of methods for finding the derivatives of a performance index in an electrical system. In this work numerical methods combined with multiple-run simulations have been used for the purpose of sensitivity analysis. Unlike other

sensitivity analysis methods, which require the system to have certain properties (e.g. linearity); numerical methods for sensitivity analysis do not add any constraint on the systems to be studied, and are only limited by the modelling capabilities of the simulation program. Therefore, these techniques can deal with a wide range of nonlinear and complex systems.

A numerical method for calculation of second-order derivatives is developed next. This method is particularly suited for the EMT simulation framework as it only relies on objective function values resulting from an electromagnetic transient simulation. For a positive incremental change $\Delta x_i$ in the variable $x_i$ of a multi-variable performance function $f(\mathbf{x})$, expression shown in (5.9) can be used to estimate the function variation using the Taylor series expansion (third and higher order terms are neglected).

$$f(x_1,\cdots,x_i + \Delta x_i,\cdots,x_n) - f(x_1,\cdots,x_n) \approx \frac{\partial f}{\partial x_i}\Delta x_i + \frac{1}{2}\frac{\partial^2 f}{\partial x_i^2}\Delta x_i^2 \tag{5.9}$$

Similarly for a negative increment, we obtain:

$$f(x_1,\cdots,x_i - \Delta x_i,\cdots,x_n) - f(x_1,\cdots,x_n) \approx -\frac{\partial f}{\partial x_i}\Delta x_i + \frac{1}{2}\frac{\partial^2 f}{\partial x_i^2}\Delta x_i^2 \tag{5.10}$$

Combining (5.9) and (5.10) yields equation (5.11) for estimated values of both first and second order derivatives of the function with respect to the variable $x_i$.

$$\begin{aligned}
\frac{\partial f}{\partial x_i} &\approx \frac{f(x_1,\cdots,x_i + \Delta x_i,\cdots,x_n) - f(x_1,\cdots,x_i - \Delta x_i,\cdots,x_n)}{2\Delta x_i} \\
\frac{\partial^2 f}{\partial x_i^2} &\approx \frac{f(x_1,\cdots,x_i + \Delta x_i,\cdots,x_n) + f(x_1,\cdots,x_i - \Delta x_i,\cdots,x_n)}{\Delta x_i^2} - \frac{2f(x_1,\cdots,x_n)}{\Delta x_i^2}
\end{aligned} \tag{5.11}$$

Note that approximation of the above partial derivatives requires two function evaluations $f(x_1,\ldots,x_i+\Delta x_i,\ldots,x_n)$ and $f(x_1,\ldots,x_i\text{-}\Delta x_i,\ldots,x_n)$, i.e., two transient simulations of the system. Having found the above derivatives, one can use a similar approach to determine mixed-partial derivatives as given in (5.12). Note that the right-hand side in (5.12) contains only function values and the previously calculated partial derivatives, which makes this method suitable for simulation-based implementation.

$$
\begin{aligned}
\frac{\partial^2 f}{\partial x_i \partial x_j} &\approx \frac{f\left(x_1,\cdots,x_i+\Delta x_i,\cdots,x_j+\Delta x_j,\cdots,x_n\right)}{2\Delta x_i \Delta x_j} + \frac{f\left(x_1,\cdots,x_i-\Delta x_i,\cdots,x_j-\Delta x_j,\cdots,x_n\right)}{2\Delta x_i \Delta x_j} \\
&- \frac{f\left(x_1,\cdots,x_n\right)}{\Delta x_i \Delta x_j} - \frac{1}{2}\frac{\Delta x_i}{\Delta x_j}\frac{\partial^2 f}{\partial x_i^{\,2}} - \frac{1}{2}\frac{\Delta x_j}{\Delta x_i}\frac{\partial^2 f}{\partial x_j^{\,2}}
\end{aligned}
\tag{5.12}
$$

The above method requires two additional simulation runs for each mixed-derivative. It is also possible to use a more classical approach for calculation of the mixed derivatives as follows; however (5.12) requires only two function evaluations whereas the method in (5.13) requires four. This has led to the adoption of (5.11) and (5.12) for the calculation of the complete set of first and second-order derivatives in this work.

$$
\begin{aligned}
\frac{\partial^2 f}{\partial x_i \partial x_j} &\approx \frac{f\left(x_1,\cdots,x_i+\Delta x_i,\cdots,x_j+\Delta x_j,\cdots,x_n\right)-f\left(x_1,\cdots,x_i-\Delta x_i,\cdots,x_j+\Delta x_j,\cdots,x_n\right)}{\Delta x_i \Delta x_j} \\
&- \frac{f\left(x_1,\cdots,x_i+\Delta x_i,\cdots,x_j-\Delta x_j,\cdots,x_n\right)-f\left(x_1,\cdots,x_i-\Delta x_i,\cdots,x_j-\Delta x_j,\cdots,x_n\right)}{\Delta x_i \Delta x_j}
\end{aligned}
\tag{5.13}
$$

From the above expressions, it can be seen that the evaluation of the full set of first and second order derivatives at a point in parameter space requires $M$ function evaluations (i.e., $M$ transient simulation runs on the transient simulation program), where:

$$M = n(n+1)+1 \qquad\qquad (5.14)$$

The above number arises due to the following terms:

- $n$ terms in the form of $\dfrac{\partial f}{\partial x_i}$ and $\dfrac{\partial^2 f}{\partial x_i^{\,2}}$, which require $2n$ simulations.

- $n^2$-$n$ terms in the form of $\dfrac{\partial^2 f}{\partial x_i \partial x_j}$, which require $2(n^2$-$n)$ simulations. However as

  $\dfrac{\partial^2 f}{\partial x_i \partial x_j} = \dfrac{\partial^2 f}{\partial x_j \partial x_i}$ the total number of required simulations is $(n^2$-$n)$.

- One simulation at the operating point

The final block diagram of the sensitivity analysis tool in shown is Figure 5.2.
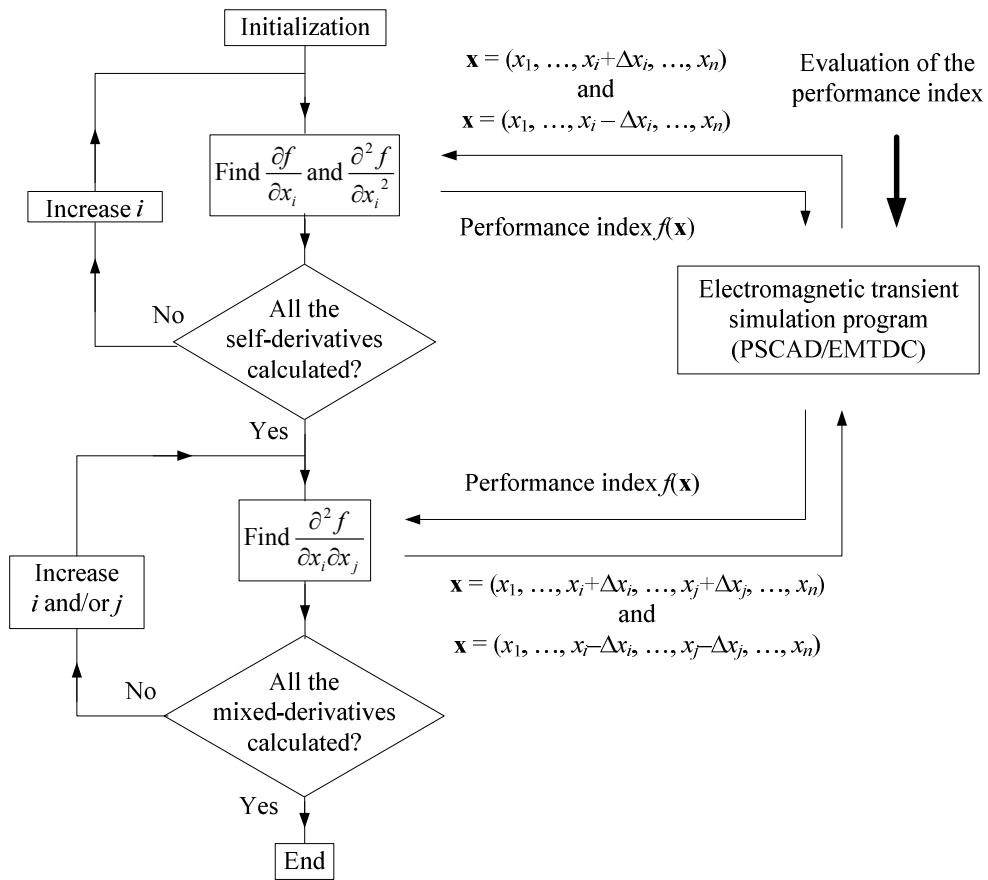


**Figure 5.2.  Block diagram of the sensitivity analysis tool**

### 5.3.7        Surrogate Models from Sensitivity Analysis

As mentioned earlier, surrogate models are simple models that capture the essential behaviour of the system but may not have any direct physical basis. The advantage of such models is that they produce outputs close to that of the actual system, but require a much smaller computational effort. In this thesis, the second-order models obtained from the simulation-based method described in the previous sections are used as surrogate models. As will be discussed in the next sections these surrogate models can be used for uncertainty analysis of the system performance. Application examples of the developed sensitivity analysis method and the surrogate models are presented in Chapter 6 of this thesis.

## 5.4        Tolerance Analysis

As mentioned before tolerance analysis is the process of finding the variations in the system performance indices when the system parameters vary within their respective ranges. In every design there is typically an acceptable performance range (referred to as a tolerance range), which is determined by the designer based on the design requirements. For example consider an induction motor connected to an ac transmission system. The maximum terminal voltage of the machine cannot exceed its rated insulation level. There is also a lower voltage limit dictated by power factor and over current considerations. In the design of the supply ac system for the induction motor these maximum and minimum voltages may define the tolerance range for the output voltage of the supply system.
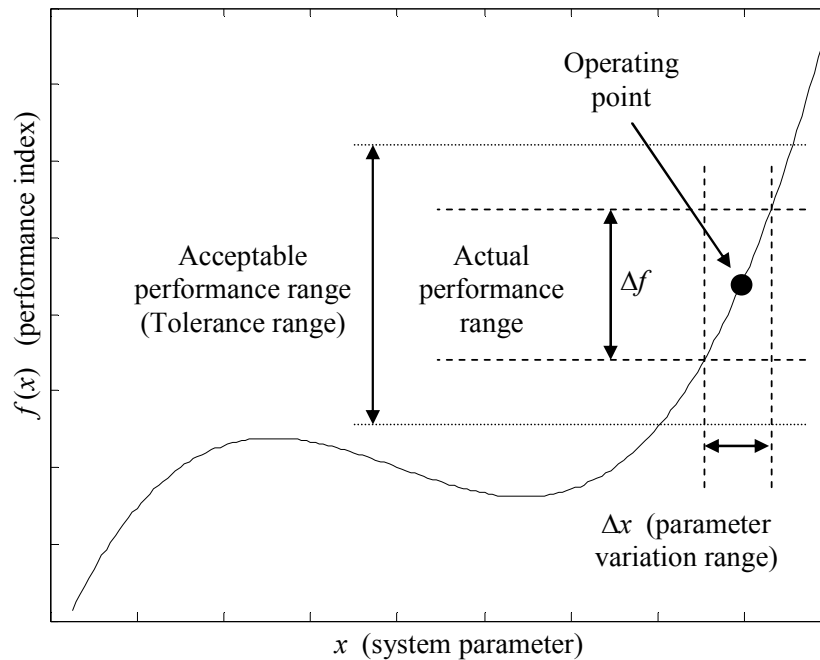
**Figure 5.3  Tolerance analysis (an acceptable design is shown)**

Figure 5.3 illustrates the tolerance analysis concept. Due to variations in the system parameters, performance of a design also varies within certain ranges. In case of our example it could be the actual voltage at the machine terminal. If the actual performance range lies within the tolerance range, then the designed system is satisfactory; otherwise, the system has to be re-designed. The purpose of tolerance analysis is to obtain an expected range for the system performance when the parameter values change in their ranges, to determine whether satisfactory performance is retained.

## 5.4.1    Types of Problems in Tolerance Analysis

In general there are two types of tolerance analysis problems. The first one is the worst-case analysis problem, in which the designer determines the potential worst-case

performance of the system, assuming that the input parameters can take any value within

a pre-specified range [41], [43], [50], [52], [53], and [56].
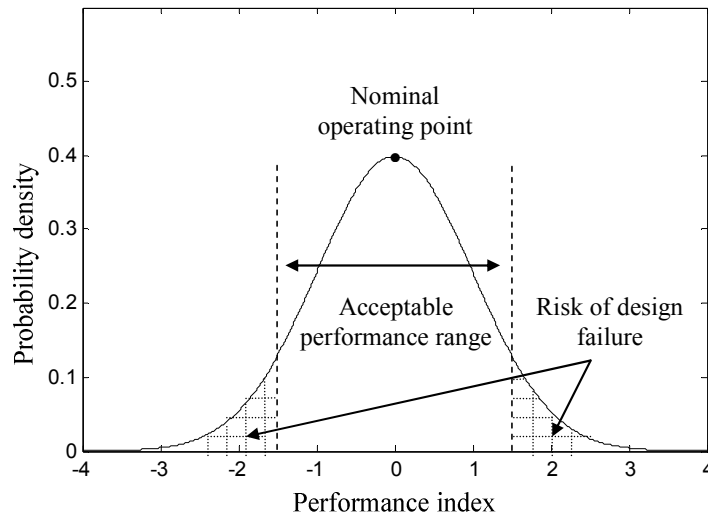


**Figure 5.4  Statistical tolerance analysis**

The other type of tolerance analysis problem is statistical tolerance analysis [39]

[49], [51], [59], [60], and [61]. Here the designer finds the probability of having different

performance levels (for example by using Monte-Carlo simulations). In such cases the

designer is usually willing to accept a certain level of performance degradation risk to

reduce the cost or to satisfy other design constraints. The concept of statistical tolerance

analysis is illustrated in Figure 5.4. The figure shows an example of a probability density

function for a performance index, which can be obtained using statistical tolerance

analysis. As shown in the figure, at the nominal operating point the value of the

performance index is zero. It is assumed that the acceptable performance range is within

±1.5 (as indicated by the dashed lines). The chance of having a non-satisfactory

performance (i.e. the risk) is determined by taking the integral of the probability density function over the entire *x*-axis excluding the area between -1.5 and +1.5. If the resulting risk is sufficiently small to be acceptable to the designer, the designed system passes the tolerance analysis stage, otherwise it should be re-designed.

## 5.4.2      Tolerance Analysis Methods

In this section, a number of tolerance analysis methods are described, and their advantages and disadvantages are discussed.

### 5.4.2.1      Direct Analytical Approach

For both types of worst-case analysis and statistical tolerance analysis problems, direct analytical approaches can be used. However, use of direct methods is only possible when the system under study is small and simple, and a closed-form representation of the system can be obtained.

### 5.4.2.2      Monte-Carlo Simulation

Monte Carlo simulation is one of the most commonly used methods for tolerance analysis of electrical systems [38], [81] − [85]. In this approach a large number of simulation runs are carried out, in which the parameter values of the system are selected randomly within their permissible tolerance ranges. After each run, the obtained values of different performance indices are recorded. At the end of this process, the results can be plotted in the form of histograms.

Monte-Carlo simulation can be used for both worst-case and statistical analysis problems. It should be noted that Monte-Carlo simulation only estimates the system performance for a given spread of parameter values, and the larger the number of simulations the closer the results to the actual distribution. Therefore, in order to obtain accurate results from this method it is necessary to conduct a large number of simulation runs, which in turn implies a long computation time.

### 5.4.2.3      Interval Arithmetic Method

In order to expedite the tolerance analysis process a number of other methods have been developed, including interval arithmetic methods [55], optimization-based methods [41], and sensitivity-based methods [52]. In the following paragraphs these methods are explained briefly.

Interval arithmetic [55] and [56] (and its improved version the affine arithmetic [42]) has been developed to find an outer range for the value of a function while its parameters vary within specified ranges. This means that the predicted performance range obtained from this method is larger than the actual performance range of the system, and it includes the actual performance range of the system. Different variants of this method have been used by researchers for finding the worst-case scenario of the system performance. These methods are sometimes combined with other tolerance analysis methods (such as optimization-based methods and Monte-Carlo simulation) to find both the inner and outer ranges of the system performance. However the problem with these methods is that they require a closed-form representation of the performance index in

terms of the system parameters, which is not easily available for large and complex system.

## 5.4.2.4      Optimization-Based Method

Another approach to worst-case problems is to use optimization-based tolerance analysis methods [41], [43], and [50]. In such methods a global optimization algorithm is used to find the worst-case value of the performance index within the permissible range of its input parameters. This method provides an inner solution for the worst-case problem.

## 5.4.2.5      Sensitivity-Based Method (and Response Surface Method)

Sensitivity-based tolerance analysis methods are capable of handling both worst-case and statistical analysis problems [39], [49], [51], [59], and [61]. In these methods instead of the actual detailed model of the system an approximated sensitivity model of the system is used for both worst-case and statistical analysis problems. This is a form of surrogate modeling described earlier. Using such surrogate models (which are usually simple) allows fast calculation of the performance indices. Thus simple function evaluations can be performed instead of time-consuming transient simulations, which results in significant time savings for the Monte-Carlo simulation.

The response surface method (RSM) is an extension of the sensitivity-based method. In RSM first a simple model (usually a first-order model) of the performance index is developed using a limited number of simulations. This model is used to detect

those system parameters, which are more important than the other ones (the ones which affect the performance index the most). The model is then improved by conducting more simulations only for the important parameters.

## 5.4.2.6       Polynomial Chaos and Stochastic Response Surface Method

Polynomial chaos (PC) expansion is a method for representing well-behaved (square-integrable) random variables in terms of orthogonal polynomial functions of standard random variables (srvs). This method was originally developed by Norbert Wiener [108] for analyzing Gaussian process [108], and later on it has been used in various engineering fields for analyzing uncertainties and noise [60], [105], [106], and [107].

Consider a function $y$ to be a function of several random inputs $x_1, \dots , x_m$. Using PC it is possible to express the above function terms of standard random variables $\xi_1, \dots \xi_n$ ($m = n$ when inputs are independent) i.e. $y = f (x_1(\xi_1, \dots \xi_n), \dots , x_m(\xi_1, \dots \xi_n))$. In classical RSM, $y$ would have been fitted directly with a response surface involving variables $x_i$-s. In contrast, in stochastic response surface methods (SRSM) that use PC, PC $y$ is fitted to a more fundamental set of random variables $\xi_i$-s. This is particularly useful when $x_i$-s themselves do not have a standard distribution. However, it is still possible to express $x_i$-s in terms of standard variables $\xi_i$, from which the PC expression for $y$ in terms of $\xi_i$-s can be determined. Hence, rather than using samples of $x_i$-s in generation the distribution of $y$, it is easier to use samples of $\xi_i$-s because their behaviour is standard. In addition, having $y$ expressed in terms of $\xi_i$-s helps to select better samples

(which have high likelihood of happening) for fitting the surface. This make the models obtained from SRSM more statistically accurate compared to the models obtained from RSM. The details of the PC approach are summarized below:

When the srvs have normal distribution (zero mean and unity standard deviation) the output $y$ can be expressed using a Hermite polynomial chaos expansion in the following form:

$$y = a_0 + \sum_{i_1=1}^{n} a_{i_1} \Gamma_1(\xi_{i_1}) + \sum_{i_1=1}^{n}\sum_{i_2=1}^{i_1} a_{i_1 i_2} \Gamma_2(\xi_{i_1},\xi_{i_2}) + \sum_{i_1=1}^{n}\sum_{i_2=1}^{i_1}\sum_{i_3=1}^{i_2} a_{i_1 i_2 i_3} \Gamma_2(\xi_{i_1},\xi_{i_2},\xi_{i3}) + \cdots \qquad (5.15)$$

where $y$ is the output, $a_i$-s are constants, and $\Gamma_p(\xi_{i_1},\cdots,\xi_{ip})$ is Hermite polynomial of degree $p$ which is calculated from the following equation:

$$\Gamma_p(\xi_{i_1},\cdots,\xi_{ip}) = (-1)^p e^{\frac{1}{2}\xi^T\xi} \frac{\partial^p}{\partial\xi_{i_1}\cdots\partial\xi_{i_p}} e^{-\frac{1}{2}\xi^T\xi} \qquad (5.16)$$

where $\xi = [\xi_{i_1},\cdots,\xi_{ip}]^T$. As the order of the polynomial chaos expansion increases the probability distribution function (pdf) of the expansion becomes closer to that of the output variable ($y$). As an example the second-order polynomial chaos expansion of a variable $y$ with respect to one standard random variable $\xi_1$ has the following form:

$$y = a_0 + \sum_{i_1=1}^{1} a_{i_1} \Gamma_1(\xi_{i_1}) + \sum_{i_1=1}^{1}\sum_{i_2=1}^{i_1} a_{i_1 i_2} \Gamma_2(\xi_{i_1},\xi_{i_2}) = a_0 + a_1\Gamma_1(\xi_1) + a_{11}\Gamma_2(\xi_1,\xi_1) \qquad (5.17)$$

For a single variable Hermite polynomial $\Gamma_1(\xi_1) = \xi_1$ and $\Gamma_2(\xi_1, \xi_1) = (1 - \xi_1^2)$; therefore the above expansion can be simplified as follows.

$$y = a_0 + a_1\xi_1 + a_{11}(1 - \xi_1^2) \tag{5.18}$$

Equation (5.18) is now the approximate formula for $y$ in terms of $\xi_i$-s, and can be used further for Monte-Carlo analysis. As the underlying distributions of $\xi_i$-s are known and easy to generate, distribution of $y$ can be easily obtained using the above formula.

Hence, stochastic response surface methodology (SRSM) in some ways is similar to RSM; but generates a response surface in terms of standard variables $\xi_i$-s to rather than in terms of the direct dependency variables $x_i$-s. This way the resulted pdf is more accurate compared to regular RSM.

## 5.4.2.7      Polynomial Chaos and Stochastic Differential Equations

Another way of handling tolerance analysis problems is to model the system under study by a set of differential equations that show the stochastic behaviour. Polynomial chaos (PC) has been proven to be an effective method in such cases. As mentioned before, the Hermite polynomials are orthogonal with respect to the following inner product:

$$\Gamma_p.\Gamma_q = E(\Gamma_p.\Gamma_q) = 0 \quad if \quad p \neq q \tag{5.19}$$

Where $E(x)$ represents the expected value of x. By expanding both system input parameters and system outputs in terms of their polynomial chaos expansions, one can

take advantage of the orthogonality feature to simplify the system solution. By re-arranging the terms in (5.15) one can represent the output as follows.

$$y = \sum_{i=1}^{\infty} \hat{a}_i \Phi_i(\xi) \tag{5.20}$$

where there is a one-to-one correspondence between the $\Phi_i$ and the Hermite polynomials functions $\Gamma_i$. Consider a simple differential equation as shown below, where the coefficient $k$ is a random variable

$$\frac{dy}{dt} = -ky \tag{5.21}$$

By expressing $k$ and the solution $y(t)$ in their PC expansion we have:

$$y = \sum_{i=1}^{\infty} y_i \Phi_i(\xi) \quad and \quad k = \sum_{i=1}^{\infty} k_i \Phi_i(\xi) \tag{5.22}$$

Using the above expansion and the orthogonality feature of $\Phi_i$-s (5.20) can be converted to the differential equation form as follows [109]:

$$\sum_{i=0}^{M} \frac{dy_i}{dt} \Phi_i = -\sum_{i=0}^{M} \sum_{j=0}^{M} \Phi_i \Phi_j k_i y_j(t) \tag{5.23}$$

Note that the above equation (5.23), can be solved for the $y_i(t)$–s. Once the $y_i$-s are obtained, one can use (5.22) to obtain distribution of $y(t)$ at any time $t$.

There are approaches that use the method described above to generate equivalent electric circuit models that can be solved using conventional circuit analyzers [105] and

[106]. The main drawback of this method for simulation-based implementation is that it requires modifications in the simulation core of the simulator program, which may not be always possible.

### 5.4.3     Tolerance Analysis for Power Systems

Monte-Carlo simulation is one of the traditional tolerance analysis approaches in power systems [81] − [85]. However as the size and complexity of power system increases the required time for Monte-Carlo simulations of such systems becomes unacceptably long. Therefore other methods have been proposed for tolerance analysis of such systems [48], [49], [50], [52], and [61].

In this thesis the sensitivity-based tolerance analysis approach discussed in the previous sections is adopted for tolerance analysis of power systems. Use of the sensitivity model instead of the actual model significantly reduces the required computation time for tolerance analysis. In order to facilitate the process in this thesis the second-order models obtained from the proposed simulation-based sensitivity analysis approach are used for tolerance analysis.

### 5.4.4     Tolerance Optimization

Although this technique has not been used in this thesis, it is briefly described in this section as it plays an important role in the future work of this thesis. In tolerance optimization [57] and [58], the designer is looking for an operating point, which results in an optimized worst-case scenario rather than an optimum operating point.
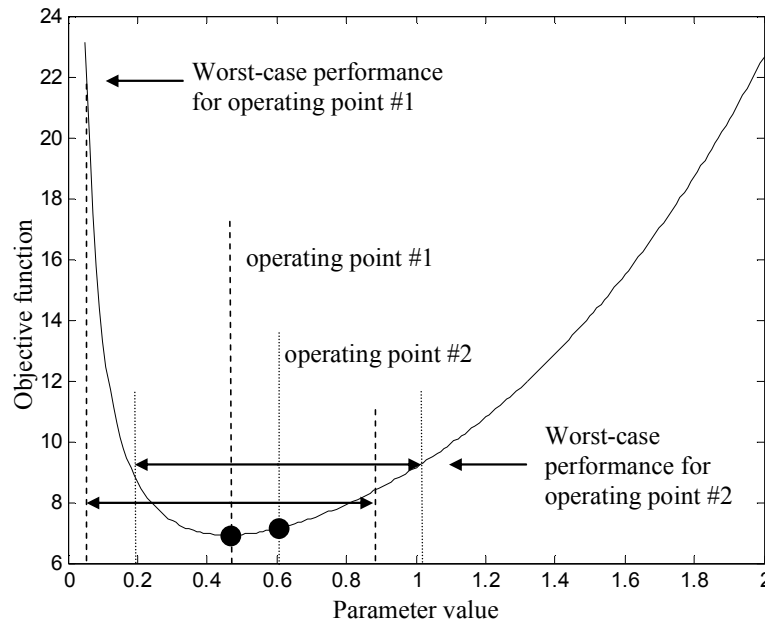
**Figure 5.5  Tolerance optimization**

The concept of tolerance optimization is illustrated in Figure 5.5. The figure

shows the objective function for a single-variable optimization problem. In a regular

optimization process the operating point #1 is selected as the optimal solution, as it

results in the lowest value of the objective function. However, assuming a tolerance range

of ±0.4 for the parameter value, the worst-case value of the objective function for this

operating point can reach 22, which is much higher than the optimal value. On the other

hand, operating point #2 is the optimal solution of the tolerance optimization process.

This is because with the same tolerance range (±0.4), the operating point #2 can only be

degraded to 9.3, even though the value of the objective function at this operating point is

higher than the operating point #1. Therefore, in such cases the designer may decide to

select the tolerance optimization solution (i.e. operating point #2) to reduce possible performance degradation in presence of parameter uncertainties.

### 5.4.5    Tolerance Analysis Using the Proposed Simulation-Based Method

As mentioned in the previous section, Monte-Carlo simulation of a system usually requires a large number of simulation runs to produce accurate results. When the system under study is large and complex, EMT simulation of the system takes a long time, which makes the Monte-Carlo simulation an unaffordably long process. Therefore, other methods have to be used for statistical tolerance analysis of such systems.

This research proposes to use the second-order models, obtained from the developed sensitivity analysis method, as surrogate models of the performance indices for tolerance analysis of the system.

### 5.4.5.1    Tolerance Analysis Using the Direct Method

Once surrogate models are obtained from the proposed simulation-based method, tolerance analysis of the system can be done directly by using those models. Direct methods are only applicable when surrogate models have simple mathematical forms; therefore, one of the advantages of the proposed surrogate models is that they make it possible to use direct methods for tolerance analysis. In the following sections, direct form of worst-case and probabilistic tolerance analyses is described.

## 5.4.5.1.1    Direct Worst-Case Tolerance Analysis

Access to a simple second-order Taylor's expansion to describe the system response makes it possible to easily address the worst-case tolerance analysis problems directly using analytical methods. There are two possible situations, namely (1) second-order terms are negligible compared to first-order terms; (2) second-order terms are considerable compared to first-order terms (e.g. when the operating point is around an optimal point or when the parameter variations are large enough that the second order terms become important). In the first case the worst-case scenario can be found by considering only the first-order terms of the Taylor's expansion given by (5.24):

$$f(x_1 + \Delta x_1, \cdots, x_n + \Delta x_n) \approx f(x_1, \cdots, x_n) + D_{x_1} \Delta x_1 + \cdots + D_{x_n} \Delta x_n$$

Where :                                                                                                              (5.24)

$$D_{x_i} \approx \frac{\partial f}{\partial x_i} \quad \text{obtained from simulation - based analysis}$$

At the worst-case scenario, $f$ has its maximum value, as given by (5.25):

$$\Delta f_{\max} \approx \left| D_{x_1} \right| \Delta x_{1\max} + \cdots + \left| D_{x_n} \right| \Delta x_{n\max}$$                                             (5.25)

Where $\Delta f_{max}$ is the maximum variations of $f$ and $\Delta x_{i\max}$ is the maximum variations of parameter $x_i$ (assuming equal positive and negative variations). For the second case, where both first and second-order terms are important, the worst-case value of $f$ cannot be easily found as it may lie on one of the vertices of the hypercube of the parameter variation space, or it may lie inside it. However, in the case that it lies on one of the

vertices (usually around an optimum) the worst-case value of $f$ can be found from equation (5.22):

$$
\begin{aligned}
\Delta f_{\max} \approx \frac{1}{2}\left|D_{x_1 x_1}\right|\Delta x_{1\max}^2 + \cdots + \frac{1}{2}\left|D_{x_n x_n}\right|\Delta x_{n\max}^2 \\
\pm \left|D_{x_1}\right|\Delta x_{1\max} + \cdots \pm \left|D_{x_n}\right|\Delta x_{n\max} \\
\pm \left|D_{x_1 x_2}\right|\Delta x_{1\max}\Delta x_{2\max} + \cdots \pm \left|D_{x_{n-1}x_n}\right|\Delta x_{n-1\max}\Delta x_{n\max}
\end{aligned}
$$

$$(5.26)$$

where

$$
D_{x_i x_j} = \frac{\partial f}{\partial x_i \partial x_j} \qquad \text{obtained from the simulation - based method}
$$

In the above equations $\pm$ sign are determined based on the vertex that corresponds to the worst-case.

## 5.4.5.1.2    Direct Statistical Tolerance Analysis

If a closed-form representation of a function is available, its probabilistic behaviour can also be calculated knowing the probabilistic behaviour of its input parameters. Before the procedure is described, it is necessary to review two definitions from probability theory, i.e., cumulative distribution function (CDF), and probability density function (PDF). The mathematical definitions of CDF and PDF of a random variable X are shown in equations (5.27) and (5.28):

$$
F_X(x) = P(X \leq x)
$$

$$(5.27)$$

$$
P(a \leq X \leq b) = \int_a^b f_X(x)dx
$$

$$(5.28)$$

where, $X$ is a random variable and $F_X$ and $f_X$ are its CDF and PDF respectively. These functions completely describe the probabilistic behaviour of the random variable. For example the mean of the random variable can be calculated from equation (5.29):

$$\overline{X} = \int_{-\infty}^{-\infty} x f_X(x) dx \tag{5.29}$$

If $Y$ is a function of $n$ random variables $X_1, \dots X_n$ as follows:

$$Y = F(X_1, \cdots, X_n) \tag{5.30}$$

The CDF of Y can be calculated from equation (5.31):

$$F_Y(y) = P(Y \le y) = \int \cdots \int_{F(x_1,\cdots,x_n) < y} f_{X_1,\cdots,X_n}(x_1, \cdots, x_n) dx_1 \cdots dx_n \tag{5.31}$$

where $f_{X_1,\cdots,X_n}$ is the joint PDF of the random variables, which in case of independent random variables can be calculated from equation (5.32) [102]:

$$f_{X_1,\cdots,X_n}(x_1, \cdots, x_n) = f_{X_1}(x_1) \times \cdots \times f_{X_n}(x_n) \tag{5.32}$$

## 5.4.5.2    Tolerance Analysis Using the Monte-Carlo Simulations

Although direct methods can be applied to simple surrogate models with a limited number of variables, as the complexity of the surrogate model and the number of variables increase use of direct methods becomes more difficult. On the other hand, as opposed to original models, which are time consuming to evaluate, surrogate models can

be evaluated in a significantly shorter time; therefore, Monte-Carlo analysis using the surrogate models could be considered as an alternative to direct methods.

In this research, a statistical tolerance analysis procedure has been developed, which uses the simulation-based sensitivity analysis results, and performs the Monte-Carlo simulations on the system performance. The block diagram of this procedure is shown in Figure 5.6.
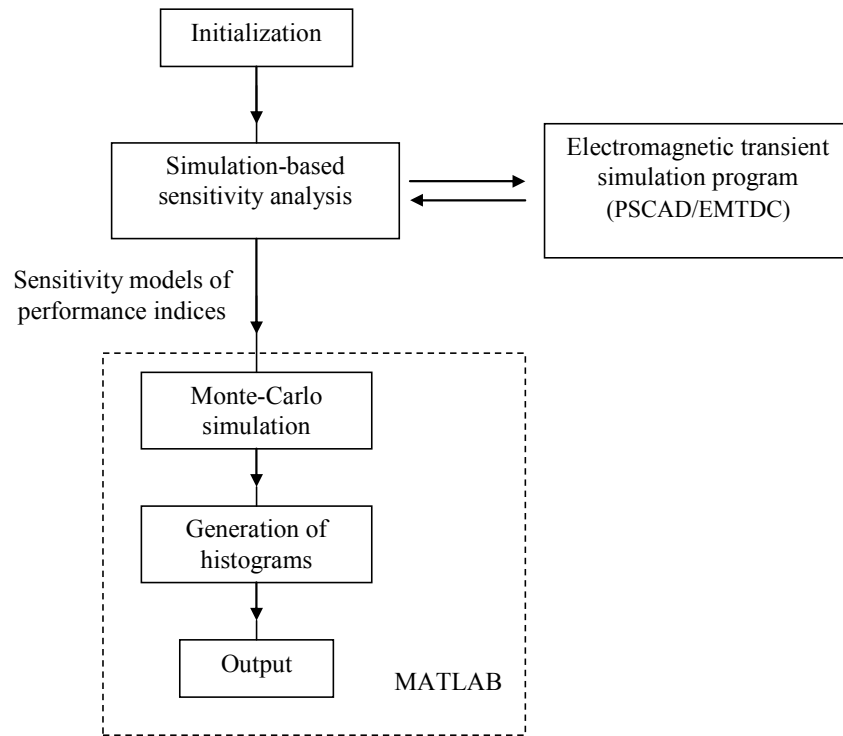


**Figure 5.6  Proposed probabilistic analysis scheme**

As it is shown in the diagram, the EMT simulations are first used to obtain surrogate models for different performance indices. Then the surrogate models are deployed to perform the Monte-Carlo Analysis. In the next chapter a few application examples of the developed tools are presented.

# Chapter 6  Application Examples of Simulation-Based Uncertainty Analysis

## 6.1      Uncertainty Analysis of Selective Harmonic Elimination Switching Pattern

In this section simulation-based uncertainty analysis is used for analyzing the performance of a power system. The procedure is explained using an example which considers the impact of an error in the firing of switches on the performance of a selective harmonic elimination (SHE) switching scheme for a voltage-sourced converter (VSC). It is shown that the low level of harmonics generated by the VSC is affected by variations in the firing instances (angles), which may happen due to accuracy limitations of the physical system.

In this example the simulation-based optimization is first used to determine SHE switching angles. After an optimal switching pattern is obtained, sensitivity of the harmonic spectrum to small variations in the switching angles is determined using the proposed sensitivity analysis approach. The problem is studied in two different stages. In the first stage a converter with three switching angles in each quarter cycle and an ideal dc-bus voltage (ripple free) is considered. Under the assumption of an ideal dc-bus, it becomes possible to obtain analytical solutions for optimization and sensitivity analysis of the problem; these analytical solutions serve to verify the results obtained from the proposed simulation-based solution. In the second stage of this example, the same switching pattern is analyzed when it is used for a two-level static compensator

(STATCOM), where the dc-bus voltage fluctuates. With the inclusion of dc-bus voltage dynamics, development of analytical solutions becomes prohibitively difficult; however it is shown that the developed methods will still be capable of handling this system.

### 6.1.1    Selective Harmonic Elimination

Repetitive switching of power electronic switches in high power converters makes them one of the largest producers of harmonic currents in the power networks. Harmonic currents cause additional losses in the network elements [87], [88], torque vibrations in electric machines [89], interference in neighbouring communication systems [90], etc. In order to eliminate these adverse impacts, different methods have been proposed to reduce the amount of harmonic currents produced by power electronic converters. Selective harmonic elimination (SHE) is one of those methods, which has gained popularity due to its relatively low switching losses [86]. In this method a number of switching instants (firing angles) are judiciously selected in order to craft a waveform with a given fundamental component and specified lower-order harmonic content.

The technique of selective harmonic elimination (SHE) is explained with reference to Figure 6.1 and Figure 6.2. This technique can be used for single-phase and three-phase voltage-sourced converters (VSC) and can be applied to two or multi-level converts. In this section a simple three-phase two-level converter is used to describe the method. To generate an ac waveform on phase a, the switches $S_1$ and $S_4$ of the voltage-source converter shown in Fig. 5.1 are operated to apply a voltage of $+V_{dc}$ or $-V_{dc}$ at the output, respectively. The resulting waveform is shown in Figure 6.2.

The harmonic spectrum of the resulting voltage waveform is clearly a function of the switching instants. The instances of switching, represented by angles $\alpha_1$, $\alpha_2$… $\alpha_N$, are adjustable degrees of freedom that can be selected so that a certain number of lower order harmonics are eliminated and the desired magnitude of the fundamental frequency voltage is obtained. By choosing $N$ switching per quarter-cycle (Figure 6.2 shows three), $N$-1 harmonics can be eliminated.
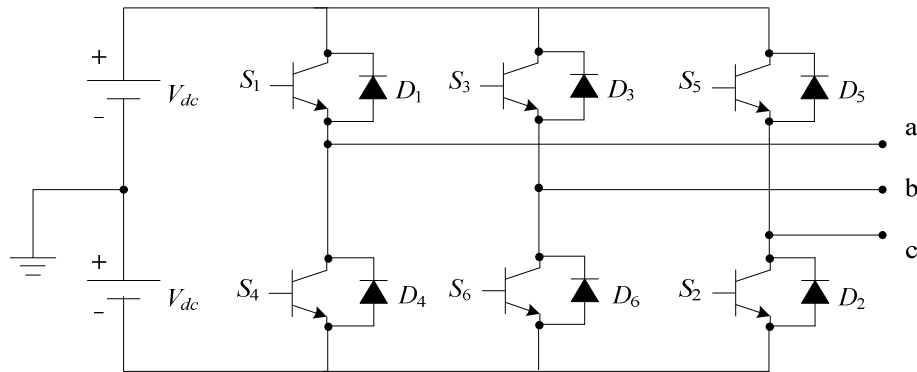


**Figure 6.1  A two-level converter**
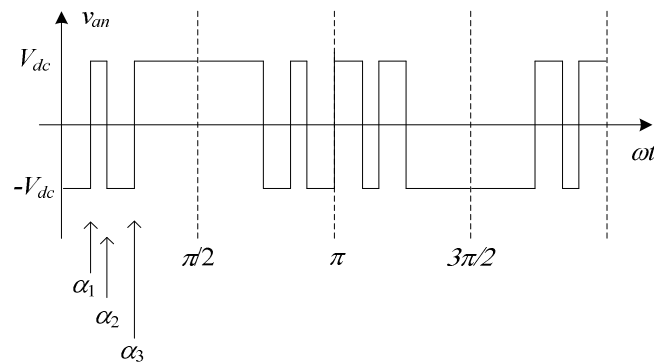


**Figure 6.2  SHE switching scheme with three switching angles in a quarter-cycle**

It can be shown that for a fixed dc voltage ($V_{dc}$ = constant) the harmonic components of the output voltage waveform are obtained using the expression given in (6.1) [86]:

$$V_1 = \left| \frac{2\sqrt{2}V_{dc}}{\pi} \left( 1 + 2\sum_{i=1}^{N} (-1)^i \cos(\alpha_i) \right) \right|$$

$$V_n = 0 = \left| \frac{2\sqrt{2}V_{dc}}{n\pi} \left( 1 + 2\sum_{i=1}^{N} (-1)^i \cos(n\alpha_i) \right) \right| \qquad (6.1)$$

$$n \in \{n_1, n_2, \cdots, n_{N-1}\}$$

In the above equations, $V_1$ is the magnitude of the fundamental voltage and $n_1$, $n_2 \ldots n_{N-1}$ are the orders of the $N$-1 harmonics targeted for elimination.

Conversely, the above system of equations can be solved for $N$ switching angles given a desired fundamental and $N$-1 harmonic components specified. Typically, the solution seeks the angles to result in matching a desired fundamental voltage and eliminate $N$-1 low order harmonics. In the 3-variable example considered here in addition to the fundamental, the 5$^{th}$ and 7$^{th}$ order harmonics are selected as they are the lowest order characteristic harmonics in a balanced 3-phase system.

## 6.1.2    Tolerance Analysis of a SHE Pattern under Ideal Conditions

In this section a selective harmonic elimination scheme with three switching angles in each quarter-cycle and an ideal dc voltage is considered. Having the ideal conditions makes it possible to use the analytical solution (6.1) for analyzing the

harmonic contents of the waveform, which can be used for verification of the results obtained from the developed simulation-based methods.

### 6.1.2.1      Optimization of the Switching Pattern

As mentioned earlier solution of the system of equations given in (6.1) yields the $N$ angles required for lower-band harmonic spectrum specified by the desired fundamental and $N$-1 harmonic components. The solution can be obtained either using a numerical method for solving nonlinear systems of simultaneous equations, or can be similarly obtained using an optimization technique.

An objective function can be defined so that it reaches its minimum when the specified harmonics are zero and the magnitude of the fundamental component is as desired. For example objective function (OF) shown in (6.2) is used for this problem.

$$f = \frac{\left(V_1 - V_{ref}\right)^2}{V_{ref}^2} + \frac{V_5^2}{V_{ref}^2} + \frac{V_7^2}{V_{ref}^2} \tag{6.2}$$

In (6.2), $V_{ref}$ is the desired fundamental voltage magnitude, and $V_1$, $V_5$, and $V_7$ are the values of the fundamental, fifth and seventh harmonics, respectively. The magnitude of the OF is represented by the function $f(\alpha_1, \alpha_2, \alpha_3)$, where $\alpha_1$, $\alpha_2$ and $\alpha_3$ are the three switching angles. Note that $f$ attains a minimum value of zero when the objectives of regulating fundamental voltage to its set-point and eliminating the required harmonics are perfectly achieved. Hence minimizing $f$ by suitable choice of $\{\alpha_1, \alpha_2, \alpha_3\}$ gives a design whose performance is as close as possible to the desired objective, provided that the

respective minimum has a vanishingly small objective function evaluation. Table 6.1 shows the optimal solution for $\{\alpha_1, \alpha_2, \alpha_3\}$ obtained using the developed optimization tool. Analytical results obtained using (6.1) are also shown in the table for comparison. Note that the solution obtained using the developed simulation-based optimization closely matches the analytical solution, thereby confirming the validity of the simulation-based method. Also note that in this simple case, the evaluation of harmonics does not necessarily require an EMT simulation and can be done analytically; however as it is shown in the next sections, for more complex cases obtaining such analytical solutions becomes prohibitively difficult.

**Table 6.1  SHE switching angles for a scheme with three chops in each quarter cycle**

| | $V_{dc} = 35\text{kV}, V_{ph} = 20\text{kV}$ | |
| --- | --- | --- |
| | Optimization Results | Analytical Results |
| $\alpha_1$ | 18.15° | 18.22° |
| $\alpha_2$ | 37.09° | 37.07° |
| $\alpha_3$ | 48.23° | 48.30° |

## 6.1.2.2     Uncertainty Analysis of the Switching Pattern

In practical implementations, due to small imperfections in the control circuit, the realized switching angles typically differ slightly from their designed values. Such limited precision in switching will introduce an error in the magnitude of the realized ac voltage waveform, and will also result in an incomplete elimination of the targeted harmonics. As will be shown in this section, uncertainty analysis can be used to study the effects of such (small) deviations in the switching angles on the harmonic spectrum of the output voltage. This section demonstrates the use of the simulation-based sensitivity

analysis approach developed in this work for determining the effect of uncertainties on the harmonic performance of the SHE scheme. As an analytical solution is also possible for the ideal SHE scheme, such analysis will be used to validate the proposed technique.

In this example the square of the harmonic distortion of voltage due to remnant 5th and 7th harmonics, as shown in (6.3), is used as a performance index. The impact of firing imprecision is then studied using this performance index.

$$D_{57}\left(\alpha_1, \alpha_2, \alpha_3\right) = \frac{V_5{}^2 + V_7{}^2}{V_{ref}{}^2} \tag{6.3}$$

For the precise angles $\{\alpha_1, \alpha_2, \alpha_3\}$ as presented in Table 6.1, $D_{57}$ is zero; however in practice it will deviate from zero due to slight deviations in these angles. The developed sensitivity analysis technique, which uses the procedure described before in Chapter 5, is used to calculate $D_{57}$. Note that in this case, as the optimized switching angle solution minimizes $D_{57}$, the first derivatives are zero and the sensitivity analysis must rely on second-order derivatives to estimate the performance index. The sensitivity analysis results, obtained from the previously-described second-order analysis method, are shown in Table 6.2, which also includes the results obtained by analytical calculation.

The sensitivities indicate the incremental $D_{57}$ per degree error in the respective switching angles. To read the table, the entry in a row marked $\partial / \partial \alpha_j$ and a column marked $\partial / \partial \alpha_k$ corresponds to the partial derivative $\frac{\partial}{\partial \alpha_j}\left(\frac{\partial}{\partial \alpha_k}\left(D_{57}\right)\right)$. The rows labelled '1' contain the first-order partial derivatives. The sensitivity analysis tool automatically generates the last four rows of Table 6.2.

**Table 6.2  Derivatives obtained for the SHE scheme with 3 chops \***

| $D_{57}$ | $\partial/\partial\alpha_1$ | $\partial/\partial\alpha_2$ | $\partial/\partial\alpha_3$ |
|---|---|---|---|
| $V_{dc}$ = 35kV, $V_{ph}$ = 20kV (rms) | | | |
| Analytical results | | | |
| 1 | 0.0* | 0.0 | 0.0 |
| $\partial/\partial\alpha_1$ | 9.9 | 5.3 | -7.1 |
| $\partial/\partial\alpha_2$ | 5.3 | 5.9 | -2.8 |
| $\partial/\partial\alpha_3$ | -7.1 | -2.8 | 5.5 |
| Values obtained using the sensitivity analysis tool | | | |
| 1 | 0.0 | 0.0 | -0.1 |
| $\partial/\partial\alpha_1$ | 10.3 | 5.1 | -7.7 |
| $\partial/\partial\alpha_2$ | 5.1 | 5.2 | -2.7 |
| $\partial/\partial\alpha_3$ | -7.7 | -2.7 | 6.1 |

**\* Unit [$10^{-3}$/Degrees]**

Having found all first and second order derivatives, the $D_{57}$ can be represented as a simple formula using the expansion in (6.4). This formula can be used as a surrogate model for $D_{57}$, which is valid for small variations in the three firing angles.

$$
\begin{aligned}
f\left(x_1 + \Delta x_1, \cdots, x_n + \Delta x_n\right) &\approx \\
f\left(x_1, \cdots, x_n\right) + \frac{\partial f}{\partial x_1}\Delta x_1 + \cdots &+ \frac{\partial f}{\partial x_n}\Delta x_n + \frac{1}{2}\frac{\partial^2 f}{\partial x_1^2}\Delta x_1^2 + \cdots \\
+ \frac{1}{2}\frac{\partial^2 f}{\partial x_n^2}\Delta x_n^2 + \frac{\partial^2 f}{\partial x_1 \partial x_2}\Delta x_1 \Delta x_2 &+ \cdots + \frac{\partial^2 f}{\partial x_1 \partial x_n}\Delta x_1 \Delta x_n \\
+ \frac{\partial^2 f}{\partial x_2 \partial x_3}\Delta x_2 \Delta x_3 + \cdots &+ \frac{\partial^2 f}{\partial x_{n-1}\partial x_n}\Delta x_{n-1}\Delta x_n
\end{aligned}
\tag{6.4}
$$

Replacing the sensitivity analysis results in the above equation, results in the surrogate model shown in (6.5):

$$
\begin{aligned}
D_{57}\left(\alpha_1, \alpha_2, \alpha_3\right) &\approx 10^{-3} \times \left( \frac{1}{2}\times 10.3 \times \Delta\alpha_1^2 + 5.1\times\Delta\alpha_1\Delta\alpha_2 - 7.7\times\Delta\alpha_1\Delta\alpha_3 \right. \\
&\left. + \frac{1}{2}\times 5.2\times\Delta\alpha_2^2 - 2.7\times\Delta\alpha_2\Delta\alpha_3 + \frac{1}{2}\times 6.1\times\Delta\alpha_3^2 \right)
\end{aligned}
\tag{6.5}
$$

## 6.1.2.2.1    Worst-Case Tolerance Analysis: Forward Problem

In a forward worst-case tolerance analysis problem, the surrogate model is used to find the maximum possible degradation in the system performance, when the parameter values are within a certain range. In case of this example the forward problem is to estimate the maximum value of the $D_{57}$ when switching angles can have a maximum deviation of $\Delta\alpha$ around the their desired values.

If the maximum uncertainty due to the electronics in the controller for each firing angle is a specified value of $\Delta\alpha = \pm0.1°$ (a typical limit for power electronic equipment in power systems), the worst case value of $D_{57}$ can be calculated by using the surrogate model (6.4) without any further need for time-consuming simulations. The resulting worst-case increase in the value of $HD_{57} = \sqrt{D_{57}}$ is shown in Table 6.3.

**Table 6.3  The worst-case scenario for 5th and 7th harmonics**

| $V_{dc}$ = 35kV, $V_{ph}$ = 20kV | | |
|---|---|---|
| Worst-case combination of switching angles: | | |
| $\Delta\alpha_1$ = -0.1° | $\Delta\alpha_2$ = -0.1° | $\Delta\alpha_3$ = +0.1° |
| Corresponding $HD_{57}$: | | |
| First-order estimation | | 0.0% |
| Second-order estimation | | 1.65% |
| Analytical result | | 1.69% |

In this example, where the simplicity of the idealized case allows derivation of a closed form expansion for $D_{57}$, it is also possible to compare the values obtained using the simulation-based approach with the result from analytical calculation. As shown in the table, the result of $HD_{57} = 1.65\%$ obtained using the surrogate model agrees well with the analytically available solution of $HD_{57} = 1.69\%$. Note also that an estimate of $HD_{57}$ based on first-order derivatives yields a totally inaccurate value of $HD_{57} = 0.0\%$.

As will be shown in the next sections, for realistic cases, where the dc bus voltage variations are also included, the simulation-based approach can still be applied, while the analytical approach becomes practically impossible.

## 6.1.2.2.2    Worst-Case Tolerance Analysis: Reverse Problem

A converse problem to the one considered in the previous section is to determine the permissible deviation of the firing angle $\Delta\alpha$, so that the harmonic distortion $HD_{57}$ remains below a specified value. Let us assume a limit of $HD_{57} < 2\%$ (or in other words $D < 0.04$) as a design objective; the permitted maximum error in the firing angles $\Delta\alpha$ can then be calculated using (6.6) and (6.7) below, which are restatements of (6.4). Note that in (6.6) and (6.7) the + or − signs are due to the fact that the deviation can be positive or negative (i.e. $+\Delta\alpha$ or $-\Delta\alpha$, where $\Delta\alpha > 0$) for each of the firing angles $\{\alpha_1, \alpha_2, \alpha_3\}$. The second-order partial derivatives required in (6.6) and (6.7) are automatically generated using the simulation-based approach at the optimum point.

$$
\begin{aligned}
\Delta D_{57} &= D_{\alpha_1\alpha_1}\Delta\alpha_1{}^2 + D_{\alpha_2\alpha_2}\Delta\alpha_2{}^2 + D_{\alpha_3\alpha_3}\Delta\alpha_3{}^2 \\
&\quad + D_{\alpha_1\alpha_2}\Delta\alpha_1\Delta\alpha_2 + D_{\alpha_1\alpha_3}\Delta\alpha_1\Delta\alpha_3 + D_{\alpha_2\alpha_3}\Delta\alpha_2\Delta\alpha_3 \\
&= \left(D_{\alpha_1\alpha_1} + D_{\alpha_2\alpha_2} + D_{\alpha_3\alpha_3}\right)\Delta\alpha^2 \\
&\quad + D_{\alpha_1\alpha_2}(\pm\Delta\alpha)(\pm\Delta\alpha) + D_{\alpha_1\alpha_3}(\pm\Delta\alpha)(\pm\Delta\alpha) + D_{\alpha_2\alpha_3}(\pm\Delta\alpha)(\pm\Delta\alpha) \\
&= \left(D_{\alpha_1\alpha_1} + D_{\alpha_2\alpha_2} + D_{\alpha_3\alpha_3} \pm D_{\alpha_1\alpha_2} \pm D_{\alpha_1\alpha_3} \pm D_{\alpha_2\alpha_3}\right)\Delta\alpha^2
\end{aligned}
$$

$$(6.6)$$

where,

$$
D_{\alpha_i\alpha_j} = \begin{cases} \left.\dfrac{1}{2}\dfrac{\partial^2}{\partial\alpha_i{}^2}D_{57}\right|_{Optimum} & i = j \\[2em] \left.\dfrac{\partial^2}{\partial\alpha_i\partial\alpha_j}D_{57}\right|_{Optimum} & i \neq j \end{cases}
$$

Hence

$$\left|\Delta\alpha_{\max}\right| \le \left(\frac{D_{57}^{\max}}{\max\left(D_{\alpha_1\alpha_1} + D_{\alpha_2\alpha_2} + D_{\alpha_3\alpha_3} \pm D_{\alpha_1\alpha_2} \pm D_{\alpha_1\alpha_3} \pm D_{\alpha_2\alpha_3}\right)}\right)^{1/2}$$

$$= \left(\frac{4\times10^{-4}}{10^{-3}\times\max\left(\frac{10.3}{2} + \frac{5.2}{2} + \frac{6.1}{2} \pm 5.1 \pm(7.7)\pm(-2.7)\right)}\right)^{1/2} = \left(\frac{0.4}{26.3}\right)^{1/2} = 0.123 \quad (6.7)$$

In the final expression of (6.7) the "max" function is used to select the combination of $+$ and $-$ signs that gives the largest value for the divisor, so as to yield the worst-case situation with the smallest magnitude for $\Delta\alpha$. Note that from (6.6) it can be concluded that in the expression (6.7), the situation of all three signs being negative is prohibited. This gives a result of $\left|\Delta\alpha\right| \le 0.123°$, for which the case was also simulated and the corresponding deviation in $HD_{57}$ was measured to be 2.1%, which is essentially the same as the maximum limit of 2%, thereby confirming the validity of this approach.

This example demonstrates that once the sensitivities are determined by the simulation-based sensitivity analysis method, further analysis can be conducted with simple mathematical calculations, and without any further need for time-consuming EMT simulations.

## 6.1.3    Tolerance Analysis of SHE Pattern for a High Power STATCOM

In the previous section a simple example of selective harmonic elimination scheme with 3 switching angles and with an ideal dc source was presented. The

assumption of a constant dc voltage made it possible to verify the results obtained from the developed simulation-based techniques by using an analytically available solution. In practice however, voltage-sourced converters are often supplied on the dc side through a capacitor. Unlike an idealized dc source a capacitor will experience voltage fluctuations during normal and transient operations of the converter. Although provisions for minimizing such fluctuations are incorporated into the design of the dc bus, small voltage ripple will still be present. Presence of ripple on the voltage waveform makes it difficult to find an analytical solution for the SHE scheme. Therefore, a simulation-based approach has to be used for analysis of this case. This thesis introduces the application of the developed simulation-based decision support tools for determining the sensitivity of the ripple harmonics to the switching angle uncertainty at the optimal operating point.

In this section, a static compensator (STATCOM) is considered as a practical application of SHE switching scheme with a non-ideal dc bus. A STATCOM is a FACTS device mainly used for fast reactive power compensation and voltage regulation in power networks, and its description is given in Chapter 4. Figure 6.3 shows the system, studied in this example.
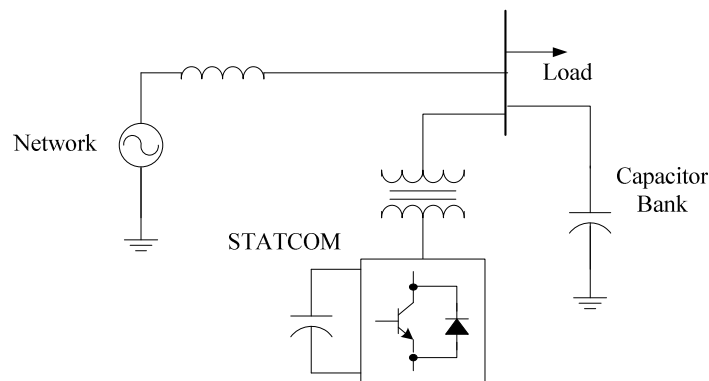


**Figure 6.3  Single line diagram of the STATCOM**

The specifications of the system are listed in Table 6.4. SHE switching pattern with five switching angles (as shown in Figure 6.4) is used in order to shape the output voltage waveform generated by the converter.

**Table 6.4  System specification: Tolerance analysis of SHE pattern**

| Network | 20 kV, 60Hz, SCR = 5 |
|---|---|
| STATCOM Transformer | 4.8 kV/20 kV, 8.0 MVA, $X_l$ = 15% |
| Capacitor Bank | 10 MVAR |
| Load | 25 MVA, pf = 0.85 |
| STATCOM Converter | 4.8 kV, ±8MVAR, C = 0.4 pu |
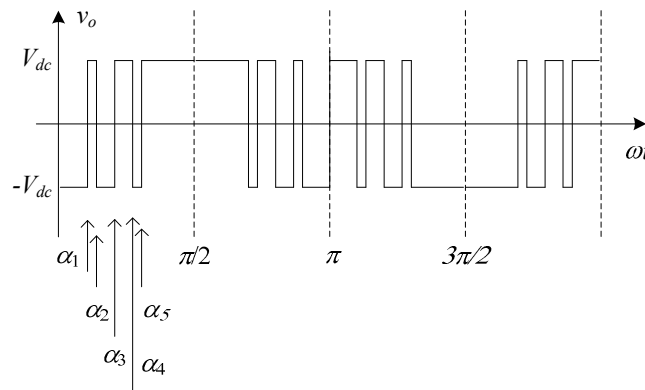


**Figure 6.4  SHE switching scheme with 5 switching angles in each quarter cycle**

## 6.1.3.1     Optimization of the Switching Pattern

In this section the developed simulation-based optimization method is used for finding an optimized set of switching angles for the STATCOM converter in order to eliminate certain harmonics while adjusting the fundamental component of the voltage. Due to the presence of capacitors, the dc side voltage of the STATCOM has ripples, and therefore, it is difficult to develop an analytical formula for the harmonic content of the

output voltage as a function of switching angles. As a result in this case simulation-based

optimization seems to be the only solution.

The method described in section 6.1.2.1 is used for the optimization using

simulation. With five switching angles in each quarter-cycle it is possible to eliminate the

four lowest dominant harmonics of the voltage waveform, i.e., $5^{th}$, $7^{th}$, $11^{th}$ and $13^{th}$ order

harmonics, while regulating the fundamental voltage as desired. Since the role of the

STATCOM is to regulate the ac voltage at the load bus, the optimization objective

function is formulated in terms of the load bus voltage, rather than the converter voltage

(as done in section 6.1.2.1). The equation (6.8) shows the objective function used in this

example.

$$f = \frac{(V_1 - V_{ref})^2}{V_{ref}^2} + \frac{V_5^2}{V_{ref}^2} + \frac{V_7^2}{V_{ref}^2} + \frac{V_{11}^2}{V_{ref}^2} + \frac{V_{13}^2}{V_{ref}^2} \tag{6.8}$$

In (6.8), $V_{ref}$ is the desired magnitude of the fundamental voltage at the load bus

(selected to be equal to the nominal ac phase voltage of the system, which is

$20kV/\sqrt{3} = 11.54kV$ rms), and $V_1$, $V_5$, $V_7$, $V_{11}$ and $V_{13}$ are the magnitudes of the

fundamental, $5^{th}$, $7^{th}$, $11^{th}$ and $13^{th}$ order harmonics obtained from the EMT simulation.

The optimization results are summarized in Table 6.5. As seen the harmonic

content of the load voltage has been reduced significantly (total harmonic distortion for

the first four harmonics was reduced from 5.2% to 1.0%), and also the fundamental value

of the ac voltage has been regulated to its nominal value (11.54kV rms). the above

optimization process required about 150 EMT simulation runs of the system.

**Table 6.5  Optimization results for the STATCOM selective harmonic elimination**

| | $V_{dc} = \pm4.5$ kV , $V_1 = 11.54$kV | | | | |
|---|---|---|---|---|---|
| | SHE Switching Angles | | | | |
| | $\alpha_1$ | $\alpha_2$ | $\alpha_3$ | $\alpha_4$ | $\alpha_5$ |
| Initial Values | 10.00° | 20.00° | 30.00° | 40.00° | 50.00° |
| Optimized Angles | 9.89° | 19.57° | 25.56° | 42.75° | 47.99° |
| | Harmonic Spectrum of the Output Voltage [kV] | | | | |
| | $V_1$ | $V_5$ | $V_7$ | $V_{11}$ | $V_{13}$ |
| Before Optimization | 10.53 | 0.14 | 0.51 | 0.06 | 0.11 |
| After Optimization | 11.53 | 0.01 | 0.01 | 0.07 | 0.09 |

The figures below show the simulation results of the operating point of the STATCOM, before and after optimization. The dc-bus voltage, the output voltage of the converter, and the ac voltage at the load bus are shown. Note that the ripple on dc voltage affects the output voltage of the converter as well. The difference can be seen by comparing the results to the ones shown in Figure 6.4. In addition harmonics injected by the STATCOM introduce distortion to the network voltage as well.
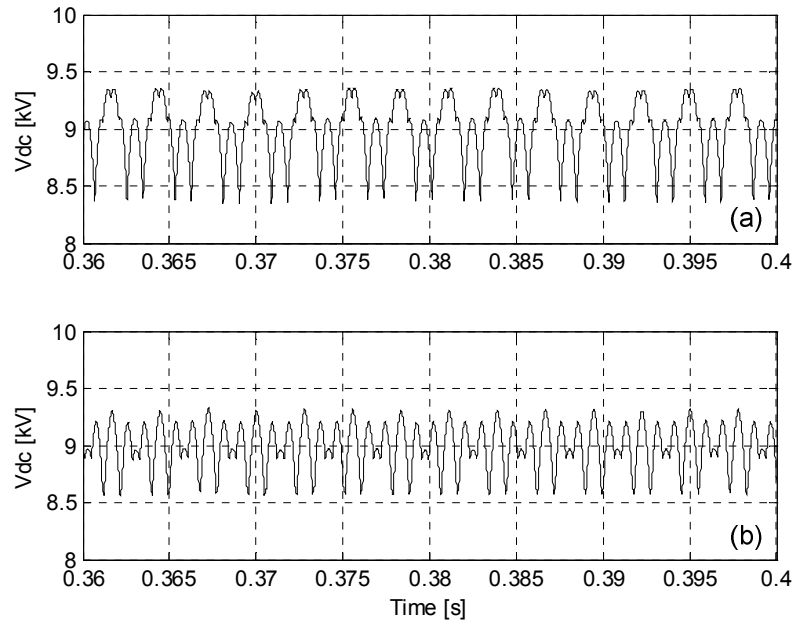


**Figure 6.5 The STATCOM dc-bus voltage**
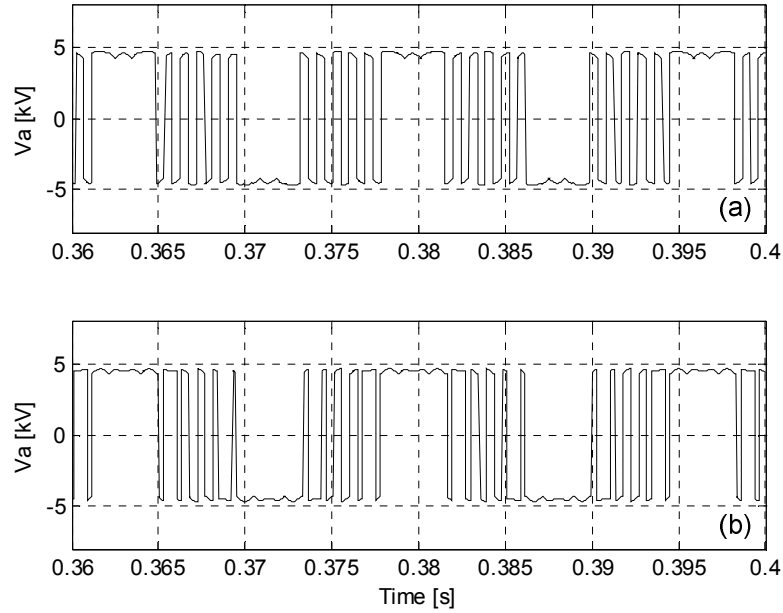
**(a) before optimization (b) after optimization**

**Figure 6.6  Output voltage of the STATCOM converter**

**(a) before optimization (b) after optimization**
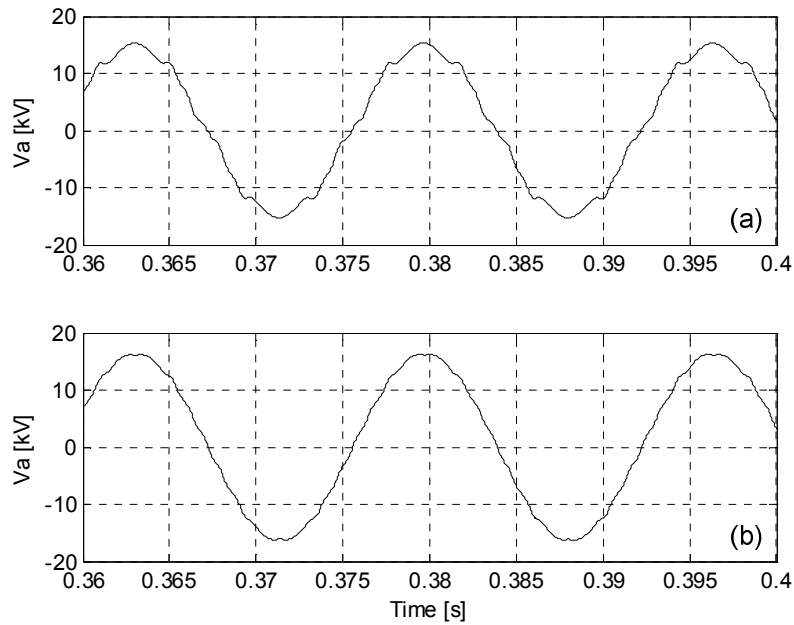


**Figure 6.7  Load ac voltage (a) before optimization (b) after optimization**

## 6.1.3.2        Worst-Case Analysis

When dc voltage fluctuations and firing mismatch are considered simultaneously, formulation of the sensitivity of the harmonics to switching angle variations becomes excessively difficult. In this section the proposed simulation-based sensitivity analysis method is used for estimating the sensitivity of the optimized harmonic spectrum of the output voltage when the switching mismatch is present. This sensitivity model is then used for tolerance analysis of the harmonic spectrum.

As an example the sensitivity of the 5$^{th}$ order harmonic to small variations in the switching angle is considered here. The performance index, shown in (6.9), is used for quantifying the 5$^{th}$ harmonic's re-appearance in the harmonic spectrum.

$$HD_5 = \frac{V_5^{\,2}}{V_{ref}^{\,2}} \qquad\qquad (6.9)$$

The above function has a minimum value of zero when 5$^{th}$ order harmonic disappears from the output voltage. It is readily seen that the optimized switching pattern obtained in the previous section is also a minimum for the performance index in (6.9). Therefore, in order to obtain meaningful results second-order representation of the performance index, as proposed in Chapter 5, is required. Table 6.6 shows the derivatives calculated by the simulation-based sensitivity analysis method.

The above derivatives are used to find the worst-case scenario for the re-emergence of the 5$^{th}$ order harmonic cause by firing angle mismatch. It is assumed that the optimal firing angles can be attained within a 0.1° tolerance. Note that the above

derivatives make it possible to develop a closed-form local representation of the performance index in the vicinity of the optimum; this closed-form formula can be used for tolerance analysis of the 5th order harmonic without any need for extra simulations. In the first two columns of Table 6.7 the worst-case combination of switching angle mismatches, which leads to the largest value of 5th order harmonic, is presented. For that combination estimations of 5th order harmonic are given when the first-order and second-order sensitivity methods are used. Results obtained using direct simulation are also shown for validation.

**Table 6.6  Sensitivity analysis results for the 5th order harmonic\***

| $HD_5$ | $\partial/\partial\alpha_1$ | $\partial/\partial\alpha_2$ | $\partial/\partial\alpha_3$ | $\partial/\partial\alpha_4$ | $\partial/\partial\alpha_5$ |
|---|---|---|---|---|---|
| 1 | 0.0146 | -0.0283 | 0.0145 | 0.0132 | -0.0548 |
| $\partial/\partial\alpha_1$ | 3.24 | -4.74 | 4.77 | 3.18 | -4.28 |
| $\partial/\partial\alpha_2$ | -4.74 | 6.76 | -5.54 | -3.57 | 5.60 |
| $\partial/\partial\alpha_3$ | 4.77 | -5.54 | 4.56 | 2.93 | -5.02 |
| $\partial/\partial\alpha_4$ | 3.18 | -3.57 | 2.93 | 2.04 | -3.41 |
| $\partial/\partial\alpha_5$ | -4.28 | 5.60 | -5.02 | -3.41 | 5.47 |

**\*Unit [$10^{-3}$/Degrees]**

**Table 6.7  Worst case scenario for the 5th order harmonic**

| $\Delta\alpha_1$ | +0.1° | 5th Order Harmonic (In Percentage of the Fundamental Voltage) | | |
|---|---|---|---|---|
| $\Delta\alpha_2$ | -0.1° | First-Order Estimation | Second-Order Estimation | Direct Simulation Result |
| $\Delta\alpha_3$ | +0.1° | | | |
| $\Delta\alpha_4$ | +0.1° | 0.4% | 2.4% | 2.4% |
| $\Delta\alpha_5$ | -0.1° | | | |

As shown the first order model gives an estimated value of 0.4%, while the value predicted by the second-order model is 2.4%. Note that direct simulation of the network for the worst-case combination of switching angles also yielded a value of 2.4% for the

fifth harmonic, which matches the second-order estimation. This confirms the necessity and also the accuracy of the proposed second-order method for sensitivity assessment around an optimum.

## 6.1.3.3        Statistical Tolerance Analysis of Harmonic Performance

In this section statistical behaviour of the harmonic content of the STATCOM voltage is determined using the proposed simulation-based surrogate modeling method. In order to verify the results obtained from the surrogate model obtained from the simulation-based sensitivity analysis, Monte-Carlo simulations were conducted on the detailed EMT simulation model. A uniform distribution with a maximum deviation of 0.1° was assumed for the switching angles, i.e. each firing angle could vary uniformly within a ±0.1° interval around its nominal value. In this case the nominal values were the optimum values obtained above. In order to quantify the harmonic content, performance indices shown in (6.10) were used.

$$HD_5 = \frac{V_5^{\,2}}{V_{ref}^{\,2}} \quad , \quad HD_7 = \frac{V_7^{\,2}}{V_{ref}^{\,2}} \quad , \quad HD_{11} = \frac{V_{11}^{\,2}}{V_{ref}^{\,2}} \quad , \quad HD_{13} = \frac{V_{13}^{\,2}}{V_{ref}^{\,2}} \tag{6.10}$$

The above performance indices show the level of each individual harmonic ($5^{th}$, $7^{th}$, $11^{th}$ and $13^{th}$). The statistical results from both methods (the actual EMT simulations and the surrogate models) are presented in Figures 6.8 to 6.11. As seen in the results, the results obtained from EMT simulation are close to the ones obtained from the surrogate models.

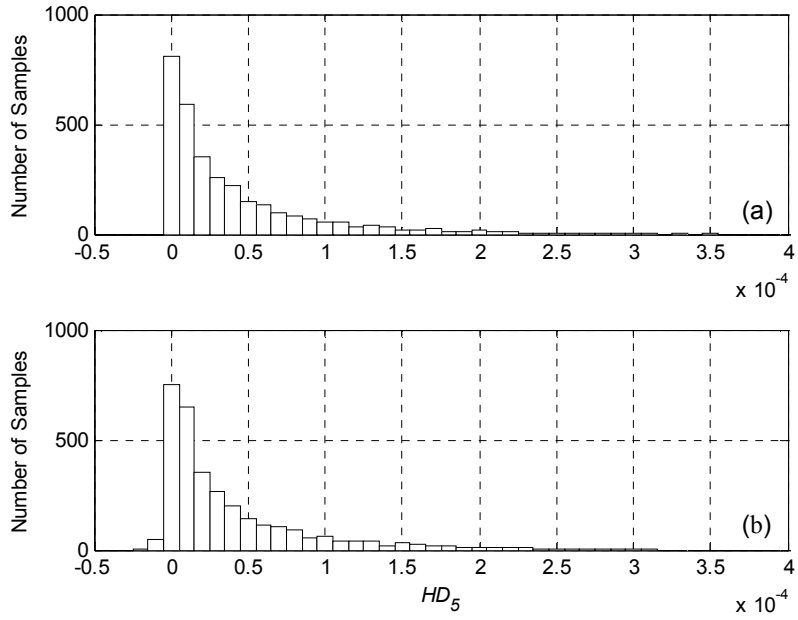**Figure 6.8  Histogram of $HD_5$ (a) EMT simulation (b) surrogate model**
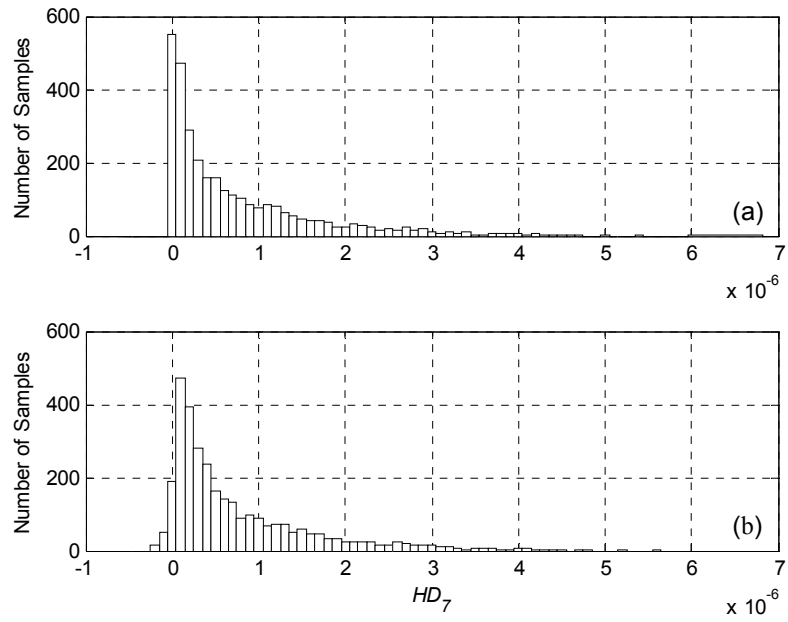


**Figure 6.9  Histogram of $HD_7$ (a) EMT simulation (b) surrogate model**
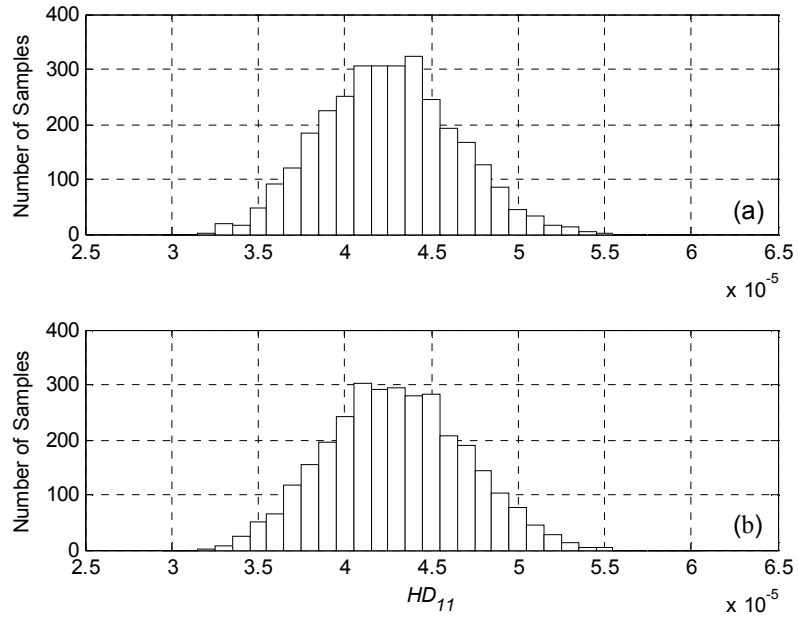
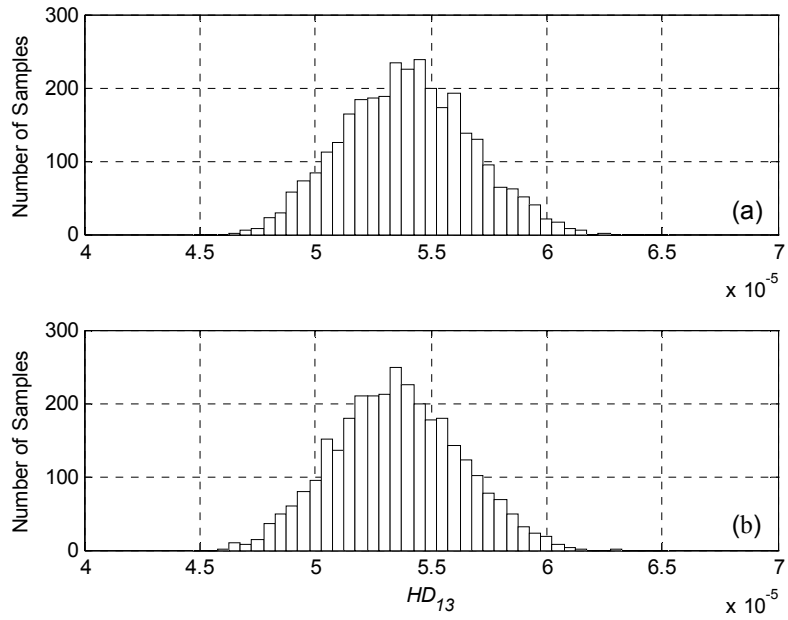**Figure 6.10 Histogram of $HD_{11}$ (a) EMT simulation (b) surrogate model**



**Figure 6.11 Histogram of $HD_{13}$ (a) EMT simulation (b) surrogate model**

As can be seen in the figures, the statistical analysis done on the actual simulation model and the ones obtained from the sensitivity models (surrogate models) are reasonably close. Note that the Monte-Carlo approach gives more accurate results as the number of samples is increased, and so the small differences could be also due to limited number of samples.

**Table 6.8  Statistical analysis results.**

| | Harmonic performance of the SHE switching pattern for the STATCOM* | | | | | |
| | Average | | Standard Deviation | | Skewness | |
| | Surrogate Model | EMT Simulation | Surrogate Model | EMT Simulation | Surrogate Model | EMT Simulation |
| $HD_5$ | 0.0361 | 0.0388 | 0.0480 | 0.0502 | 2.2675 | 2.1405 |
| $HD_7$ | 0.0007 | 0.0007 | 0.0008 | 0.0009 | 1.8480 | 1.8627 |
| $HD_{11}$ | 0.0430 | 0.0425 | 0.0039 | 0.0038 | 0.0922 | 0.0984 |
| $HD_{13}$ | 0.0534 | 0.0540 | 0.0027 | 0.0027 | 0.1088 | 0.0725 |

* All values to be multiplied by $10^3$

Table 6.8 presents the average value and the standard deviation of each parameter obtained from both the surrogate models and the actual simulations. In the table the results are based on 3125 samples for each method. As seen in Table 6.8, the average, standard deviation, and the skewness obtained from the actual simulations are close to the ones obtained from the surrogate models. The simulation time required for the first method, which uses direct EMT simulations of the network, is about 8.6 hours; whereas the required evaluation time for the second method using surrogate models is about 6 minutes (Using a computer with 4GB of RAM and a 3GHz AMD Athlon™ 64 X2 Dual Core Processor) a saving of 9900% in computing time. This is due to the fact that the proposed sensitivity analysis approach requires only 31 EMT simulation runs, based on

(5.13), to obtain the parameter values of the sensitivity models. Once the sensitivity models are obtained, Monte-Carlo-type evaluations can be done on these simple models, which take only a few seconds. On the other hand performing Monte-Carlo simulation of the fully detailed model requires 3125 simulations of the full system (each simulation takes about 10s, which results in total simulation time of 8.6 hours).

Statistical analysis results provide important information that help the designer in the decision making process. For example assume that in the above example one of the design requirements is to keep each individual harmonic below 1.5% of the fundamental component. Based on the above results, although at the worst-case scenario the magnitude of the $5^{th}$ order harmonic exceeds 1.95% of the fundamental voltage (equivalent to $HD_5$=3.8 as shown in Figure 6.8), statistical analysis shows that the probability of having a $5^{th}$ order harmonic level more than 1.4% (equivalent to $HD_5$>2) is very low (less than 100 samples out of 3125 samples). In such a situation the designer may accept a small risk of design failure (having $5^{th}$ order harmonic level above 1.5%) to reduce the price of the system by using smaller-size filters, for example.

## 6.2    Uncertainty Analysis of a Static Compensator (STATCOM)

As another application of the proposed methods, in this section the uncertainty analysis methods are utilized for studying distribution of the dynamic behaviours of a static compensator controlling the ac voltage at its point of common coupling (PCC).

## 6.2.1 System Description

In this section the same static compensator case, presented in Chapter 4 is used to demonstrate the effectiveness of the proposed optimization methods. Figure 6.12 shows the schematic diagram of the network used for this example with the system data as given Chapter 4.
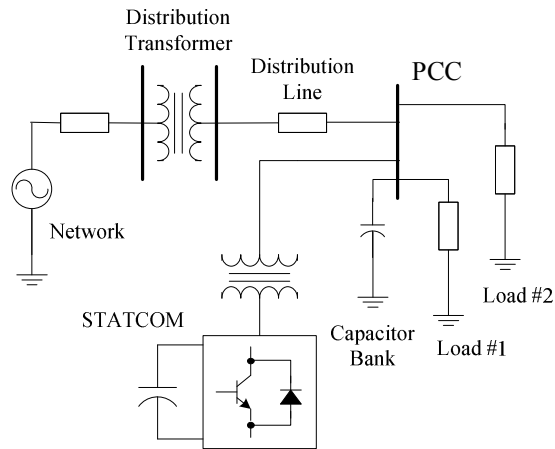


**Figure 6.12  The STATCOM system**

**Table 6.9  Control system parameters of the STATCOM**

| DC-capacitor | $K_1$ | $0.23 \times 10^{-1}$ |
|---|---|---|
| voltage controller | $T_1$ | 0.16 |
| $i_d$ controller | $K_2$ | 4.5 |
| | $T_2$ | $0.87 \times 10^{-2}$ |
| Network voltage | $K_3$ | $0.18 \times 10^{-1}$ |
| controller | $T_3$ | $0.57 \times 10^{-1}$ |
| $i_q$ controller | $K_4$ | 6.5 |
| | $T_4$ | $0.87 \times 10^{-3}$ |
| Filter time | $T_{f1}$ | $0.1 \times 10^{-1}$ |
| constants | $T_{f2}$ | $0.1 \times 10^{-2}$ |
| | $T_{f3}$ | $0.5 \times 10^{-3}$ |

The STATCOM in Figure 6.12 uses a three-level SPWM controlled voltage sourced converter. Control of the dc-bus voltage and the ac network voltage is conducted

through a de-coupled control system. The control system parameters for this part are shown in Table 6.9 (see Figure 4.4 for controller structure).

## 6.2.2      Uncertainty Analysis

In this section the effect of variations of the system parameters on the variations in the transient response of the STATCOM is studied. The parameters of concern considered here are the hardware components: distribution line resistance and inductance ($R_{DL}$ and $L_{DL}$), distribution transformer leakage inductance ($L_{DT}$), size of the capacitor bank ($C_B$), STATCOM transformer leakage inductance ($L_{ST}$), and load resistance and inductance ($R_L$ and $L_L$). However, as in the system $L_{DL}$ and $L_{DT}$ are in series with each other and the same tolerance is considered for both, they have been replaced by one inductance ($L_D$) to simplify the problem to some extent. Note that although in this example only the above parameters are considered, in general the choice and the number of uncertain parameters will depend on the specifics of the case at hand. In this case it is also assumed that the control system parameters do not change.

In order to be able to assess the transient behaviour of the system, it is first necessary to apply a disturbance to the system. In this case, in order to generate a transient phenomena, at $t = 0.5$s, load #1 is disconnected from the system, to which the STATCOM responds by adjusting its injected reactive power to maintain the network voltage at its desired level. In order to quantify the system performance during this transient phenomenon, the transient performance index, give in (6.11), was defined.

$$f_T\left(R_{DL},L_D,C_B,L_{ST},R_L,L_L\right)=\int_{t=0.45s}^{t=0.95s}\left(\frac{v\left(t,R_{DL},L_D,C_B,L_{ST},R_L,L_L\right)-V_{ref}}{V_{ref}}\right)^2 dt \qquad (6.11)$$

The above performance index penalizes the difference between the actual network voltage ($V_{ref}$) and its reference value. Therefore, the higher the value of $f_T$ the worse is the system performance. Figure 6.13 shows the system response at the nominal operating point where the performance index has a value of $f_T = 3.69 \times 10^{-3}$.
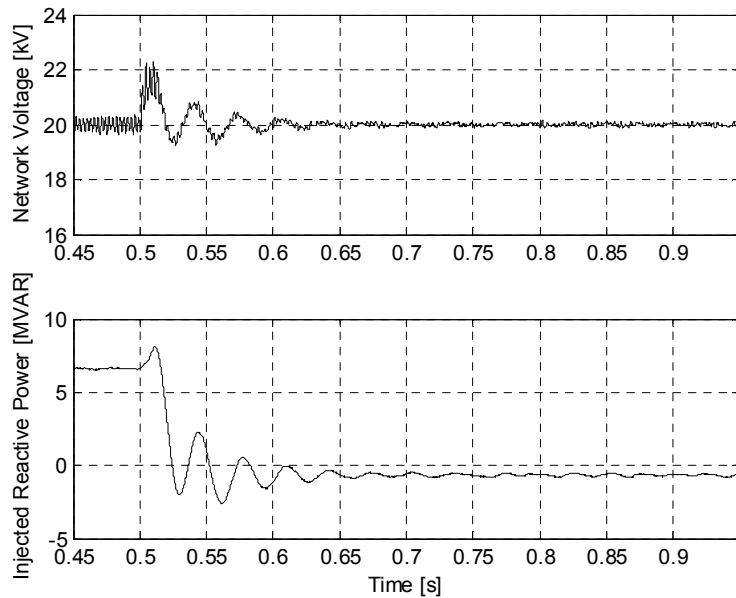


**Figure 6.13  The STATCOM response at the nominal operating point**

## 6.2.2.1     **Worst-Case Analysis**

It is assumed that the system parameters ($R_{DL}$, $L_D$, $C_B$, $L_{ST}$, $R_L$, $L_L$) each have a normal distribution with a standard deviation of $\sigma$ = 5%. Mathematically, the normal distribution does not impose any limits on its minimum or maximum values. For practical reasons, however, the spread of values in the computer experimentation was limited to $\pm 3\sigma$ , as 97% of the values will be covered within this range.

The tolerance analysis was carried out using the proposed sensitivity-based method described in the previous chapter. Similar to the previous example in section 6.1.3.2, the worst-case scenario of the system response was determined using a surrogate model, and verified using the fully detailed EMT simulation. The results of the worst-case analysis are shown in Table 6.10. Note that at the worst-case condition the value of $f_T$ increases from $3.69 \times 10^{-3}$ to $10.9 \times 10^{-3}$, an increase of 295%.

$$
\begin{aligned}
f_T\left(R_{DL}, L_D, C_B, L_{ST}, R_L, L_L\right) &= 3.69 \times 10^{-3} - 5.91 \times 10^{-5} \Delta R_{DL} + 1.14 \times 10^{-2} \Delta L_D \\
&+ 1.26 \times 10^{-3} \Delta C_B + 3.95 \times 10^{-3} \Delta L_{ST} - 1.00 \times 10^{-4} \Delta R_L + 1.24 \times 10^{-4} \Delta L_L \\
&+ \frac{1}{2} 1.38 \times 10^{-3} \Delta R_{DL}{}^2 - 1.55 \times 10^{-2} \Delta R_{DL} \Delta L_D + 2.10 \times 10^{-3} \Delta R_{DL} \Delta C_B \\
&- 4.33 \times 10^{-3} \Delta R_{DL} \Delta L_{ST} + 2.33 \times 10^{-3} \Delta R_{DL} \Delta R_L - 5.95 \times 10^{-3} \Delta R_{DL} \Delta L_L \\
&+ \frac{1}{2} 6.41 \times 10^{-2} \Delta L_D{}^2 + 1.12 \times 10^{-2} \Delta L_D \Delta C_B + 7.07 \times 10^{-2} \Delta L_D \Delta L_{ST} \\
&+ 5.02 \times 10^{-3} \Delta L_D \Delta R_L - 2.30 \times 10^{-3} \Delta L_D \Delta L_L + \frac{1}{2} 1.25 \times 10^{-2} \Delta C_B{}^2 \\
&- 4.52 \times 10^{-4} \Delta C_B \Delta L_{ST} - 1.45 \times 10^{-3} \Delta C_B \Delta R_L - 5.86 \times 10^{-3} \Delta C_B \Delta L_L \\
&+ \frac{1}{2} 1.87 \times 10^{-2} \Delta L_{ST}{}^2 + 1.62 \times 10^{-3} \Delta L_{ST} \Delta R_L - 3.73 \times 10^{-3} \Delta L_{ST} \Delta L_L \\
&+ \frac{1}{2} 1.40 \times 10^{-2} \Delta R_L{}^2 - 6.61 \times 10^{-3} \Delta R_L \Delta L_L + \frac{1}{2} 1.17 \times 10^{-2} \Delta L_L{}^2
\end{aligned}
$$

$$(6.12)$$

**Table 6.10  Worst-case scenario of the STATCOM case**

| | $\Delta R_{DL}$ | $\Delta L_D$ | $\Delta C_B$ | $\Delta L_{ST}$ | $\Delta R_L$ | $\Delta L_L$ |
|---|---|---|---|---|---|---|
| Change in the Parameter | -15% | 15% | 15% | 15% | -15% | 15% |
| | First-Order Appr. | | Second Order Appr. | | EMT Simulation | |
| $f_T$ value | $6.4 \times 10$-3 | | $10.0 \times 10$-3 | | $10.9 \times 10$-3 | |

The results show that although the operating point is not an optimal one, the second-order approximation still provides a more accurate result. This is likely because the perturbation in the performance index ($f_T$) is close to 300%, and a linear fit is too

simplistic, necessitating a higher order surrogate model. In Figure 6.14 the system response with the original parameter values is compared with the system response for the worst possible operating condition. Figure 6.14 shows that the uncertainty in the values of the STATCOM components leads to significant differences in the damping of the network voltage.
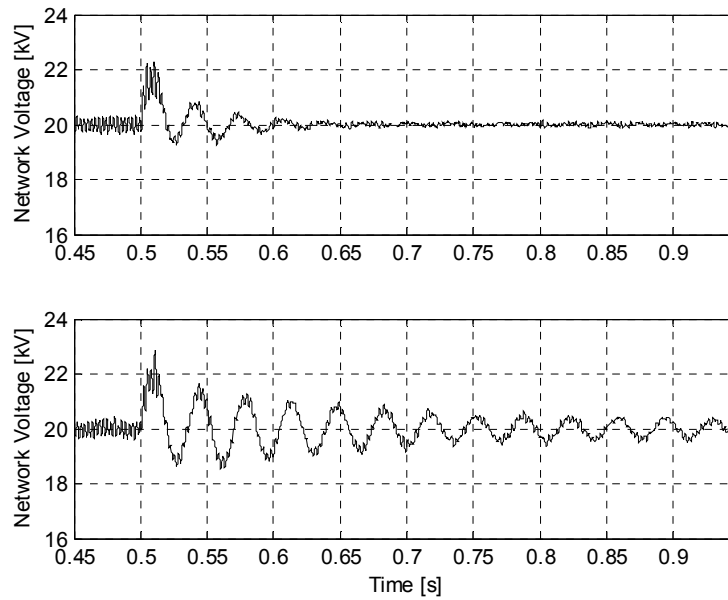


**Figure 6.14  The STATCOM response at the nominal operating point**

**(Top) and the worst-case operating point (Bottom)**

## 6.2.2.2    Statistical Tolerance Analysis of the STATCOM Dynamic Response

In the design process, a compromise is often required where the risk is reduced to a small and acceptable value rather than completely eliminated. This is done in order to reduce the cost or to meet some other design constraints. Therefore it is necessary to perform statistical tolerance analysis to evaluate the risk level involved in each design. In this section statistical analysis has been carried out using two different methods, namely

(i) Monte-Carlo EMT simulation, and (ii) Monte-Carlo simulation with the surrogate models of (6.12). Figure 6.15 shows the histogram of the results obtained from both methods after 2500 runs.
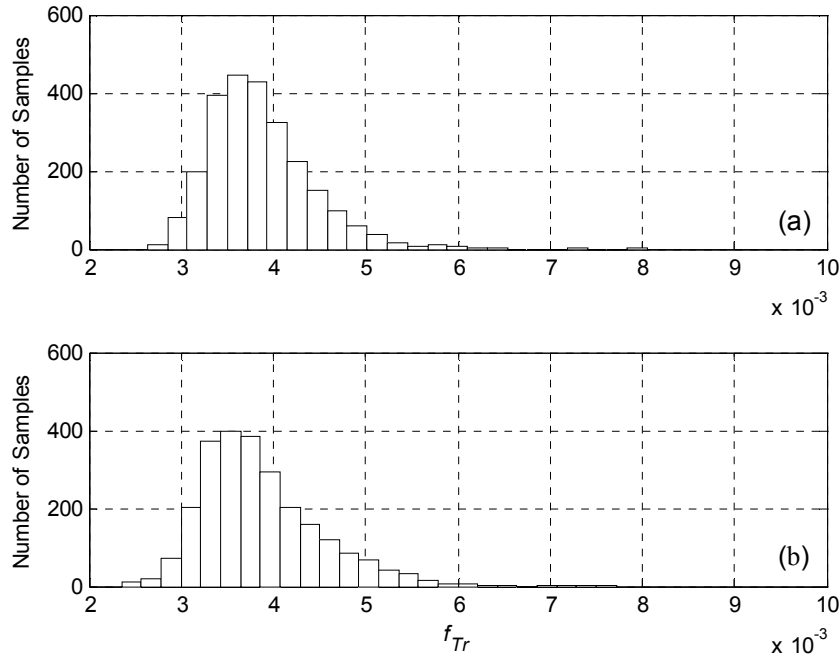


**Figure 6.15 Histogram of $f_T$ for the STATCOM case**
**(a) EMT simulation results (b) results obtained from the surrogate model**

Use of surrogate models instead of the EMT simulation results in a significant time saving. For the above results, use of EMT simulation took about 14 hours, whereas use of the surrogate models took about 15 minutes (on a computer with 3.0GHz AMD Athlon 64 Dual Core Processor and 4GB of RAM).

Assume that the design specification dictates that the performance index $f_T$ be no greater than $4.5 \times 10^{-3}$. The detailed Monte Carlo analysis shows that the number of samples higher than this value is 335 out of the total of 2500, giving a probability of

13.6% of exceeding the design specification. The simplified model essentially gives a similar result of 14.8%. If this risk is unacceptable, then the tolerances on the components must be made more stringent and the components will most likely cost more money.

# Chapter 7  Concluding Remarks

## 7.1      Contributions

The thesis introduces new decision support tools that can be used to facilitate the design of power systems. These tools assist the design process by conducting multiple run simulations in an intelligent manner, so that the design information required by the user is automatically extracted from the system.

Specifically, the thesis introduces a new gradient-based optimization approach for electromagnetic transient simulation and shows that it is often more effective than direct optimization methods. The thesis introduces supervisory optimization algorithms that handle multiple objectives, and include the effects of uncertainty in the design of power equipment and systems.  The use of an electromagnetic transient (EMT) simulation program makes the developed decision support tools especially suitable for power system and power electronic applications. The details of the contributions made by the author are outlined in three categories below.

### 7.1.1      Gradient-Based Optimization

The main highlights of the thesis contributions in the area of gradient-based optimization are as follows.

- A gradient-based optimization algorithm was adopted for simulation-based optimization.

- The developed gradient-based simulation facility was equipped with a constraint handling feature.

Previous work on simulation based optimization [13] considered direct methods (non-gradient based) for optimization. The belief was that gradient-based techniques would be too time-consuming due to the considerable number of simulations required for numerically computing a gradient. However, this thesis showed that by using a suitably conditioned gradient-based method, the total number of steps needed to be taken to reach to an optimum can be significantly reduced. Therefore, although in the developed gradient-based method the required number of simulation runs in each step is more than that of the direct method, the overall optimization time of the gradient-based method is often comparable to that of the direct method. This is an important conclusion as the gradient-based methods can be easily parallelized, which provides the opportunity to develop fast optimization facilities. Moreover, a constraint handling feature was added to the optimization process that helps the designer to limit the design parameters within a user defined ranges.

## 7.1.2    Multi-Objective Optimization

The main highlights of the thesis contributions in the area of multi-objective optimization are as follows.

- The thesis adopts the Pareto method as a structured way for handling multi-objective optimization problems.

- A multiple-run optimization process was developed, which is capable of efficiently generating the Pareto frontier.

- The proposed method was successfully utilized for analysing two practical cases namely (1) a three level STATCOM and (2) an induction motor drive system.

The developed Pareto Frontier graphically identifies the tradeoffs between multiple objectives and enables the designer to select the optimum parameters that provide an acceptable compromise between competing objectives. The usefulness of the optimization tool has been demonstrated by using two design examples, (1) a three-level STATCOM and (2) an induction motor drive system. The results showed that the proposed multi-objective optimization method is capable of handling multi-objective optimization problems.

### 7.1.3    Uncertainty Analysis

The main highlights of the thesis contributions in the area of uncertainly-analysis are as follows.

- The thesis creates a surrogate model that replaces the detailed simulation by a second-order sensitivity model which can be used to calculate the performance indices of the system. The higher order allows the uncertainty analysis to be done for optimal operating points.

- A multiple-run uncertainty analysis process was developed that automatically calculates the parameters of the second-order models.

- The surrogate models were used to solve the worst-case case tolerance analysis problems. In addition, the simplicity of the models makes it possible to solve the inverse problem easily and with less computational effort.

- The above surrogate models can also be used for Monte-Carlo simulation to obtain statistical distributions. Using surrogate models instead of the actual EMT simulations makes the uncertainty analysis significantly faster as the evaluation of a surrogate model needs considerably less computational effort compared to detailed EMT simulations.

- By using two practical application examples namely (1) the selective harmonic elimination and (2) the three-level STATCOM, it was shown that the developed technique is capable of producing accurate results in a significantly shorter time.

The capability of the uncertainty analysis tool was demonstrated by using two examples, (1) uncertainty analysis of the selective harmonic elimination (SHE) switching pattern, and (2) uncertainty analysis of the dynamic response of a three-level STATCOM. In the first example, the sensitivity information was effectively used to calculate the permitted deviations of switching angles to keep the key harmonics below a satisfactory level. In addition, statistical analysis provided an estimation of the expected harmonic levels of the output voltage. In the second example, the uncertainty analysis tool was used to analyze the dynamic behaviour of a STATCOM, when the system parameters varied within their permissible ranges. The analysis not only resulted in an estimation of the worst-case performance, but also provided statistical information about the distribution of system

response. In both examples, Monte-Carlo EMT simulations were used to verify the accuracy of the results.

## 7.2     Recommendations for Future Work

In this section some of the suggestions for future work based on this research are summarised. As two different decision support algorithms were developed during the course of this research, the future work is explained separately for each one.

### 7.2.1     Optimization

The main highlights for the future expansions of the simulation-based optimization method are as follows.

- Combining the sensitivity analysis methods and gradient-based optimization in order to increase the optimization speed;

- Employing other optimization techniques such as response surface methodology (RSM) and heuristic methods for the purpose of the optimization;

- Investigating other methods for handling multi-objective problems;

- Using heuristic methods for generation of Pareto Frontier;

- Addressing the problem of optimization under uncertainties and tolerance optimization.

In this research in order to obtain the gradient vector required by the optimization algorithm, multiple-run approach has been used; for the electrical networks, sensitivity analysis techniques can be used for fast calculation of the gradient vector. Using such methods the gradient vector can be obtained in much fewer number of simulations, thus the speed of the optimization tool can be increased.

Other modern optimization techniques such as response surface methodology and heuristic methods can be also implemented for simulation-based optimization to compare their performance with the available techniques and to study their advantages and their short-comings. This way the user can select the optimization method based on the design requirements.

In this work the concept of Pareto optimality has been introduced for handling multiple objective problems. In order to obtain the Pareto frontier a sequence of optimization runs has been used. However, the Pareto frontier is not the only way for handling multiple objective problems and other methods for handling such problems should be also investigated.

The capability to handle uncertainties in an optimization procedure is one of the important issues in the optimization area. There are many examples in which certain parameters (such as the size of the load, the impedance of the network, etc.) are not exactly known, and therefore special care should taken for handling such problems. Therefore as part of the future work, the problem of optimization under uncertainty has to be addressed.

### 7.2.2        Uncertainty Analysis

In this thesis second-order estimation has been done using a multiple-run simulation approach. The method was based on estimation of the first and second-order terms of the Taylor's expansion of the performance index. However, this method can be improved by using a Response Surface Method (RSM), in which the sampling of the simulation points and the accuracy of the model changes based on the properties of the case at hand to minimize the required number of simulation runs. In addition Stochastic Response Surface Method (SRSM) can be used to improve the probabilistic convergence of the surrogate models.

In order to obtain the second-order estimation, this thesis proposes to use a multiple-run simulation approach. When the number of system parameters is large, this approach requires a large number of simulation runs to find the model, which could lead to a long processing time. However, for a large number of cases (where the simulation model is simple enough) faster sensitivity analysis methods such as adjoint network approach can be used. Therefore, an important future work could be examining these methods in the context of power system simulation.

## 7.3        List of Publications Related to This Thesis

Here is a list of publications related to this work.

*Journal Papers*

- M. Heidari, S. Filizadeh, and A. M. Gole, "Electromagnetic Transients Simulation Based Surrogate Models for Tolerance Analysis of FACTS Apparatus", in Progress.

- M. Heidari, S. Filizadeh, and A. M. Gole, "Support Tools for Simulation-Based Optimal Design of Power Networks with Embedded Power Electronics", *IEEE Trans. Power Delivery*, vol. 23, no. 3, pp. 1561 – 1570, Jul 2008

- S. Filizadeh, M. Heidari, A. Mehrizi-Sani, J. Jatskevich, and J. A. Martinez, "Techniques for Interfacing Electromagnetic Transient Simulation Programs with General Mathematical Tools", *IEEE Trans. Power Delivery*, vol. 23, no. 4, pp. 2610 – 2622, Oct 2008

*Conference Papers*

- M. Heidari, S. Filizadeh, A. M. Gole, "Application of simulation support tools in control system design of FACTS elements", *in Proc. 2008 National Power Systems Conference (NPSC 08)*, Mumbai, India.

- M. Heidari, S. Filizadeh, and A. M. Gole, "Computer-Aided Sensitivity Analysis for Optimal Systems", *in Proc. 7th International Conference on Power Systems Transients (IPST'07)*, Lyon, France, Jun 2007

- S. Filizadeh and M. Heidari, "Interfacing Methods for Design-Oriented Electromagnetic Transient Simulation", *in Proc. 2009 IEEE Power and Energy Society General Meeting (2009 IEEE PES General Meeting)*, Calgary, AB, Canada, pp. 1 – 5, Jul 2009

# Appendix A    Gradient-Based Optimization

An optimization problem can be defined as finding the minimum (or maximum) of a mathematical function, commonly referred to as an objective function (OF), within a specified parameter space. Even though analytical solutions can be found for simple objective functions it is generally difficult to find the optimum point of a nonlinear multivariable function. As a result optimization algorithms are used for solving such problems. In these methods the optimal point of the OF is found by following an iterative search process. The search starts by selecting an initial point(s). A set of mathematical techniques are then used to move the initial point(s) in the search space until the best value of the objective function (the minimum value for a minimization problem) is found. As in this work a gradient-based optimization algorithm has been implemented, in this section some the common gradient-based optimization methods are explained and the advantages and disadvantages of each method is briefly discussed.

Gradient-based optimization methods use the information obtained from the derivatives of the objective function to find a suitable direction for movement in the search space. As a result these methods are generally faster compared to other optimization techniques. However, there are two main disadvantages for these methods. Firstly since these methods use the derivative information they cannot be applied to discontinuous objective functions (OF). Secondly the calculation of derivatives could be a time consuming task, which sometime makes the whole procedure considerably slow. In this section, some of the commonly used gradient-based methods are explained.

# A.1    Cauchy's Method

Cauchy's method can be classified as one of the steepest descent methods, in which only the first-order derivatives of the function are used. Generally in a steepest descent method, the problem is to find a direction vector so that the initial velocity of function change in that direction is maximized, while the vector has unity norm. In other words, the direction vector should be chosen so that it maximizes $\Delta f$ and makes $\|\mathbf{d}\| = 1$, where $\mathbf{d}$ is the direction vector. Based on the kind of norm being used different steepest descent methods can be obtained. If the Euclidean norm (2-norm) is used, it yields the Cauchy's method of optimization, in which the direction vector is obtained as follows [62].

$$\mathbf{d} = -\frac{\nabla f}{\|\nabla f\|} \tag{A.1}$$

Having the above direction vector, in each interaction of Cauchy optimization method the decision vector (vector of the current values of the parameters) is updated using the following equation, in which $s$ is the step length and it is found using a line search algorithm.

$$\mathbf{x}^{(k+1)} = \mathbf{x}^{(k)} - s^{(k)} \frac{\nabla f\left(\mathbf{x}^{(k)}\right)}{\left\|\nabla f\left(\mathbf{x}^{(k)}\right)\right\|} \tag{A.2}$$

The main advantage of Cauchy's steepest descent method is its simplicity. Simplicity is an important factor in practice, not only because it makes the implementation easier but also it causes the method to be less vulnerable to numerical

errors. Application of this method for optimization of power electronic systems is reported in [17].

## A.2    Newton's Method

The Cauchy's method only uses the first-order information of the objective function; however, one can take second-order terms into account as follows.

$$f(\mathbf{x}) = f(\mathbf{x}_0) + \nabla f(\mathbf{x}_0)\Delta\mathbf{x} + \frac{1}{2}\Delta\mathbf{x}^T\nabla^2 f(\mathbf{x}_0)\Delta\mathbf{x} + \cdots \tag{A.3}$$

Neglecting the third and higher order terms one can approximate the function using the first and second order terms. Knowing the fact that the gradient of a function at its optimum is zero, one can solve the above estimation to find the $\mathbf{x}_0$ for which the gradient vector is zero; this leads to Newton's method of optimization, which is formulated as follows.

$$\mathbf{x}^{(k+1)} = \mathbf{x}^{(k)} - \nabla^2 f\left(\mathbf{x}^{(k)}\right)^{-1}\nabla f\left(\mathbf{x}^{(k)}\right) \tag{A.4}$$

Similar to Cauchy's method, the Newton's method can be also classified as a steepest descent method, in which the quadratic norm defined by the Hessian is used [97]. The Hessian quadratic norm can be calculated as follows.

$$\|\mathbf{u}\|_{\nabla^2 f(x)} = \left(\mathbf{u}^T\nabla^2 f(x)\mathbf{u}\right)^{1/2} \tag{A.5}$$

It has been observed that Newton's method does not work well for non-quadratic functions, especially when the starting point is far from the optimum point. However, it is possible to improve this method by combining Newton's method with a line search algorithm [62], as shown below.

$$\mathbf{x}^{(k+1)} = \mathbf{x}^{(k)} - s^{(k)} \nabla^2 f\left(\mathbf{x}^{(k)}\right)^{-1} \nabla f\left(\mathbf{x}^{(k)}\right) \tag{A.6}$$

In the above equation, $s$ should be determined so that it minimizes the objective function (OF).

## A.3     Marquardt's Method

Since Cauchy's method is more effective when the point is far from the optimal point, and Newton's method is better when the point is close to the optimal point, Marquardt introduced a method to have both advantages at the same time. This method is shown in the following equation [74].

$$\mathbf{x}^{(k+1)} = \mathbf{x}^{(k)} - \left[\nabla^2 f\left(\mathbf{x}^{(k)}\right)^{-1} + s^{(k)}\mathbf{I}\right]^{-1} \nabla f\left(\mathbf{x}^{(k)}\right) \tag{A.7}$$

It can be seen that when $s$ is large, Marquardt's method tends to Cauchy's method, and when $s$ is small it tends to Newton's method. On the other hand, it is known that usually step length is large when the point is far from the optimum point, and it is small when the point is close to optimum point, so Marquardt's method has both advantages of Cauchy's and Newton's methods.

## A.4       Conjugate Gradient Methods

It was mentioned that Marquardt's method exhibits both positive characteristics of Cauchy's and Newton's methods. However, the drawback of this method is that it uses second-order derivatives to find the optimum point. Calculation of second-order derivatives of a function using numerical methods is a time-consuming process, and is likely to introduce numerical errors. In this section, the conjugate gradient methods are introduced, which have a fast convergence rate and only use the first-order derivatives of the objective function.

Given an $N \times N$ arbitrary matrix (**C**) directions, $\mathbf{d}_1$, …, $\mathbf{d}_N$ are called conjugate directions if we have:

$$\mathbf{d}_i^{\mathrm{T}} \mathbf{C} \mathbf{d}_j = 0 \qquad \text{for all} \quad i \neq j \tag{A.8}$$

It can be shown that the optimal solution of the following quadratic function can be found by $N$ line searches in the directions of $\mathbf{d}_1$, …, $\mathbf{d}_N$ [74].

$$f(\mathbf{x}) = \mathbf{a} + \mathbf{b}^{\mathrm{T}} \mathbf{x} + \mathbf{x}^{\mathrm{T}} \mathbf{C} \mathbf{x} \tag{A.9}$$

The above theorem is useful for optimization process, considering the fact that every function can be approximated by a quadratic function around its optimum. The only remaining question is how to find the above conjugate directions. Fletcher and Reeves suggested the following method for finding the directions [53].

$$\mathbf{d}^{(k+1)} = -\nabla f^{(k+1)} + \frac{\left\|\nabla f^{(k+1)}\right\|^2}{\left\|\nabla f^{(k)}\right\|^2}\mathbf{d}^{(k)}$$

$$\mathbf{d}^{(0)} = -\nabla f^{(0)}$$

(A.10)

Comparing the Fletcher-Reeves method with other gradient-based methods shows that this method is capable of effectively handling objective functions with complex shapes [74].

## A.5     Quasi-Newton Methods

Quasi-Newton methods also have appealing characteristics of Newton's method while still using only the first-order derivatives of the OF. Quasi-Newton methods have the following form.

$$\mathbf{x}^{(k+1)} = \mathbf{x}^{(k)} - s^{(k)}\mathbf{A}^{(k)}\nabla f\left(\mathbf{x}^{(k)}\right)$$

(A.11)

where matrix $\mathbf{A}$ called the metric matrix. Recalling from the previous sections, if $\mathbf{A}$ is the inverse of Hessian matrix, the above equation is exactly Newton's method. However, in Quasi-Newton methods in order to avoid the use of second-order derivatives, instead of inversed Hessian matrix, the metric matrix is used. In each iteration this matrix is modified so that it eventually converges to the inverse of Hessian matrix. The sequence is usually traced in the following form.

$$\mathbf{A}^{(k+1)} = \mathbf{A}^{(k)} + \mathbf{A}_c^{(k)}$$

(A.12)

where $\mathbf{A}_c$ is the correction matrix. There are different types of correction matrices proposed by different researchers. One of them is the method proposed by Davidon, Fletcher and Powell (DFP), which has the following form [62].

$$\mathbf{A}^{(k+1)} = \mathbf{A}^{(k)} + \frac{\Delta\mathbf{x}^{(k)}\Delta\mathbf{x}^{(k)^T}}{\Delta\mathbf{x}^{(k)^T}\Delta\mathbf{g}^{(k)}} - \frac{\mathbf{A}^{(k)}\Delta\mathbf{g}^{(k)}\Delta\mathbf{g}^{(k)^T}\mathbf{A}^{(k)}}{\Delta\mathbf{g}^{(k)^T}\mathbf{A}^{(k)}\Delta\mathbf{g}^{(k)}} \tag{A.13}$$

where $\Delta\mathbf{g}$ can be calculated as follows:

$$\Delta\mathbf{g}^{(k)} = \nabla f\left(\mathbf{x}^{(k+1)}\right) - \nabla f\left(\mathbf{x}^{(k)}\right) \tag{A.14}$$

Another method similar to DFP was proposed by Broyden, Fletcher, Goldfarb, and Shanno (BFGS), and it is formulated as follows [62]:

$$\mathbf{x}^{(k+1)} = \mathbf{x}^{(k)} - s^{(k)}\mathbf{B}^{(k)^{-1}}\nabla f\left(\mathbf{x}^{(k)}\right) \tag{A.15}$$

$\mathbf{B}$ is updated using the following equation.

$$\mathbf{B}^{(k+1)} = \mathbf{B}^{(k)} + \frac{\left(\Delta\mathbf{g}^{(k)} - \mathbf{B}^{(k)}\Delta\mathbf{x}^{(k)}\right)\left(\Delta\mathbf{g}^{(k)} - \mathbf{B}^{(k)}\Delta\mathbf{x}^{(k)}\right)^T}{\Delta\mathbf{x}^{(k)^T}\left(\Delta\mathbf{g}^{(k)} - \mathbf{B}^{(k)}\Delta\mathbf{x}^{(k)}\right)} \tag{A.16}$$

Having a complicated form makes these methods prone to numerical error.

# Appendix B    Computer-Aided Sensitivity Analysis

The method developed in the thesis for sensitivity calculations (Chapter 5) is generally applicable to all systems - linear or non-linear. However, as described in the main thesis body there are other methods, used in the past, for sensitivity analysis of circuits. These methods are not applicable to all circuits, and can only be used specifically with linear circuits. They exploit linear system properties to generate more rapid and accurate calculation of sensitivities. These methods are presented here for completeness. The method introduced in the thesis, is completely general and has the following advantages and disadvantages.

Advantages:

1.  As opposed to other computer-aided sensitivity analysis techniques which require the system to have certain characteristics (e.g. to be linear), this method does not impose limitation to the system.

2.  The method can be implemented without altering the main core of the simulation program, and therefore, it can be implemented on almost any simulation program.

Disadvantages:

1.  Numerical methods always involve numerical errors, which makes the sensitivity calculations inaccurate.

2.   If the number of system parameters is large, this method requires a large number of simulation runs, which makes this method time-consuming.

# B.1   Incremental Network Approach

If the circuit under study has certain properties, it is possible to reduce the simulation burden of the sensitivity analysis by using some mathematical methods and taking advantage of those properties. In this section and the next section two of such sensitivity analysis techniques are briefly explained. In this section the incremental network approach (INA) for sensitivity analysis of electrical networks is described based on [27].

Suppose it is desired to perform sensitivity analysis on the network $N$. If the elements of the network vary from their original values, a new network, the perturbed network $N_p$, is obtained as shown in Figure B-1. In the figure the original network ($N$) and the perturbed network ($N_p$) are shown. KVL and KCL can be written for both networks as follows.

Network $N$:
$$KCL: \quad \mathbf{AI} = 0 \quad , \quad KVL: \quad \mathbf{BV} = 0 \tag{B.1}$$

Network $N_p$:
$$KCL: \quad \mathbf{A}(\mathbf{I} + \Delta\mathbf{I}) = 0 \quad , \quad KVL: \quad \mathbf{B}(\mathbf{V} + \Delta\mathbf{V}) = 0 \tag{B.2}$$

Where, $\mathbf{V}$ and $\mathbf{I}$ are the vectors of the network branch currents and the network branch voltages.
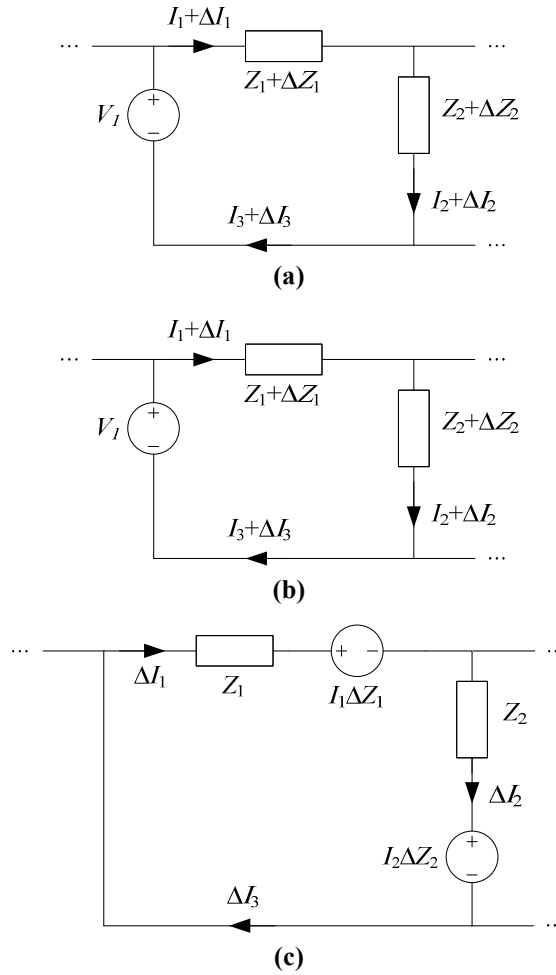
**Figure B-1  Original network (a), perturbed network (b) and incremental network (c)**

In the sensitivity analysis, we are interested in finding the currents and the voltages of the perturbed network. However, in order to find the values of the currents and the voltages in the perturbed network, it is just enough to calculate the changes in the currents and the voltages of the original network ($\Delta \mathbf{V}$ and $\Delta \mathbf{I}$). This is where the incremental network $N_i$, can be used. Combining the original network equations with the perturbed network equations, we have:

$$\mathbf{A}\Delta \mathbf{I} = 0 \quad , \quad \mathbf{B}\Delta \mathbf{V} = 0 \tag{B.3}$$

The above equation shows that the incremental values $\Delta\mathbf{V}$ and $\Delta\mathbf{I}$ have the same constraints as the original network, so those values can be currents and voltages of a network (incremental network $N_i$) with the similar topology as the original one.

Now the question is how we can find the incremental network. Consider an impedance branch in the original network ($N$), and the same branch in the perturbed network ($N_p$). The equations for that branch can be written as follows.

$$V = ZI$$
$$(V + \Delta V) = (Z + \Delta Z)(I + \Delta I)$$

(B.4)
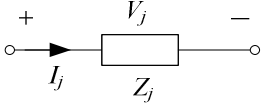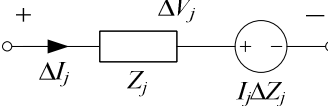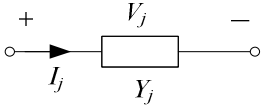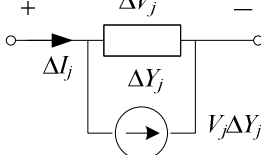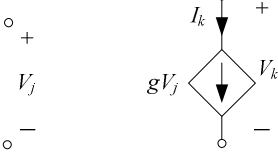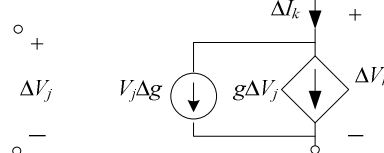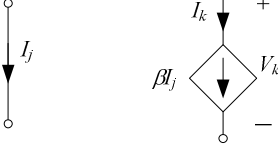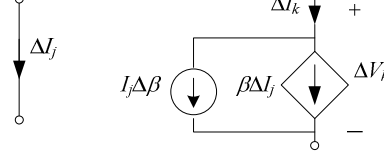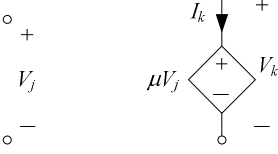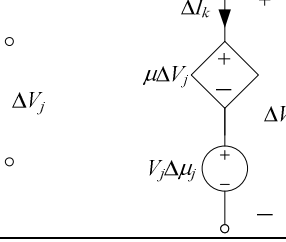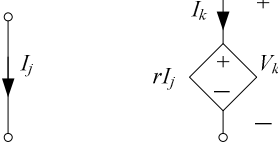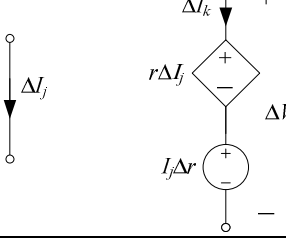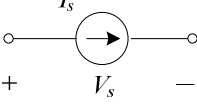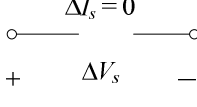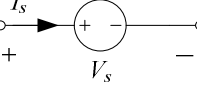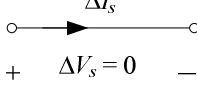
Neglecting the second order term ($\Delta Z \Delta I$) and combining the equations in B.11 we get:

$$\Delta V = Z\Delta I + I\Delta Z \quad \Rightarrow \quad \Delta V - I\Delta Z = Z\Delta I$$

(B.5)

Equation (B.12) shows that the incremental voltage and current of an impedance branch can be voltage and current of the same branch in the incremental network if a series voltage source with the value of $I\Delta Z$ is added to the incremental network.

Using this technique one can obtain the incremental network equivalent of each element in the original network $N$ as shown in Figure B-1. Using a similar method, one can obtain the equivalent incremental models for different network elements. Table B-1 shows the incremental network equivalents for different elements [27].

**Table B-1  Incremental network equivalents for different elements**

| Original Network (N) | Incremental Network (Ni) |
|---|---|
|  |  |

Having the incremental network, one can calculate the sensitivities in three steps as follows.

1.  Analyze the original network ($N$)

2.  Use the results from the original network to make the incremental network ($N_i$)

3.  Analyze the incremental network to find the sensitivities

Note that since the incremental network ($N_i$) and the original network ($N$) are only different in the placement of the independent sources, they have the same admittance matrix. This makes the solution of the incremental network much faster. In general the incremental network approach (INA) has the following advantages.

1.  Compared to the method described in the previous section, INA method takes much less simulation time.

2.  Since INA visualizes the effects of the parameter variation (by adding independent sources into the network), it provides a better insight on the sensitivities.

3.  Using INA, the incremental currents and voltages in all branches will be obtained. This information might be useful in some studies.

For more information about INA refer to [27] and [28].

# B.2     Adjoint Network Approach

The adjoint network approach (ANA) for sensitivity analysis at first was proposed by Director and Rohrer in 1969. The main purpose of this approach was to find a quick way of calculating the gradient vector for automatic network design using gradient-based optimization techniques [21]. Since one of the most time consuming steps in gradient-based optimization is the calculation of the gradient vector, ANA made those methods significantly faster.

In ANA Tellegen's theorem is used to set up a new network, i.e. adjoint network, which has the same topology as the original network; and the elements of original network are replaced by their adjoint equivalents. It can be shown that having the simulation results of the original network and the adjoint network makes it possible to calculate the first-order derivatives of an arbitrary selected network function [27]. The detailed explanation of this method is beyond the scope of this thesis; however readers may refer to [27] for such information.

In general Adjoint networks can be used for time-domain sensitivity analysis of linear circuits [27], [29], [32]; however there are methods available for applying adjoint networks for special kinds of nonlinear and switching systems [30], [31], [33], [14]. In addition, even thought the original ANA was developed for calculation of the first-order derivatives, higher order derivatives can be found using adjoint networks [23]. For more information about adjoint networks, readers may refer to [98] – [100].

# References

[1]   B. Stott, "Review of load-flow calculation methods", Proc. IEEE, vol. 62, pp. 916 – 929, 1974

[2]   Z. Ao, R. J. Fleming, and T. S. Sidhu, "A Transient Stability Simulation Package (TSSP) for Teaching and Research Purposes", *IEEE Trans. Power Systems*, Vol. 10, No. 1, pp. 11 – 17, February 1995

[3]   P. Kundur, G.J. Rogers, D.Y. Wong, L. Wang, M.G. Lauby, "A comprehensive computer program package for small signal stability analysis of power systems", *IEEE Trans. Power Systems*, Vol. 5, No. 4, pp. 1076 – 1083, Nov 1990

[4]   H.W. Dommel, "Digital Computer Solution of Electromagnetic Transients in Single and Multiphase Networks", *IEEE Trans. Power Apparatus and Systems*, vol. PAS-88, no. 4, pp. 388–399, Apr. 1969

[5]   V. K. Sood and A. M. Gole, "A static compensator model for use with electromagnetic transients simulation programs", IEEE Trans. Power Delivery, Vol. 5, No. 3, pp. 1398 – 1407, July 1990

[6]   Jiang Shan, U. D. Annakkage, and A. M. Gole ,"A platform for validation of FACTS Models", IEEE Trans. Power Delivery, Vol. 21, No. 1, pp. 484 – 491, Jan 2006

[7]   D.A. Woodford, A.M. Gole, R.W. Menzies, "Digital Simulation of DC Links and AC Machines", *IEEE Trans. Power Apparatus and Systems*, Vol. PAS-102, No. 6, pp. 1616 – 1623, June 1983

[8]   EMTDC User's Guide, Manitoba HVDC Research Center, Winnipeg, MB, Canada, 2003

[9]   A. M. Gole, "Electromagnetic transient simulation of power electronic equipment in power systems: challenges and solutions", *in Proc. 2006 IEEE Power Engineering Society General Meeting*, Jun 2006

[10]  Juan A. Martinez, and Jacinto Martin-Arnedo, "Expanding Capabilities of EMTP-Like Tools: From Analysis to Design", *IEEE Trans. Power Delivery*, Vol. 18, No. 4, Oct 2003

[11]  E. Rahimi, S. Filizadeh, A. M. Gole, "Commutation Failure Analysis in HVDC Systems Using Advanced Multiple-Run Methods", *in Proc. 2005 International Conference on Power System Transients*, Montreal, Canada, 2005

[12]  Mansour Eslami and Richard S. Marleau, "Theory of Sensitivity of Network: A Tutorial", *IEEE Trans. Education*, Vol. 32, No. 3, pp. 319 – 334, Aug 1989

[13]  M. Gole, S. Filizadeh, R. W. Menzies, and P. L. Wilson, "Optimization-Enabled Electromagnetic Transient Simulation", *IEEE Trans. Power Delivery*, Vol. 20, pp. 512 – 518, Jan 2005

[14]  Dietbert V. J. Essl, Rudolf W. Niitterer, Bert F. Rehn, and Joseph R. Domitrowich, "Automated Design Optimization of Integrated Switching Circuits", *IEEE Journal of Solid-State Circuits*, vol. SC-9, no. 1, pp. 14 – 20, Feb. 1974.

[15]  Andrew R. Conn, Paula K. Coulman, Ruud A. Haring, Gregory L. Morrill, Chandu Visweswariah, and Chai Wah Wu, "JiffyTune: Circuit Optimization Using Time-Domain Sensitivities", *IEEE Trans. Computer-Aided Design of Integrated Circuits and Systems*, vol. 17, no. 12, pp. 1292 – 1309, Dec. 1998.

[16]  Henrik Kragh, Frede Blaabjerg, and John K. Pedersen, "An Advanced Tool for Optimised Design of Power Electronic Circuits", *in Proc. IEEE Industry Applications Conference*, pp. 991 – 998, 1998.

[17]  S. Filizadeh, A. M. Gole, "A Gradient Based Approach for Power System Design Using Electromagnetic Transient Simulation Programs", *in Proc. IEEE Power Systems Transients Conf. (IPST'05)*, Montreal, Canada, Jun 2005

[18]  John W. Bandler, Qi-Jun Zhang, Jian Song, and Radoslaw M. Biernacki, "FAST Gradient Based Yield Optimization of Nonlinear Circuits", *IEEE Trans. Microwave Theory and Techniques*, Vol. 38, No. 11, pp. 1701 – 1710, Nov 1990

[19]  John W. Bandler, Shao Hua Chen, Shahrokh Daijavad, and Kaj Madsen, "Efficient Optimization with Integrated Gradient Approximations", *IEEE Trans. Microwave Theory and Techniques*, Vol. 36, No. 2, pp. 444 – 455, Feb 1988

[20]  Natalia K. Nikolova, Reza Safian, Ezzeldin A. Soliman, Mohamed H. Bakr, and John W. Bandler, "Accelerated Gradient-Based Optimization Using Adjoint Sensitivities", IEEE Trans. Antennas and Propagation, Vol. 52, No. 8, pp. 2147 – 2157, August 2004

[21]  Stephen W. Director, Ronald A. Rohrer, "Automated Network Design-The Frequency Domain Case", *IEEE Trans. Circuits Theory*, Vol. CT-16, No. 3, pp. 330 – 337, Aug 1969

[22]  J. W. Bandler, R. E. Seviora, "Current Trends in Network Optimization", *IEEE Trans. Microwave Theory and Techniques*, Vol. 18, No. 12, pp. 1159 – 1170, Dec 1970

[23] Mahmoud A. El Sabbagh, Mohamed H. Bakr, and John W. Bandler, "Adjoint Higher Order Sensitivities for Fast Full-Wave Optimization of Microwave Filters", *IEEE Trans. Microwave Theory and Techniques*, Vol. 54, No. 8, Aug 2006

[24] Eckart Zitzler and Lothar Thiele, "Multiobjective Evolutionary Algorithms: A Comparative Case Study and the Strength Pareto Approach", *IEEE Trans. Evolutionary Computation*, vol. 3, no. 4, pp. 257 – 271, Nov. 1999.

[25] Timothy C. Neugebauer, and David J. Perreault, "Computer-Aided Optimization of DC/DC Converters for Automotive Applications", *IEEE Trans. Power Electronics*, Vol. 18, No. 3, pp. 775 – 783, May 2003

[26] Sergio Busquets-Monge, Jean-Christophe Crebier, Scott Ragon, Erik Hertz, Dushan Boroyevich, Zafer Gürdal, Michel Arpilliere, and Douglas K. Lindner, "Design of a Boost Power Factor Correction Converter Using Optimization Techniques", *IEEE Trans. Power Electronics*, Vol. 19, No. 6, pp. 1388 – 1396, November 2004

[27] Leon O. Chua and Pen-Min Lin, *Computer-Aided Analysis of Electronic Circuits*, Prentice-Hall Inc, Englewood Cliffs, New Jersey, 1975

[28] L. M. Vallese, "Incremental versus Adjoint Models for Network Sensitivity Analysis", *IEEE Trans. Circuits and Systems*, Vol. CAS-21, No. 1, pp. 46 – 49, Jan 1974

[29] Stephen W. Director, Ronald A. Rohrer, "The Generalized Adjoint Network and Network Sensitivity", *IEEE Trans. Circuits Theory*, Vol. CT-16, No. 3, pp. 318 – 323, Aug 1969

[30] Fei Yuan and Ajoy Opal, "Sensitivity Analysis of Periodically Switched Linear Circuits Using an Adjoint Network Technique", *in Proc. IEEE International Symposium on Circuits and Systems (ISCAS'99)*, Vol. 5, pp. 331 – 334, June 1999

[31] P. Feldmann, T. V. Nguyen, S. W. Director, R. A. Rohrer, "Sensitivity Computation in Piecewise Approximate Circuit Simulation", *IEEE Trans. Computer-Aided Design*, Vol. 10, No. 2, pp. 171 – 183, Feb 1991

[32] Chung-Wen Ho, "Time-domain Sensitivity Computation for Networks Containing Transmission Lines", *IEEE Trans. Circuits and Systems*, Vol. 18, No. 1, pp. 114 – 122, Jan 1971

[33] Y. Kuroe, T. Yamamoto, "Computer Aided Sensitivity-Analysis of Power Electronic Control Systems and its Applications", *in Proc. Power Electronics Specialists Conference (PESC'92)*, Vol. 2, pp. 1293 – 1300, 1992

[34] N. K. Nikolova, J. W. Bandler, M. H. Bakr, "Adjoint Techniques for Sensitivity Analysis in High-Frequency Structure CAD", *IEEE Trans. Microwave Theory and Techniques*, Vol. 52, No. 1, Part 2, pp. 403 – 419, Jan 2004

[35] Seth, "Comments on Time - Domain Network Sensitivity Using the Adjoint Network Concept", *IEEE Trans. Circuits and Systems*, Vol. 19, No. 4, pp. 367 – 370, Jul 1972

[36] H. Schjaer-Jacobsen, and Kaj Madsen, "Algorithms for Worst-Case Tolerance Optimization", *IEEE Trans. Circuits and Systems*, Vol. CAS-26, No. 9, Sep 1979

[37] T. Kato and Y. Arai, "Parallel tolerance analysis of a power electronic converter", *in Proc. IEEE Workshop on Computers in Power Electronics*, pp. 88 – 93, 2002

[38] Jerry C. Hamann, John W. Pierre, Stanislaw F. Legowski, and Francis M. Long, "Using Monte Carlo Simulations to Introduce Tolerance Design to Undergraduates", *IEEE Trans. Education*, Vol. 42, No. 1, pp. 1 – 7, Feb 1999

[39] Fimmel, S. Quitzk, and W. Schwarz, "Large-Scale Tolerance Analysis", *in Proc. International Conference on Parallel Computing in Electrical Engineering (PARELEC 2004)*, pp. 33 – 38, Sep 2004

[40] S. R. Nassif, A. J. Strojwas, S. W. Director, "A Methodology for Worst-Case Analysis of Integrated Circuits", *IEEE Trans. Computer-Aided Design of Integrated Circuits and Systems*, Vol. 5, No. 1, pp. 104 – 113, Jan 1986

[41] Nicola Femia, and Giovanni Spagnuolo, "True Worst-Case Circuit Tolerance Analysis Using Genetic Algorithms and Affine Arithmetic", *IEEE Trans. Circuits and Systems-I: Fundamental Theory and Applications*, Vol. 47, No. 9, Sep 2000

[42] V. K. Manaktala and G. L. Kelly, "Computer-Aided Worst Case Sensitivity Analysis of Electrical Networks Over a Frequency Interval", *IEEE Trans. Circuits Theory*, Vol. 19, No. 1, pp. 91 – 93, Jan 1972

[43] De Vivo, G. Spagnuolo, M. Vitelli, "Worst-Case Tolerance Analysis of Non-Linear Systems Using Evolutionary Algorithms", *in Proc. International Symposium on Circuits and Systems (ISCAS'03)*, Vol. 4, pp. 576 – 579, 2003

[44] M. G. Rezai-Fakhr and Gabor C. Temes, "Probabilistic Large-Tolerance Analysis of Nonlinear Circuits in the Time Domain", *IEEE Trans. Circuits and Systems*, Vol. CAS-22, No. 1, Jan 1975

[45] Juan A. Martinez Velasco, and Ferley Castro-Aranda, "EMTP Implementation of a Monte Carlo Method for Lightening Performance Analysis of Power Transmission Lines", *Ingeniare. Revista Chilena de Ingeniería*, vol.16, no.2, pp. 169 – 180, June 2008

[46]  S. J. Shelemy and D. R. Swatek, "Monte Carlo Simulation of Lightning Strikes to the Nelson River HVDC Transmission Lines", *in Proc. 2001 International Conference on Power System Transients*, Brazil, Jun 2001

[47]  Thomas K. Soerensen, Joachim Holboell, "Insulator and Clearance Requirements in Overhead Line Transmission Systems without Shield Wires", *in Proc. 43rd International Universities Power Engineering Conference (UPEC2008)*, Italy, Sep 2008

[48]  J. Langston, M.Steurer, S. Suryanarayanan, T. Baldwin, N. Senroy, S. Woodruff, M. Andrus and J. Simpson, "Characterization of the Transient Behavior of an AC/DC Conversion System for a Notional All-Electric Ship Simulation Using Sequential Experimental Design Methodology", *in  Proc. ACM 2007 Summer Computer Simulation Conference*, pp. 91 – 97, 2007

[49]   J. Langston, M. Steurer, T. Baldwin, J. Taylor, F. Hover and J. Simpson, "Uncertainty Analysis for a Large-Scale Transient Simulation of a Notional All-Electric Ship Pulse Load Charging Scenario" , *in Proc. 2008 International Conference on Probabilistic Methods Applied to Power Systems*, May 2008

[50]  T. Kato, K. Inoue, Y. Yano, S. Oshio, "Parallel Tolerance Analysis of a Power Electronic Converter by the Genetic Algorithm with the Island Model", *in Proc. International Power Electronics and Motion Control Conference (IPEMC 2004)*, Vol. 3,  pp. 1659 – 1664, 2004

[51]  A. Graupner, W. Schwarz, R. Schuffny, "Probabilistic analysis of analog structures through variance calculation", *IEEE Trans. Circuits and Systems I: Fundamental Theory and Applications*, vol. 49, no. 8, pp. 1071 – 1078, August 2002

[52]  T. Kato, T. Fukuyama, "Tolerance computation of harmonics in a power electronic circuit by parameter sensitivity analysis", *in Proc. 32nd IEEE Power Electronics Specialists Conference (PESC. 2001)*, vol. 3, 1730 – 1735, Vancouver, BC, Canada, 2001

[53]  T. Fukuyama, T. Kato, "Tolerance Computation of a Power Electronic Circuit by Higher Order Sensitivity Analysis Method", *Transactions of the Institute of Electrical Engineers of Japan. D*, vol. 121-D, no. 8, pp. 835 – 840, 2001

[54]  Jun-Fa Mao, Ernest S. Kuh, "Fast simulation and sensitivity analysis of lossy transmission lines by the method of characteristics", *IEEE Trans. Circuit and Systems-I: Fundamental Theory and Applications*, vol. 44, no. 5, May 1997

[55]  Lubomir V. Kolev, Valeri M. Mladnev, and Simeon S. Vladov, "Interval Mathematics Algorithms for Tolerance Analysis", *IEEE Trans. Circuits and Systems*, vol. 35, no. 8, 967 – 975, August 1988

[56] Lubomir Kolev, "Worst-Case Tolerance Analysis of Linear DC and AC Electric Circuits", *IEEE Trans. Circuits and Systems-I: Fundamental Theory and Applications*, vol. 49, no.12, pp. 1693 – 1701, December 2002

[57] A. Lemke, L. Hedrich, E. Barke, "Analog circuit sizing based on formal methods using affine arithmetic", *in Proc. 2002 IEEE Computer Aided Design Conference (ICCAD 2002)*, 486 – 489, November 2002

[58] Dale E. Hocevar, Ping Yang, Timothy N. Trick, Berton D. Epler, "Transient Sensitivity Computation for MOSFET Circuits", IEEE Trans. Computer-Aided Design, vol. CAD-4, no. 4, pp. 609 – 619, October 1985

[59] Lei Junzhao, P. Lima-Filho, M.A. Styblinski, C. Singh, "Propagation of variance using a new approximation in system design of integrated circuits", in Proc. 1998 IEEE Aerospace and Electronics Conference (NAECON 1998), 242 – 246, July 1998

[60] S.S. Isukapalli, S. Balakrishnan, P.G. Georgopoulos, "Computationally efficient uncertainty propagation and reduction using the stochastic response surface method", in Proc. 43rd IEEE Decision and Control Conference, pp. 2237 – 2243, December 2004

[61] James R. Hockenberry and Bernard C. Lesieutre, "Evaluation of Uncertainty in Dynamic Simulations of Power System Models: The Probabilistic Collocation Method", IEEE Trans. Power Systems, vol. 19, no. 3, pp. 1483 – 1491, August 2004

[62] Harvey J. Greenberg, *Mathematical Programming Glossary*, University of Waterloo, 1995 – 2005

[63] M. A. Murray-Lasso, "Analysis of linear integrated circuits by digital computer using black-box techniques", *Computer-Aided Integrated Circuit Design*, G. J. Herskowitz, Ed. New York: McGraw-Hill, 1968, pp. 113-159

[64] Klaus Rigbers, Stefan Schroder, Thomas Durbaum, Matthias Wendt, and Rik W. De Doncker, "Integrated Method for Optimization of Power Electronic Circuits", *in Proc. 35th Annual IEEE Power Electronics Specialists Conference*, pp. 4473 – 4478, 2004

[65] Gary D. Hachtel, Michael R. Lightner, and H. J. Kelly, "Application of the optimization program AOP to the design of memory circuits", *IEEE Trans. Circuits and Systems*, vol. CA.922, no. 6, June 1975.

[66] William Nye, Daviod C. Riley, Alberto Sangiovanni-Vincentelli, Andre L. Tits, "DELIGHT.SPICE: An Optimization-Based System for the Design of Integrated

Circuits", *IEEE Trans. Computer-Aided Design*, vol. 7, no. 4, pp. 501 − 519, Apr. 1988.

[67] M. Gole, S. Filizadeh, and Paul L. Wilson, "Inclusion of Robustness Into Design Using Optimization-Enabled Transient Simulation", *IEEE Trans. Power Delivery*, Vol. 20, No. 3, pp. 1991 − 1997, Jul 2005

[68] N. E. Franca, J. L. Viegas, M. A. Lanca, and J. E. Franca, "Automatic Generation of Optimization Programs Using an Electrical Simulator with an Optimization Package", *in Proc. IEEE Circuits and Systems Symposium*, pp. 65 − 68, 1996

[69] Yong-Hua Song and Malcolm R. Irving, "Optimisation Techniques for Electrical Power Systems. II. Heuristic Optimisation Methods", *Power Engineering Journal*, Vol. 15, pp. 151 − 160, Jun 2001

[70] J. Michael Johnson, Yahya Rahmat-Samii, "Genetic Algorithms in Engineering Electromagnetics", *IEEE Antennas and Propagation Magazine*, Vol. 39, pp. 7 − 21, Aug 1997

[71] M. R. AlRashidi, M. E. El-Hawary, "Emission-Economic Dispatch Using a Novel Constraint Handling Particle Swarm Optimization Strategy", *in Proc. 19$^{th}$ Canadian Conference on Electrical and Computer Engineering (CCECE/CCGEI'06)*, Ottawa, Canada, pp. 1315 − 1319, 2006

[72] John W. Bandler, Shao Hua Chen, "Circuit Optimization: The State of the Art", *IEEE Trans. Microwave Theory and Techniques*, Vol. 36, No. 2, Feb 1988

[73] Y. Kang, J. D. Lavers, "Power Electronics Simulation: Progress and Future Trends", *IEEE 4$^{th}$ Workshop on Computers in Power Electronics*, pp. 169 − 174, 1994

[74] A. Ravindran, K. M. Ragsdell, and G. V. Reklaitis, *Engineering Optimization, Methods and Applications*, John Wiley and Sons Inc, Second Edition 2006

[75] U. Baumgartner, Ch. Magele, and W. Renhart, "Pareto Optimality and Particle Swarm Optimization", *IEEE Trans. Magnetics*, Vol. 40, No. 2, pp. 1172 − 1175, March 2004

[76] Zhao Yuan and Yu Xinjie, "Pareto Competition Based Evolution Strategy for Two-Objective Optimization Design of SMES Solenoids", *IEEE Trans. Applied Superconductivity*, Vol. 18, No. 2, pp. 1513 − 1516, June 2008

[77] N. Krami, M. A. El-Sharkawi, M. Akherraz, "Pareto multiobjective optimization technique for reactive power planning", *in Proc. IEEE Power and Energy Society General Meeting*, pp. 1 − 6, July 2008

[78] J. H. Van Sickel, P. Venkatesh, K. Y. Lee, "Analysis of the pareto front of a multi-objective optimization problem for a fossil fuel power plant", *in Proc. IEEE Power and Energy Society General Meeting*, pp. 1 – 8, July 2008

[79] D.I. Olcan, B.M. Kolundzija, "Comparison of NSGA and ELM for finding the Pareto front of multiple-criteria antenna optimization problem", *in Proc. IEEE Antennas and Propagation Society International Symposium*, Vol. 2A, pp. 53 – 56, July 2005

[80] M. Martinez, S. Garcia-Nieto, J. Sanchis, X. Blasco, "Pareto Frontier Construction. A GA vs Gauss-Newton Optimization for Normalized Normal Constraint Method", in Proc. IEEE Intelligent Engineering Systems (INES'06), pp. 184 – 189, 2006

[81] K. C. Lee and K. P. Poon, "Probabilistic Switching Overvoltage Analysis of the First B. C. Hydro Phase Shifting Transformer Using the Electromagnetic Transients Program", *IEEE Trans. Power Systems*, Vol. 5, No. 4, November 1990

[82] P. Guerin, M. Machmoum and R. Le Doeuff, "Probability Distributions of Harmonic Currents in Multiple Phase-Controlled Loads", *in Proc. IEEE Power Electronics Specialists Conference (PESC'95)*, Vol. 2, pp. 1021 – 1027, 1995

[83] P. Gomez, "Validation of ATP Transmission Line Models for a Monte Carlo Study of Switching Transients", *in Proc. IEEE North American Power Symposium*, pp. 124 – 129, Oct 2007

[84] J. A. Martinez and F. Castro-Aranda, "Lightning performance analysis of transmission lines using the EMTP", *in Proc. 2003 IEEE Power Engineering Society General Meeting*, Vol. 1, pp. 295 – 300, July 2003

[85] M. Bemardi, A. Borghetti, C. A. Nucci, F. Napolitano, M. Paolone, F. Rachidi, R. Vitale and K. Yamabuki, "Lightning-Correlated Faults in Power Distribution Networks", *in Proc. IEEE 2007 Lausanne Power Tech*, pp. 585 – 591, July 2007

[86] John N. Chiasson, Leon M. Tolbert, Keith J. McKenzie, and Zhong Du, "A Complete Solution to the Harmonic Elimination Problem", *IEEE Trans. Power Electronics*, Vol. 19, No. 2, pp. 491 – 499, Mar 2004

[87] A. Basak, A. Moses, "Harmonic losses in a three phase transformer core", *IEEE Trans. Magnetics*, Vol. 14, No. 5, pp. 990 – 992, Sep 1978

[88] Paul G. Cummings, "Estimating Effect of System Harmonics on Losses and Temperature Rise of Squirrel-Cage Motors", *IEEE Trans Industry Applications*, Vol. IA-22, No. 6, pp. 1121 – 1126, Nov. 1986

[89]  T. A. Lipo, P. C. Krause, H. E. Jordan, "Harmonic Torque and Speed Pulsations in a Rectifier-Inverter Induction Motor Drive", *IEEE Trans. Power Apparatus and Systems*, Vol. PAS-88, No. 5, pp. 579 – 587, May 1969

[90]  J.A. Orr, A.E. Emanuel, D.J. Pileggi, and F.J. Levitsky, "Determination of Harmonic Interference Voltages Induced in Paired-Cable Communications Circuits by Harmonic Currents in Adjacent Power Lines", IEEE Trans. Power Apparatus and Systems, Vol. PAS-102, No. 7, pp. 2278 – 2283, July 1983

[91]  P. Rao, M.L. Crow, Z. Yang, "STATCOM control for power system voltage control applications", *IEEE Trans. Power Delivery*, Vol. 15, No. 4, pp. 1311 – 1317, Oct. 2000

[92]  C. Hochgraf, R.H. Lasseter, "Statcom controls for operation with unbalanced voltages", *IEEE Trans. Power Delivery*, Vol. 13, No. 2, pp. 538 – 544, April 1998

[93]  K.V. Patil, J. Senthil, J. Jiang, R.M. Mathur, "Application of STATCOM for damping torsional oscillations in series compensated AC systems", *IEEE Trans. Energy Conversion*, Vol. 13, No. 3, pp. 237 – 243, Sept. 1998

[94]  C. K. Sao, P. W. Lehn, M. R. Iravani, and J. A. Martinez, "A Benchmark System for Digital Time-Domain Simulation of a Pulse-Width-Modulated D-STATCOM", *IEEE Trans. Power Delivery*, vol. 17, no. 4, pp. 1113 – 1120, Oct. 2002

[95]  C. Schauder and H. Mehta, "Vector Analysis and Control of Advanced Static VAR Compensators", *in Proc. IEE Generation, Transmission and Distribution*, vol. 140, Issue 4, pp. 299 – 306, July 1993.

[96]  R. W. Menzies, Yiping Zhuang, "Advance Static Compensation Using a Multi-Level GTO Thyristor Inverter", *IEEE Trans. Power Delivery*, vol. 10, no. 2, pp. 732 – 738, Apr. 1995.

[97]  Stephen Boyd and Lieven Vandenberghe, *Convex Optimization*, Cambridge University Press, 2004

[98]  A. Desoer, "Teaching Adjoint Networks to Juniors", *IEEE Trans. Education*, Vol. E-16, pp. 10 – 14, Feb. 1973

[99]  G. W. Roberts, A. S. Sedra, "Adjoint networks revisited", *IEEE International Symposium on Circuits and Systems*, Vol. 1, pp. 540 – 544, May 1990

[100] Desoer, "On the Description of Adjoint Networks", *IEEE Trans. Circuits and Systems*, Vol. 22, No. 7, pp. 585 – 587, Jul 1975

[101] A. M. Gole, *HVDC Transmission Systems*, Course Notes, Electrical and Computer Engineering Department, University of Manitoba, 2006

[102] Neil A. Weiss, *A Course in Probability*, Pearson Addison Wesley, 2006

[103] F. Crusca and M. Aldeen, "Multivariable Frequency-Domain Techniques for the Systematic Design of Stabilizers for Large Scale Power Systems", *IEEE Trans. Power Systems*, vol. 6, no. 3, pp. 1133 − 1139, August 1991

[104] C.T. Chang and Y.Y. Hsu, "Design of UPFC Controllers and Supplementary Damping Controller for Power Transmission Control and Stability Enhancement of a Longitudinal Power System", *IEE Proc. Generation Transmission and Distribution*, vol. 149, no. 4, pp. 463 − 471, July 2002

[105] Qianli Su and Kai Strunz, "Stochastic Polynomial-Chaos-Based Average Model of Twelve-Pulse Diode Rectifier for Aircraft Applications", *in Proc. IEEE COMPEL Workshop*, Troy, NY, 2006

[106] Kai Strunz and Qianli Su, "Stochastic Formulation of SPICE-Type Electronic Circuit Simulation with Polynomial Chaos", *ACM Trans. Modeling and Computer Simulation*, vol. 18, no. 4, article 15, September 2008.

[107] Sastry Isukapalli, *Uncertainty Analysis of Transport-Transformation Models*, PhD Dissertation in Chemical and Biochemical Engineering, State University of New Jersey, 1999

[108] N. Wiener, "The Homogeneous Chaos", *American Journal of Mathematics*, vol. 60, pp. 897 − 936, 1938

[109] Dongbin Xiu, Didier Lucor, C.-H. Su, and George Em Karniadakis, "Performance Evaluation of Generalized Polynomial Chaos", in Proc. 2003 International Conference on Computational Science (ICCS), pp. 346−354, 2003